Metop-A GOME Annual In-Flight Performance Report 2014

Doc.No. : EUM/OPS-EPS/REP/14/770718
Issue : v2A
Date : 19 February 2015
WBS/DBS :

EUMETSAT
Eumetsat-Allee 1, D-64295 Darmstadt, Germany
Tel: +49 6151 807-7
Fax: +49 6151 807 555
http://www.eumetsat.int

This page intentionally left blank.

Document Change Record

Issue / Revision	*Date*	*Changed Pages / Paragraphs*
v1	06 October 2014	First issue
V1C	15 October 2014	Updated draft following internal review
V1D	31 October 2014	Updated following discussion during Annual review 2014
V2	03 February 2015	Final issue
V2A	19 February 2015	Document template updated (no content changes)

Table of Contents

List of Tables

List of Figures

1 INTRODUCTION

1.1 Purpose and Scope

The primary purpose of the instrument annual reports is to provide input to the Metop-A lifetime extension review process, in particular for the objective; *Assess the feasibility and need to extend Metop-A lifetime until 2018.* The health and performance of various functions of each instrument is assessed both to report on the performance during the reporting period and provide indications of degradations which may affect instrument performance in the period before 2018.

By assessment of instrument functional performance, cumulative life limited item usage and instrument outage during the reporting period, these reports are also used to trigger any necessary operational changes, software updates or studies which will be required to maximise instrument performance and life time both for this spacecraft and future recurrent spacecraft.

The main reporting cycle is typically September-August, with a draft version of the report generated in September and reviewed during a formal In-flight performance review held in October. This review includes representatives from EUMETSAT Operations, EUMETSAT Program Development, SSST and Industry or Cooperating Agencies. A lighter mid-term review is also typically held in the second quarter of the year. This report covers the period 2013-09-01 to 2014-08-31.

1.2 Document Structure

This document is structured in eight sections as follows:

- Section 1: General introduction presenting purpose, scope and structure of this document, the list of applicable and reference documents and the open issues contained in this document.
- Section 2: Presentation of all events in the reporting period, according to the four event categories anomaly, routine, operational request and external.
- Section 3: Statistics on the duration and cause of outages and on the operational mode budgets.
- Section 4: Discussion of all open anomaly and non-conformance reports.
- Section 5: Assessment of the in-flight performance, providing sufficient data and analysis as is necessary to conclude on the behaviour and trending over the period of the report.
- Section 6: Operational configuration and evolution plan of hardware, software, documentation, procedures and database. Status of lifetime limited items.
- Section 7: Conclusion summarising the trending results and providing operational recommendation if any.

1.3 Applicable Documents

Number	*Document Name*	*EUMETSAT Reference Number*
AD 1	GOME-2 Instrument Operations Manual	MO.MA.ESA.GO.0304
AD 2	GOME Annual In-flight Performance Report Jan 2007 - Sep 2008	EUM/OPS-EPS/REP/08/0668
AD 3	GOME-2 FM3 Long-Term In-Orbit Degradation - Status After 1st Throughput Test	EUM/OPS-EPS/TEN/8/588
AD 4	GOME-2 in-flight performance review Minutes of Meeting	EUM/OPS-EPS/MIN/08/0578
AD 5	GOME-2 FM3 long-term in-orbit QTH lamp blackening - analysis, test proposal and mitigating action plan	EUM/OPS/DOC/09/1504
AD 6	GOME-2 FM3 Long-Term In-Orbit Degradation - Status After 2nd Throughput Test	EUM/OPS-EPS/TEN/09/0318
AD 7	GOME-2 FM3 Long-Term In-Orbit Degradation - Basic Signatures After 2nd Throughput Test	EUM/OPS-EPS/DOC/09/0426
AD 8	Investigation on GOME-2 throughput degradation version 2	EUM/LEO/REP/09/0732
AD 9	GOME-2 / Metop-A Level 1B Product Validation Report No. 5: Status at Reprocessing G2RP-R2, version 1E.	EUM/OPS-EPS/REP/09/0619
AD 10	GOME Annual In-flight Performance Report 2009	EUM/OPS/DOC/09/1092
AD 11	GOME Annual In-flight Performance Report 2010	EUM/OPS-EPS/REP/10/0018
AD 12	GOME Annual In-flight Performance Report 2011	EUM/OPS-EPS/REP/11/0057
AD 13	GOME Annual In-flight Performance Report 2012	EUM/OPS-EPS/DOC/12/0407
AD 14	GOME Annual In-flight Performance Report 2013	EUM/OPS-EPS/DOC/13/726897
AD 15	Investigation on GOME-2 throughput degradation – Final Report	MO.TN.ESA.GO.0985

1.4 Reference Documents

Number	*Document Name*	*EUMETSAT Reference Number*
RD 1	GOME-2 L1 Product Generation Specification	EPS.SYS.SPE.990011, version 6.1
RD 2	GOME-2 Level 1B Product Validation Report No 4: Status at Reprocessing G2RP-R1	EUM.MET.REP.08.0327
RD 3	GPDU FM3 electrical test report	MO-TR-FIN-GO-647
RD 4	GOME-2 PMD band definitions 3.0 and PMD calibration	EUM/OPS-EPS/DOC/07/0601
RD 5	Operational Incident 58 - Metop Event – GOME-2 HDM Latch-up	EUM/OPS-EPS/REP/14/744121
RD 6	GOME-2 on MetOp-A Support for Analysis of GOME-2 In-Orbit Degradation and Impacts on Level 2 Data Products, Final report, v1.	EUM/TSS/TEN/13/730011

1.5 Additional Information

This report, other reports and additional information are available on the EPS OPS Extranet. See http://www.eumetsat.int/EPS-OPS-Extranet/

1.6 Open Issues

Issue	*Section*	*Description*	*Due Date*	*Status*
		NONE		

Table 1-1: Open Issues

2 OVERVIEW OF INSTRUMENT MAIN EVENTS

In this section, the main events that have impacted the instrument over the reporting period are presented. These events are categorised to allow easier assessment of instrument and system performance. Also, instrument and mission outage are distinguished. For the GOME instrument, for example, the instrument is fully recovered after a switch off when the PMD flight line is selected and dale resistor relay disabled. However, the mission outage extends until L1 data dissemination resumes after quality checks have been made.

2.1 Event Categorisation

The events and activities are categorized into four categories. These categories have been further broken down into classes as follows:

Anomaly	This category is for those activities/events that are the result of an instrument-specific anomaly. It is broken down into the following classes:
SEU/MEU	anomalies where the root cause in a single- or multiple-event-upset affecting the software or software registers of the instrument
SET	a single-event-transient affecting the physical state of a relay or other equipment of the instrument
OB Monitoring	anomalies caused by on-board limit exceptions
OG Monitoring	anomalies detected by on-ground monitoring
Software	anomalies caused by incorrect behaviour of the OB software, if not caused by SEU/MEU and SET
Hardware	anomalies caused by unexpected hardware behaviour
Other	anomalies without a clearly identified cause, hardware failures requiring reconfiguration, and anomaly reports raised on unexpected behaviour

Routine	This category is for those activities/events that are of routine nature. It is broken down into the following classes:
OOP	for out-of-plane manoeuvres all instruments must be put into a safe configuration
IP	for in-plane manoeuvres some instruments must be put into a safe configuration in-plane manoeuvre
Calibration	for routine instrument calibration activities
Other	any other routine activities

Operational Requests	This category is for special activities initiated at the request of operational entities, It is broken down into the following classes:
Calibration	requests for special instrument calibration activities
SW Maintenance	requests for modifications of the onboard software
HW Maintenance	requests for modifications of the onboard hardware
Onboard Tables	requests to update on-board tables to tune instrument performance
Timelines	requests to update operational timelines
Tandem Ops	requests to update onboard sequence or timeline activations to support the two spacecraft working in tandem, with one in a reduced swath-width configuration

External	This category is for those activities/events that are external to the instrument but still have an impact. It is broken down into the following classes:
PL-SOL	PL-SOL is a spacecraft anomaly external to the instrument but still resulting in a switch off of the instrument
PLM	PLM operations or anomalies that cause outages
NIU	NIU operations or anomalies that cause outages, only applicable to NIU instruments
FDS	related to space mechanics events, e.g. ANX, Eclipse, etc.
[Instrument]	related to other instrument, e.g. *GOME-2*, *ASCAT*, *IASI*, etc.
Other	any other external influence

2.2 Chronology of Main Events

This table reports relevant main events during the reporting period.

Date UTC yyyy-mm-dd hh:mm:ss	*Category*	*Event Title*	*Description*	*Class*	*Reference*	*Instrument Outage*	*Mission Outage*
2013-09-04 13:35:23	Routine	In-Plane Manoeuvre	Safing Action: Mirror Parked	IP	IP_21	0d 01:41:22	0d 01:41:22
2013-09-24 07:43:18	Routine	Mooncal	September 2013 Mooncal	Calibration		N/A	N/A
2013-10-24 05:45:01	Routine	Mooncal	October 2013 Mooncal	Calibration		N/A	N/A
2013-11-22 19:18:36	Routine	Mooncal	November 2013 Mooncal	Calibration		N/A	N/A
2013-12-04 12:21:37	Routine	In-Plane Manoeuvre	Safing Action: Mirror Parked	IP	IP_22	0d 01:41:22	0d 01:41:22
2013-12-22 15:35:57	Routine	Mooncal	December 2013 Mooncal	Calibration		N/A	N/A
2014-01-21 23:32:22	Anomaly	Standby Refuse	HDM Latch-Up	SEU	AR15267	1d 17:43:00	1d 17:43:00
2014-02-05 12:15:38	Routine	In-Plane Manoeuvre	Safing Action: Mirror Parked	IP	IP_23	0d 01:41:22	0d 01:41:22
2014-03-26 11:54:33	Routine	Out-Of-Plane Manoeuvre	Safing Action: Mirror Parked	OOP	OOP_07	0d 01:41:20	0d 01:41:20
2014-04-09 10:22:06	Routine	Out-Of-Plane Manoeuvre	Safing Action: Mirror Parked	OOP	OOP_08	0d 01:41:21	0d 01:41:21
2014-06-04 10:59:55	Routine	In-Plane Manoeuvre	Safing Action: Mirror Parked	IP	IP_24	0d 01:41:21	0d 01:41:21
2014-08-15 02:10:20	Routine	Mooncal	August 2014 Mooncal	Calibration		N/A	N/A

Table 2-1: Overview of Significant Events

2.3 Event Details

This section expands on the details of events, especially those which have had an impact on instrument performance.
Note: For the category Operational Request, there were no outages during the reporting period.

2.3.1 Anomaly

2.3.1.1 EUM/EPS/AR/15267 – Standby Refuse due to HDM Latchup

On 21 January 2014 at 23:32 UTC, the Metop-A GOME-2 instrument experienced a latchup on the Housekeeping Data Module (HDM) Board. As a result of this anomaly, the instrument entered Standby/Refuse mode.

This is the first instance of such a latch-up occurring onboard either Metop spacecraft.

Recovery required a complete restart of the instrument, which was performed at 10:31 on 22 January as recommended by the ARB. The restart of the instrument allowed immediate confirmation that the latch-up had been reset, and was therefore not a permanent failure. The following six passes were utilised to upload the necessary patches for the onboard software and bring the instrument back to a nominal operational configuration.

Execution of timelines was resumed at 20:33 UTC, with a sequence of 28 calibration timelines which include day-side Earth scanning. Due to a loss of thermal stability during the anomaly and subsequent recovery operations, data dissemination was not resumed until dissemination was resumed at 17:15 UTC on 23 January, with a sensing time of 15:20. The total data outage was therefore 1d 17h 43m.

Full details of the anomaly, investigation and recovery actions taken are given in [RD 6].

2.3.2 Routine

2.3.2.1 Calibration

Most GOME-2 calibration measurements are handled in the routine cycle of timeline activations and so are not mentioned in this report. The exception to this is the Moon calibration. Whenever an opportunity arises, the scan mirror is directed such that the Moon will enter the field of view so that it can be used as a calibration source. Moon calibrations occur on a synodic period (approximately 29 days) throughout the year, except January-June.

Moon calibrations only ever occur on the dark side of the orbit, so do not result in a mission outage – shortened timelines are used which leave most of the night side of the orbit free. Moon opportunities occur on several successive orbits and so it is not necessary to miss daily calibrations. Also, Moon calibration opportunities are linked to the synodic period, which is nearly at the same frequency as the 412 orbit repeat cycle, so clashes with the monthly calibration sequence are a once per mission event. As a result of this, Moon calibrations have no impact on other aspects of the mission.

Table 2-2 below indicates the dates of Moon calibration campaigns during the reporting period, and the number of orbits used for each campaign.

Date UTC yyyy-mm-dd	*Description*	*Number of calibration orbits*
2013-09-24/25	September 2013 Mooncal	14
2013-10-24/25	October 2013 Mooncal	12
2013-11-22/23	November 2013 Mooncal	15
2013-12-22/23	December 2013 Mooncal	13
2014-08-15/16	August 2014 Mooncal	13

Table 2-2 Moon calibrations during the reporting period

2.3.2.2 Out-Of-Plane Manoeuvre

Out-of-plane (OOP) manoeuvres are required in-frequently to maintain the orbit of Metop within the requirements. The current orbit maintenance strategy foresees one OOP manoeuvre at the autumn equinox per year. This may consist of one or two burns and is usually followed by an In-Plane "touch-up" manoeuvre.

Since the start of tandem operations (July 2013), all GOME timelines end with the mirror parked internally (launch position) with all lamps off and the diffuser closed. For the orbit on which the OOP occurs, GOME is safed by simply not issuing a "timeline activate" command, thereby leaving GOME in this configuration. As a result, there is a 1 orbit outage for GOME.

Date UTC yyyy-mm-dd hh:mm:ss	*Category*	*Event Title*	*Description*	*Class*	*Reference*	*Instrument Outage*	*Mission Outage*
2014-03-26 11:54:33	Routine	Out-Of-Plane Manoeuvre	Safing Action: Mirror Parked	OOP	OOP_07	0d 01:41:20	0d 01:41:20
2014-04-09 10:22:06	Routine	Out-Of-Plane Manoeuvre	Safing Action: Mirror Parked	OOP	OOP_08	0d 01:41:21	0d 01:41:21

Table 2-3 OOP Manoeuvres during the reporting period

2.3.2.3 In-Plane Manoeuvre

In Plane (IP) manoeuvres are required in-frequently to maintain the Metop ground track, avoid debris in case of conjunction warnings (MIAMI) and to "touch-up" the orbit after an OOP. During the reported period there were six IP manoeuvres performed.

As with the Out-Of-Plane manoeuvres described above, for the orbit on which the IP occurs, GOME is "safed" by not issuing a "timeline activate" command. As a result, there is a one-orbit outage for GOME.

Date UTC yyyy-mm-dd hh:mm:ss	*Category*	*Event Title*	*Description*	*Class*	*Reference*	*Instrument Outage*	*Mission Outage*
2013-09-04 13:35:23	Routine	In-Plane Manoeuvre	Safing Action: Mirror Parked	IP	IP_21	0d 01:41:22	0d 01:41:22
2013-12-04 12:21:37	Routine	In-Plane Manoeuvre	Safing Action: Mirror Parked	IP	IP_22	0d 01:41:22	0d 01:41:22
2014-02-05 12:15:38	Routine	In-Plane Manoeuvre	Safing Action: Mirror Parked	IP	IP_23	0d 01:41:22	0d 01:41:22
2014-06-04 10:59:55	Routine	In-Plane Manoeuvre	Safing Action: Mirror Parked	IP	IP_24	0d 01:41:21	0d 01:41:21

Table 2-4 IP Manoeuvres during the reporting period

2.3.3 External

This category is for those activities/events that are external to the instrument but still have an impact.

2.3.3.1 PL-SOL

PL-SOLs cause a switch down of the entire payload module and instruments. During the reporting period, no PL-SOL occurred. The outage for GOME following a PL-SOL is mainly due to the time required to re-upload software and regain thermal stability.

Date UTC yyyy-mm-dd hh:mm:ss	*Category*	*Event Title*	*Description*	*Class*	*Reference*	*Instrument Outage*	*Mission Outage*
None							

Table 2-5 PLSOLs during the reporting period

2.3.3.2 FDS

This category includes events that are due to geometric events. During the reporting period, the only such event type was Eclipses of the Sun by the Moon, which do not result in an instrument outage.

Date UTC yyyy-mm-dd hh:mm:ss	*Category*	*Event Title*	*Description*	*Class*	*Reference*	*Instrument Outage*	*Mission Outage*
2013-11-03 11:38:46	External	Sun Eclipse by the Moon	General Temperature Reduction	FDS		none	none
2014-04-29 04:09:56	External	Sun Eclipse by the Moon	General Temperature Reduction	FDS		none	none
2014-04-29 06:05:01	External	Sun Eclipse by the Moon	General Temperature Reduction	FDS		none	none

3 OPERATIONAL AVAILABILITY AND OUTAGE STATISTICS

3.1 Instrument Outages

This table details the mission outages over the reported period:

CAT.	*CLASS*	*Instrument Outage %*	*Mission*	*EVENT / DESCRIPTION*	*# OF*	*CUMULATIVE outage (DAYS)*
Anomaly	SEU/MEU	0.24	0.48	None	1	01 days 17:43
	SET	0.00	0.00	None	0	00 days 00:00
	Software	0.00	0.00	None	0	00 days 00:00
	OB Monitoring	0.00	0.00	None	0	00 days 00:00
	OG Monitoring	0.00	0.00	None	0	00 days 00:00
	Other	0.00	0.00	None	0	00 days 00:00
	SUBTOTAL	**0.24**	**0.48**		**1**	**01 days 17:43**
Routine	Calibration	0.00	0.00	Mooncal does not cause outage	0	00 days 00:00
	OOP	0.04	0.04	Safing action for manoeuvre	2	00 days 03:23
	IP	0.08	0.08	Safing action for manoeuvre	4	00 days 06:45
	Other	0.00	0.00	None	0	00 days 00:00
	SUBTOTAL	**0.12**	**0.12**		**6**	**00 days 10:08**
Request	Calibration	0.00	0.00	None	0	00 days 00:00
	SW Maintenance	0.00	0.00	None	0	00 days 00:00
	HW Maintenance	0.00	0.00	None	0	00 days 00:00
	Timeline Update	0.00	0.00	None	0	00 days 00:00
	Onboard Table Update	0.00	0.00	None	0	00 days 00:00
	SUBTOTAL	**0.00**	**0.00**		**0**	**00 days 00:00**
INS	**TOTAL**	**0.36**	**0.60**		**8**	**02 days 03:51**
External	PL-SOL	0.00	0.00	None	0	00 days 00:00
	PLM	0.00	0.00	None	0	00 days 00:00
	NIU	0.00	0.00	None	0	00 days 00:00
	Instrument	0.00	0.00	None	0	00 days 00:00
	FDS	0.00	0.00	Sun Eclipse by the Moon	3	00 days 00:00
	Other	0.00	0.00	None	0	00 days 00:00
	SUBTOTAL	**0.00**	**0.00**		**3**	**00 days 00:00**
	TOTAL	**0.36**	**0.60**		**11**	**02 days 03:51**

Table 3-1: Instrument Outage Breakdown

From Table 3-1, it can be seen that the overall availability of the GOME-2 instrument was over 99 %. The only outages were due to manoeuvres and the HDM latch-up event of January 21.

3.2 Operative Modes Budget

The only outages during the reporting period have been due to manoeuvres. Note that calibration timelines and solar eclipses do not cause an outage. During the reporting period, a timeline has been running for 99.6 % of the elapsed flight time.

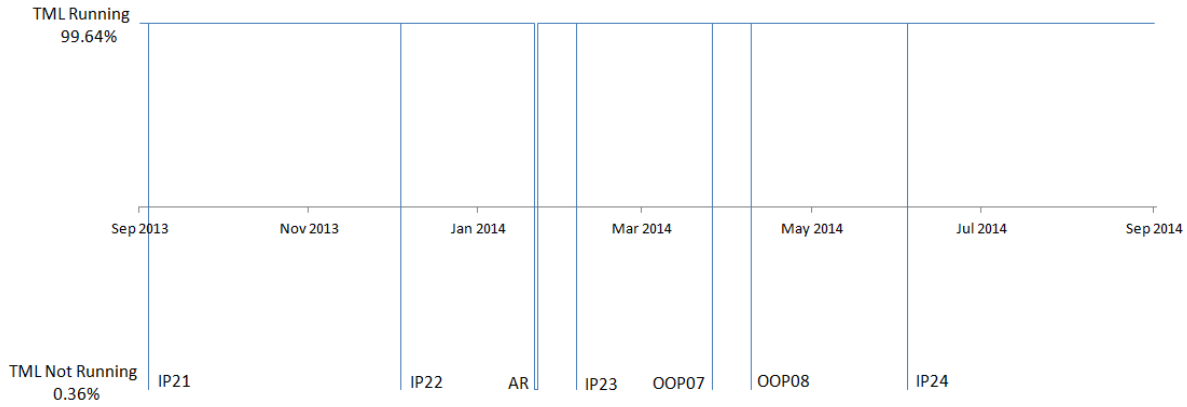

Figure 3-1 Timeline status 01 Sep 2013 – 31 Aug 2014

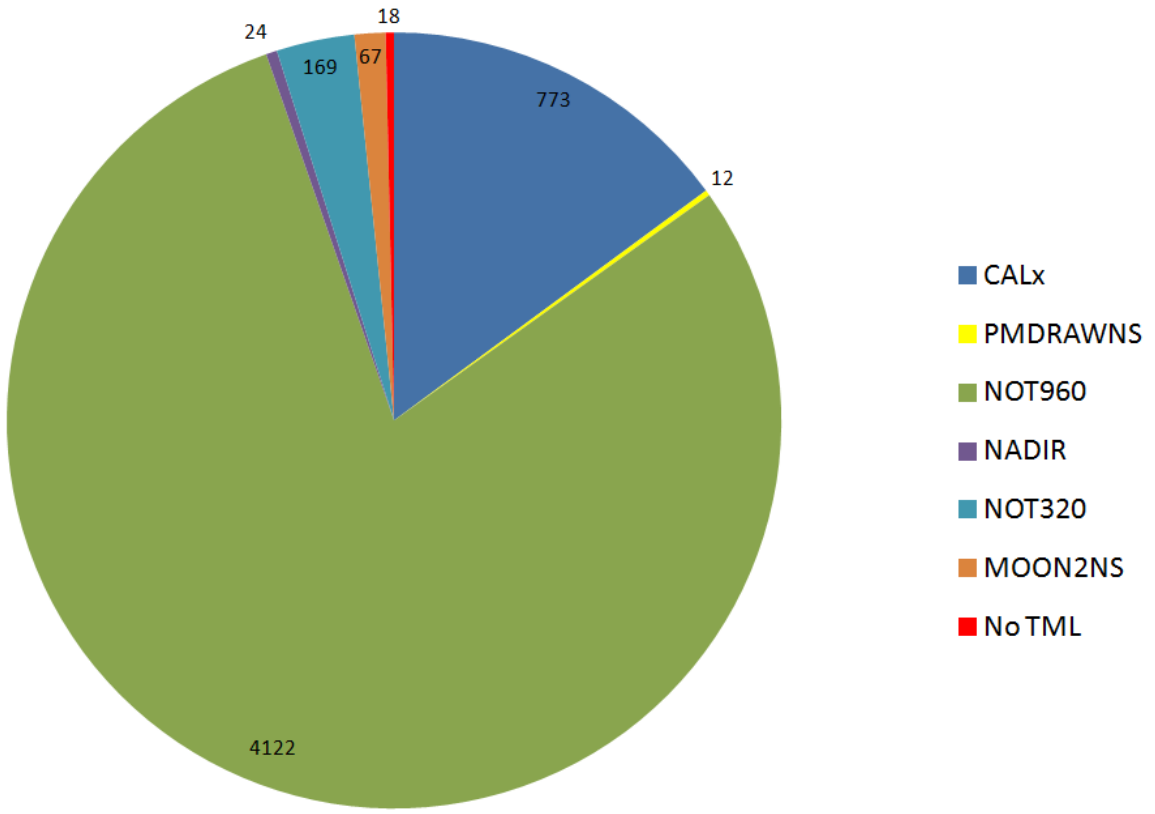

Figure 3-2 Timelines executed 01-Sep-2013 to 31-Aug-2014 by type.

4 ANOMALY AND NON-CONFORMANCE REPORTS

This section outlines the status of anomalies and non-conformances relating to the GOME-2 instrument. For completeness, a description of the anomalies is given even if they are closed and have not occurred during the reporting period.

Note: This list only includes Anomalies that are really related to the GOME-2 instrument itself. In the EUMETSAT anomaly processing tool there are other anomalies assigned to GOME-2 that actually relate to other items such as the IOM, procedures or timelines

4.1 AR and NCR Overview

Sect.	*Ref*	*Title*	*Class*	*Occurrences in Reporting Period*	*Disposition*
4.2	AR.6203	Onboard Monitoring Limits	SW	On-going	Closed
4.3	AR.6210 NCR.3115	Spurious EQSOL	SET	Approx 2 per day	Closed
4.4	AR.6241	Thermistor Noise Sensitivity	HW	On-going	Closed
4.5	AR.6537	Spurious SU switch on	SET	0	Closed
0	AR.6674 AR.6933 AR.7385 NCR.3116 NCR.3117 NCR.3121	GOME Coffee Break	SW	N/A	Closed
4.7	AR.6702	Dale Resistor Relay Toggling	HW	1	Closed
4.8	AR.6736	PMD Array Temperature OOLs	HW	0	Closed
4.9	AR.6886	Radience/Irradience Jumps Between Channels	HW	On-going	Closed
4.10	AR.6892	Light Tightness	HW	0	Closed
4.11	AR.6963 AR.8283	Spurious SU Off	SW	2	Closed
4.12	AR.7050	Spectral jumps between channel 3 & 4 for inhomogeneous scenes	SW	N/A	Closed
4.13	AR.7304	Loss of throughput for the GOME-2 Instrument	HW	On-going	Closed
4.14	AR.7446	SU Torque evolution	HW	N/A	Closed
4.15	AR.8078	Calibration Key Data for GOME-2 Polarisation Measurement Devices (PMD)	HW	N/A	Closed
4.16	AR.8602	Spurious TLM Spikes during MOON1 and MOON2 timelines	HW/SW	N/A	Closed
4.17	AR.9064	FM-3 Key Data for PMD Spectral Calibration and Slit Function	HW	N/A	Closed

Sect.	*Ref*	*Title*	*Class*	*Occurrences in Reporting Period*	*Disposition*
4.18	AR.9234	HCL lamp signal drop and degradation impacting GOME-2 spectral calibration	HW	N/A	Closed
4.19	AR.9559	HCL Voltage Anomaly	HW	0	Closed
4.20	AR9899	Spurious SU Off	SEU	0	Closed
4.21	AR.10369	PMD signal throughput degradation	HW	N/A	Limitation
4.22	AR.10874	EQSOL after MCMD xfer ack failure	SW	1	Closed
4.23	AR.11085	QTH Lamp Throughput	HW	1	Closed
4.24	AR.11644	Signal decrease after 2nd GOME-2 instrument throughput test	HW	N/A	Limitation
4.25	AR.11840	Scan angle dependence of polarization sensitivity (-45/45) PMD key-data not correctly applied	HW	N/A	Closed
4.26	AR.11839	Key-data not stray-light corrected	HW	N/A	Closed
4.27	AR.13706	GOME-2 radiometric key-data for FM3	HW	N/A	Closed
4.28	AR.14786	Reduced radiometric accuracy due to overlap shift	HW	N/A	Closed
4.29	AR.15102	GOME anomaly counter incremented by scan torque monitoring	HW	1	Closed
4.30	AR.15133	Evolution of GOME scan unit torque during 960km swath about M02	HW	N/A	Closed
4.31	AR.15267	GOME HDM Latch-up	SEU	1	Closed
4.32	AR.15517	GOME SU behaviour at static mirror positions	HW	On-going	Open

Table 4-1: Anomaly & Non-Conformance Report Overview

4.2 On-board Monitoring Limits (AR.6203)

At initial switch on, GOME immediately entered Standby/Refuse as overall temperatures were slightly lower than expected. Monitoring limits are now set as part of the switch on sequence.
As Metop has aged, temperatures have generally increased which means that post PL-SOL switch on temps are now high enough to prevent entry into Standby/Refuse, instead just triggering a few anomalies. This anomaly is officially closed in the Anomaly Database, however Metop-A operational experience should be used to define appropriate monitoring limits for all Flight Models.

4.3 Spurious EQ-SOL (AR6210)

GOME-2 was found to be susceptible to spurious EQ-SOL signals due to the sensitivity of the opto-coupler. GOME ICU RAM has since been patched (and is patched at every activation) to ignore all EQ-SOL signals. Subsequent flight models have an RC circuit to filter out any spurious signals.

Spurious EQ-SOLs still generate type 15 entries in the history area. As a result, occurrences of Spurious EQ-SOLs can be mapped as shown in Figure 4-1.

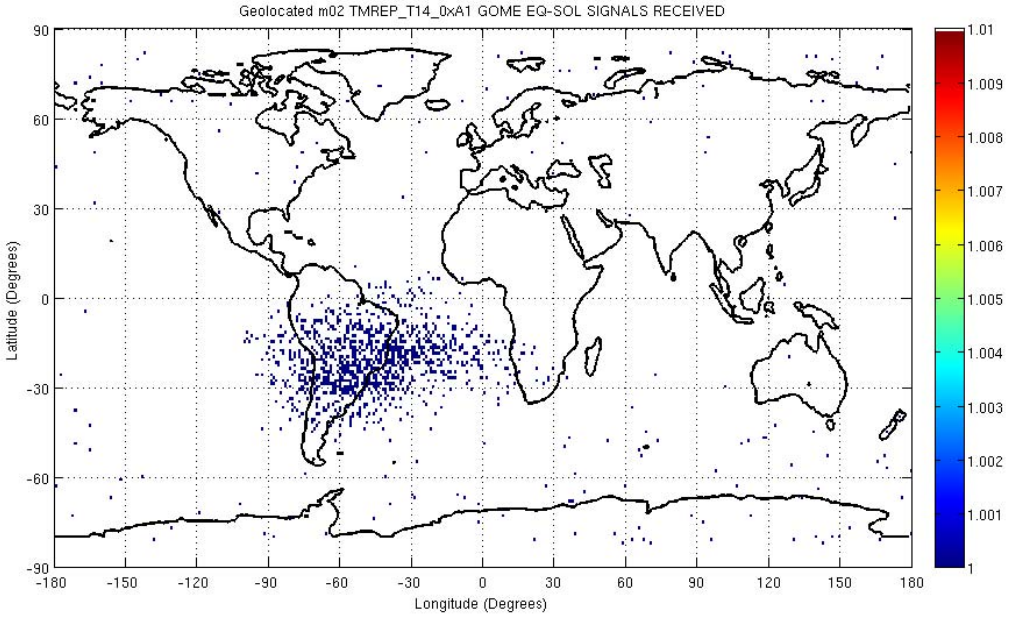

Figure 4-1 GOME-2 EQSOL Splat-o-gram

4.4 Thermistor Noise Sensitivity (AR.6241)

Thermistor Noise sensitivity is evident for several thermistors onboard GOME-2. The following sensors can exhibit step changes when activating lamps, resistors etc. ONA0023, ONA0024, ONA0025, ONA0026, ONA0106, ONA0109, ONA0281. The cause is understood and the behaviour is now documented in AD1 (GOME-2 IOM) §9

4.5 Spurious SU On Anomaly (AR.6537)

During SIOV, there was a period where GOME was left in Idle mode with the Equipment Bus powered, but without a parameter MCMD having been issued to activate the SU. A Radiation event had hit an optocoupler HCPL523K (same type as responsible of AR 6210), controlling the SU power switch. This caused the SU to come on, but without knowledge of the ICU. This was only noticed retrospectively by looking at GOME-2 EQ bus current telemetry. As a result, the SU/ICU had no communication and the SU was in autoscan mode. When a parameter command was issued to activate the SU, the ICU could not communicate it, so switched the SU off, raising an anomaly in the history area. The SU was switched on at the next timeline command.

This anomaly has no impact since it can only occur in non-nominal operating conditions and the recovery is autonomous anyway. The IOM has been updated to explain this behaviour and also that the optocoupler type is present on power switches of all FPAs, PMDs and SU, therefore all above units could potentially be affected by spurious switch on events in certain conditions. This behaviour is documented in AD1 (GOME-2 IOM) §9.

4.6 Coffee Break Anomaly (AR.6674)

The GOME Coffee Break anomaly was initially considered fairly benign. GOME would occasionally skip 1 HKTLM format. The format counter would go as follows *n-1, n, n, n+1*. After the second HKTLM format with a counter of n, the PMC would raise 2 anomalies, set the next expected format to n+1 and there would be no further impact.

However, if this anomaly occurred around the time that an extended format was being acquired from another instrument or PLM, the PMC would react to the incorrect format length of the repeated format and not look at any other aspect of the format, including the counter. The PMC would then assume that the format counter of the repeated format was n+1, so would set the next expected format counter to n+2 rather than n+1. The PMC would then see the next format from the GOME ICU had the incorrect format counter. Having inferred two bad formats in a row, the PMC would send an EQ-SOL signal to the GOME ICU and suspend the processor.

This anomaly eventually triggered two occurrences of GOME suspend mode, resulting in 10 days mission outage in total – primarily due to loss of thermal stability. A short RAM patch was prepared which was first uploaded after the second ICU suspend and is now uploaded at each ICU activation.

4.7 Dale Resistor Relay Toggling (AR.6702)

During SIOV, as the FPA detectors were first operated at 235K, instability in the detector temperatures was observed. It was found that the cause was the thermostatically controlled Dale Resistor toggling. The Dale resistor has two relays in series – a commanded relay and a thermostatically controlled relay. Procedures were updated to open the Dale Resistor after any transition to Idle mode, and a note added to the AD1 (GOME-2 IOM) §9 to this effect.

4.8 PMD Array Temperature OOLs (AR.6736)

During SIOV, as the PMD cooler flight lines were activated, PMD array temperatures started breaching the yellow lower limit and getting very close to the red limit. Since the PMD array temperatures are uncontrolled, they vary throughout the orbit, so several anomalies per orbit were registered by the ICU due to the Type 6 LIMITX entry created by the on-board monitoring. At this point the spacecraft was cooling, so the problem was becoming worse. It was decided to lower the Yellow lower limits of these parameters to 229K, just 1K from the Red lower limits.

These limits also need to be carried across to FM1 and FM2. The IOM has also been updated to recommend that the PMD cooler flight line is not activated with optical bench temperatures (as measured by ONA0113) below 275.5K. This needs to be considered for the Metop B/C SIOV Plan.

4.9 Radience/Irradience Jumps between Channels (AR.6886)

Jumps in calibrated radiance (backscattered Earthshine spectra) and solar irradiance spectra were observed in GOME-2 level 1b data products produced by the PPF and also by the GPP when compared with key data.

The source of these shifts could not be explicitly identified; however, they were consistent with physical movements within the instrument caused by the launch phase or different thermal environment. This anomaly is now closed. Now that the issues of Key Data are understood more clearly, separate ARs will be raised to allow easier tracking of problems.

4.10 Light Tightness (AR.6892)

During light tightness tests in commissioning, it was found that stray Earth light signals were observable in dark signal measurements made on the day side of the orbit. All relevant operational timelines were updated such that all calibration measurements necessary for the processing (with the exception of the sun measurements) were taken during eclipse. GOME-2 FM1 and 3 will inherit these timelines.

4.11 Spurious SU off Anomaly (AR.6963)

Frequently, when a report format is requested from the GOME ICU, the ICU registers a bad TLM format from the SU. This is normally only observable in science data packets and has no impact. However, this anomaly occasionally leads to SU protocol exceptions which force the ICU to switch the SU off. The anomaly tends to generate so many Type 14 entries that the History Area often fills up.

Since SU commands are embedded in Routine Parameter MCMDs in timelines, the SU is always reactivated autonomously. Since the anomaly is related to report format acquisition, it always occurs over Svalbard. At this point even if Earth scanning has started, the Integration Times are being frequently updated. So this anomaly rarely causes a significant outage.
This anomaly has now been fixed with the upload of SW 2.6.2.

4.12 Spectral jumps between channel 3 and 4 for inhomogeneous scene (AR.7050)

Spectral jumps were observed in level 1b and raw data between channel 3 and 4 for very inhomogeneous scenes (cloud edges for example). This problem was only been observed when channel three integration time was set to 93.75 ms co-added. Analysis showed that co-added 93.75 ms co-added data was shifted by 93.75 ms with respect to 187.5 ms data without co-adding.

As a work-around, all timelines had to be updated so that co-adding was not used. A consequence of this was that scenes including bright objects such as tropical cloud tops were saturated. This only impacted about 1% of data, but its impact was concentrated on one type of data. As a long term solution, the CDHU SCIuP software was updated. The scale of the update meant that the software had to be re-compiled to give v2.6. Before this was uplinked to the spacecraft, further testing revealed that the new software did not allow co-adding for channel 1 or 2, so further patch had to be applied. After 2 unsuccessful attempts at loading this software in September 2008, the new software was successfully loaded in March 2009. Since the upload there are very occasional instances of Channel 4 saturation, believed to be due to specular reflection from ice crystals in bright tropical cloud tops.

4.13 Loss of throughput for the GOME-2 Instrument (AR.7304)

Since very early in the commissioning phase, it was noticed that the throughput for the GOME-2 instrument had been reducing. It is believed that the main sources for this throughput loss are Scan Mirror Degradation and Detector Contamination This loss of throughput was declared to have stabilised in September 2012, with limited performance degradations. A test was made in January 2009 to warm the FPA detectors in 5K steps to 260K and run the PMD coolers on ground line. This test did show some positive results, however it is believed that having the Dale resistor disabled during the test had a major impact on the results and the achieved higher target temperature. In 2013, a dedicated “darkness test” was executed on Metop-B, which was showing similar rates of degradation. This test ruled out exposure to UV radiation as the source of the degradation.

4.14 SU Torque Evolution (AR.7446)

Shortly after launch, the Scan Unit Torque profile over a 1920km 6s scan cycle (4.5 s scan, 1.5 s flyback) was seen to rapidly deteriorate, becoming much more noisy. GOME-2 has a full-rotation feature implemented and a torque telemetry shift, allowing pseudo-170Hz torque profiles to be created for careful monitoring. This allowed a 10-minute period of continuous rotation to be implemented in the daily calibration timeline and for the profile to be carefully monitored. Since the daily maintenance has started, the torque profile is greatly improved. This maintenance will be carried forward to GOME FM1 and 2 onboard Metop B and Metop C.

4.15 Calibration Key Data for GOME-2 Polarisation Measurement Devices (PMD) (AR.8078)

Radiometrically calibrated raw PMD Sun measurements show clear differences (4-5%) between PMD-p and PMD-s. As the Sun is an unpolarised source, radiometrically calibrated PMD-p and PMD-s spectra should be the same within the error bounds. However, taking into account the complicated nature of the analysis and the indications that more than one effect are implicated in the observed behaviour (in addition to the fact that primary polarisation data and products are no longer believed to be affected) the AR was closed. The investigations will be continued in the frame of the overall degradation analysis and correction, and the activities of the GOME-2 polarisation study (through which all aspects of GOME-2 polarisation products including PMD spectral and radiometric calibration & degradation will be analysed). This issue is open and the AR will be re-opened and rephrased to describe better the issue.

4.16 Spurious TLM Spikes during MOON1 and MOON2 timelines (AR.8602)

It was observed that spikes in the Pre-disperser Prism Temperature (ONA0113) were occurring during MOON1 and MOON2 timelines. The Spikes are of the order 1K and last for just 1 sample, so do not represent a physical increase in temperature. Due to the low impact of this anomaly and the difficulties finding the root cause, no further action is taken.

4.17 FM-3 Key Data for PMD Spectral Calibration and Slit Function (AR.9064)

The in-flight PMD spectral calibration is unstable if the spectral fitting window from 348 – 382 nm is used in the operational data processing. Additionally, the PMD-p and PMD-s spectral calibration derived in-orbit shows a shift of ~2 spectral pixels which is not believed to be real. As a result of the analysis described below the PMD spectral calibration key data is believed to be inadequate in the region 320 – 400nm. The issue has been resolved by using an improved set of spectral fitting windows together with a full-grid fitting approach (replacing the polynomial representation of spectral grids for PMDs)

4.18 HCL lamp signal drop and degradation impacting GOME-2 spectral calibration (AR.9234)

Due to the overall loss of throughput for the GOME-2 Instrument, the spectral line at 320 nm was verging on the level of detectability. In order to rectify this, the integration time for the spectral calibration was increased in the daily and monthly calibrations and the acceptance threshold in the PPF was reduced from 80 to 50 BUs. At the same time, the daily calibration timeline was split into 2 – a CAL6 and a CAL0 so that the spectral calibration could be performed before SMR measurements. Metop B and Metop C will inherit this split daily calibration, however the increased integration time

must be assessed before use to prevent saturation of strong lines. This will be performed as the normal work. Also, the use of Fraunhofer lines may be considered as a future back-up to spectral calibration.

4.19 HCL Voltage Anomaly (AR.9559)

During the HCL ignition on 1 April 2008, the current and voltage of the HCL lamp did not follow the usual pattern. This resulted in the ICU switching the HCL Lamp off due to the current OOL. This anomaly was most likely caused by the Lamp finding a lower impedance discharge path. This anomaly is not considered to be a sign of Low Voltage Mode (LVM) and no further action is required, other than monitor for re-occurrence.

4.20 Spurious SU Off (AR.9899)

On 21 Jun 2008, as Metop-A was flying over the SAA, the ICU lost communication with the Scan Unit. The ICU reacted to the SU Torque reading 0xFFFF and switched the SU Off. On the execution of the next line of the running timeline, the SU was re-activated and has behaved correctly since then. Due to the rare occurrence and low impact, no action is necessary for any Flight Model.

4.21 PMD signal throughput degradation (AR.10369)

The GOME-2 main channel and PMD signals are known to be degrading. The largest degradation is observed in the UV. At a certain point in time the PMD signal for UV PMD bands will fall below the pre-defined threshold of currently 35 BU for processing resulting in the loss of polarisation correction of main channel radiances. The exact mechanism of throughput loss is not yet completely understood. For details we refer to the investigation of the ESA led “tiger team” activities [AD8].

4.22 EQSOL after MCMD xfer ack failure (AR.10874)

On 16 Feb 2009, the PMC suspended the GOME ICU due to a failure of the ICU to correctly acknowledge reception of a routine activate timeline MCMD. A memory dump of the history area revealed that the MCMD reception and ICU report format time were only two OBT ticks apart. It is therefore considered likely that the cause of this anomaly was similar to AR.6963 and that the fix for AR.6963 will coincidentally fix this anomaly too. Recreating the anomaly on ground using the EGSE will be extremely difficult and since there was only one occurrence in 2.5 years, it was decided to close this anomaly and potentially re-open on re-occurrence.

4.23 QTH Lamp Throughput (AR.11085)

During the instrument annual in-flight performance review process, it was noticed that optical throughput from Radiometric Calibration measurements were falling more quickly compared to other sources (SMR, SLS, LED), which are mutually consistent. It is believed that this may be caused by Lamp Blackening due to the lamp being run too cold.

Based on OMI experience, an operation was executed (AD5), where the QTH Lamp was ignited at 360, 380 and 400mA for 10-15 minutes to see if any improvement could be made. The test proved inconclusive – there was no improvement in throughput. However, it is understood that the GOME-2 lamp operates at a lower voltage than that of OMI and GOME-1, so the lamp would not reach the same temperatures. There is no concern regarding lamp life and the loss of throughput could always be remedied by increasing integration times or lamp operating current. Signal decrease after a second GOME-2 instrument throughput test (AR.11644)

A continuous throughput degradation has been observed. The signal at the output of the instrument decreased with a spectral signature: the losses are around 20% per year in the UV part of the spectra and 10% per year in the visible. These losses have been estimated as the linear annual rate of degradation since the beginning of life.

This leads to the degradation of the products and, in a long-term frame, possibly to the loss of the operational status of some products. Up to now the quality of all the operational products is within the specifications. Investigations are being performed in order to understand the phenomenon and to define possible actions for mitigating the on-going degradation and/or for avoiding the same problem on the Metop-B and C satellites.

4.24 Signal decrease after 2nd GOME-2 instrument throughput test (AR.11644)

After the 2nd GOME-2 instrument test started 7th of September 2009 and ended in orbit 15041 with sensing time 9:50. During the test the temperatures of the main detectors FPA 1 to 4 have been put at various temperature levels in order to evaluate the throughput response. The second part of the test was a dedicated outgassing phase with detectors set to 305K (OB temperatures at around 275 K). After the end of the test the temperatures were brought back from an intermediate 280 K to 235 K as nominal.

After the instrument was brought back to nominal configuration (including stable processing of level 1b data) it was noted that the throughput (signal levels) of the instrument had dropped with respect to previous levels by between 25 and 10% in the UV/vis and 5% or less in the NIR. This drop was unexpected. An expected throughput loss during one week of operations should have been on the order of 1 to 4% overall.

Following investigation by a “tiger team” from SSST, the GOME-2 degradation is now considered a feature. For more details, see [AD.8] Investigation on GOME-2 throughput degradation and [AD.15] Investigation on GOME-2 throughput degradation – Final Report.

4.25 Scan angle dependence of polarization sensitivity (-45/45) PMD key-data not correctly applied (AR.11840)

It was noted that sensitivity for PMD detectors was applying an interpolation of key-data provided for the FPA detectors, which was invalid. Updated key-data files were provided, and it is also important to make sure that these key-data files are delivered for the following flight models FM2 and 1.

4.26 Key-data not stray-light corrected (AR.11839)

A substantial part of the FM3 key-data was not corrected for stray-light during the derivation of key-data from raw calibration measurements. The key-data files were updated, and it was noted EUMETSAT should check that stray-light correction for polarisation key-data derivation from raw measurements is turned on following analysis of the delta calibration campaign of FM2 and 1 and subsequent derivation of key-data.

4.27 GOME-2 radiometric key-data for FM3 (AR.13706)

During the FM2-2 delta-calibration campaign systematic biases in the radiometric key-data for FM2 (Metop-B) were identified, which have been traced back to measurement setup problems and which are therefore to various degree also applicable to FM-3 key-data on Metop-A. The calibration data has since been updated in June 2013.

4.28 Reduced radiometric accuracy due to overlap shift (AR.14786)

After seven years in orbit the overlap point between channel 2 and 3 (less between channel 1 and 2) has shifted considerably, since the initial adjustment to account for on-ground to in-orbit changes. In addition, the observed delta Etalon between on-ground and in-orbit has been growing quite large, which also increases the error on the applied correction from in-flight data. The issue has been corrected with new key-data being integrated in CGS1 on 13th June 2013.

4.29 GOME anomaly counter incremented by scan torque monitoring (AR.15102)

During Metop-A pass #36252 the GOME anomaly counter was increased by 1, and the associated alarm pointed at a high (YOOL) scan mirror torque reading (23mNm) at 09:55:09.2
This highlighted the following:

- the onboard monitoring limits (21mNm) did not reflect those used on ground (35mNm), and have since been updated to 35mNm.
- the anomaly was raised by a single high value (the recorded value) preceeded by several points below the yellow low limit. The combination of both low and high OOL values into the filtering is a software feature which was not expected. This was addressed in IOM version 8 (March 2014).
- the points below the yellow low limit are common at the start of a timeline, but not explained. See AR.15517

4.30 Evolution of GOME scan unit torque during 960km swath about M02 (AR.15133)

Following the change of scan swath aboard Metop-A from 1920km to 960km the daily increase in torque between daily spinning activities showed an increasing trend, implying the reduced range of angular motion and/or speed of the scan unit associated with the new scan swath led to a worsening of the evolution of the torque profile between these maintenance activities. However, the trend did not continue.

4.31 GOME HDM Latch-up (AR.15267)

On 21 January 2014 at 23:32 UTC, the Metop-A GOME-2 instrument experienced a latchup on the Housekeeping Data Module (HDM) Board. As a result of this anomaly, the instrument entered Standby/Refuse mode. Recovery required a complete restart of the instrument, which was performed at 10:31 on January 22nd as recommended by the ARB. The restart of the instrument allowed immediate confirmation that the latch-up had been reset, and was therefore not a permanent failure. The following six passes were utilised to upload the necessary patches for the onboard software and bring the instrument back to a nominal operational configuration. Full details of the anomaly, investigation and recovery actions taken are given in RD.6.

4.32 GOME SU behaviour at static mirror positions (AR.15517)

For six of the seven nominal scenarios in which the GOME scan mirror is in a fixed position, the SU reports a non-zero torque. This is reported immediately before the start of scanning for each timeline, where the torque values reported are large (greater than 20mNm) and appear to be increasing over time. This is applicable to both Metop A/B, and assumed to also affect Metop-C. In two of the scenarios, the torque profile exhibits a well-defined but unexplained saw-wave pattern.

5 FUNCTIONAL PERFORMANCE ASSESSMENT AND TRENDING

5.1 Analysis Method description

Instruments are monitored per **physical signature** to which indicators are assigned to reflect its performance and trending.

A **physical signature** is a sub-set of correlated parameters which describes a vital function of the instrument or a particular observed behaviour. These signatures are interpreted and then apportioned to the instrument **component**, and a status is assigned (ref. to test coverage matrix in annex A
A function is provided by a set of instrument **components generally** linked to the instrument subsystem.

For each **component**, several ***test unit***s are created. A unit test can cover anything from simple trending of a group of parameters and inspection of the average, standard deviation etc., to performing detailed analysis on a particular set of parameters to determine the state of a particular component (e.g. principle component analysis, derived parameter calculations, comparison of a group of parameters against another group etc.), and raise **indicators**.

Indicators are then monitored on different timescale, then apportioned to the instrument component.
Some additional physical signature may also be performed under certain specific conditions (e.g. troubleshooting, to analyse decontamination etc.), while others are performed routinely.
For all physical signatures the immediate and lasting effects of system level events (e.g. PL-SOL, OOP) or instrument events (e.g. anomalies, operating strategy changes) will be identified and discussed.

Trends indicating a long term change of physical signature will be identified, discussed and compared against the operating limits. Nevertheless, it must be noted that even if the analysis is based on these observations, all parameters remain available for troubleshooting or deeper analysis.

In the plots contained in the following sections the following colour convention applies:

1) *Graphs with three coloured lines (Black/Blue/Magenta):* The black line represents the orbital averages of the parameter, while the blue and the magenta lines represent respectively the minimum and maximum on the orbit.
2) *Graphs with a single blue line:* The red line represents the value of that parameter.
3) *Graphs with multiple coloured lines (other colours, red, green, blue)*: As specified in the plot labels.

This colour convention is applicable to the plots produced for all the physical signatures.
Plots are either covering the reporting period, the entire time since the instrument has been declared operational or a shorter time period related to a specific event.

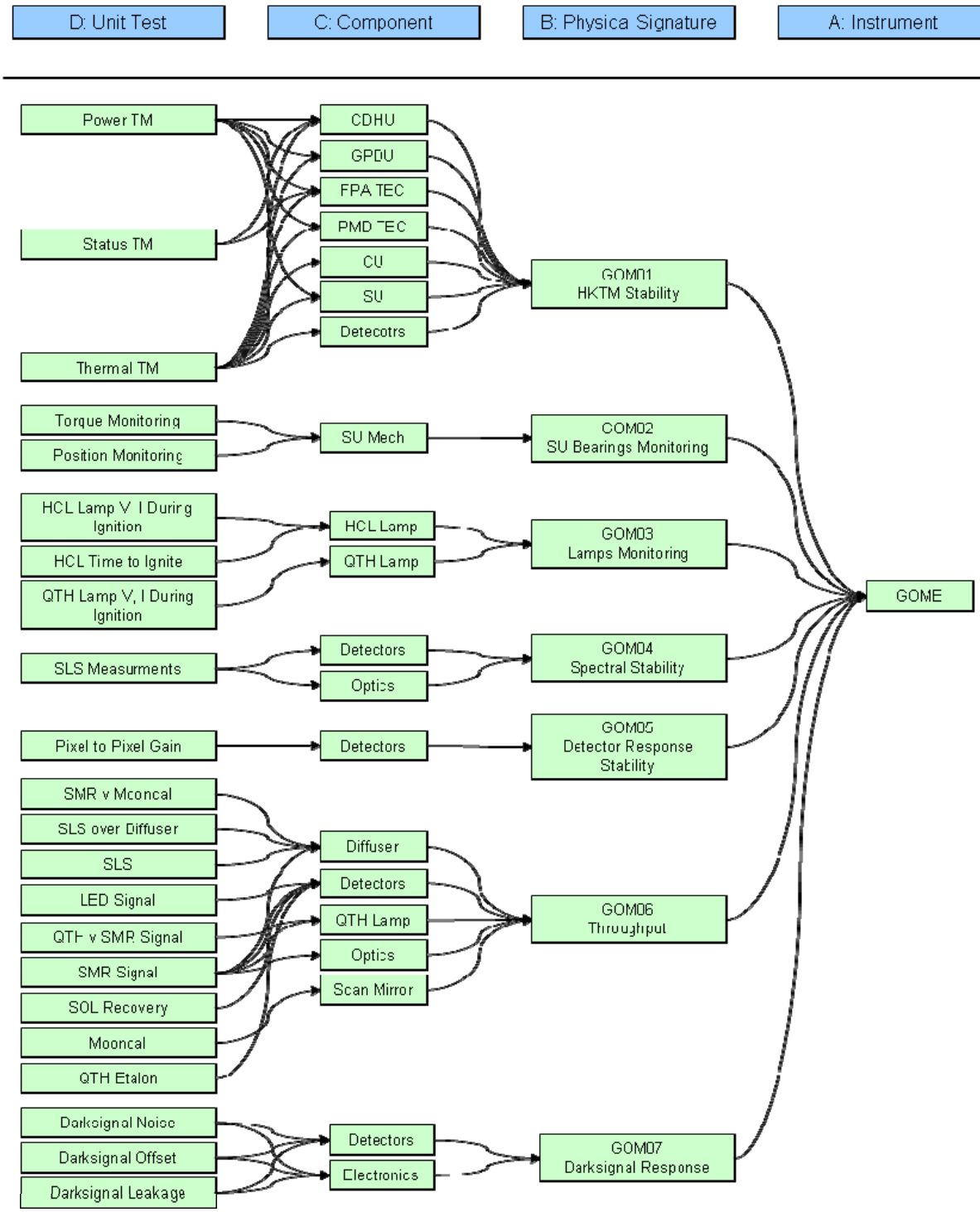

Figure 5-1: Test Unit Breakdown

5.2 Physical Signature Synopsis

Section	*PS*	*Title*	*Component*	*Status*	*Trend*	*Conclusion*
5.3	GOM01	HKTM stability	Functional health and trending analysis (including SVM/PLM TM correlation, ageing factors, etc) covering below aspects: • Thermal HKTM stability (detector cooler) • Power HKTM stability (GPDU, CDHU) • Software stability (type 14 entries)	GREEN	⇒	GOME Healthy
5.4	GOM02	SU Bearings Monitoring	• Torque monitoring • Position Error monitoring	GREEN	⇒	Mechanism Healthy, torque profile noisy but stable. Spinning on Metop B/C recommended
5.5	GOM03	HCL and QTH Lamps Monitoring	• HCL Output and Electrical Stability • QTH Output and Electrical Stability	GREEN	⇒	QTH Lamp Blackening possible, but does not look serious HCL Lamp Output Stability Questionable No signs of HCL LVM or similar. Usage of lamps indicates plenty of life remains
5.6	GOM04	Spectral Stability	Stability of Spectral Calibration	GREEN	⇒	Some correlation with known events, but well within specs.
5.7	GOM05	Detector response stability	Pixel to Pixel Gain	GREEN	⇒	
5.8	GOM06	Throughput Stability	Overall throughput assessment based on the below analysis • SLS, SMR Throughput • Earthshine • WLS Etalon Monitoring • WLS vs. SMR • SLS vs. SLS Over Diffuser • SMR vs. Mooncal	YELLOW	⇘	Throughput loss in UV stabilised with limited performance degradations
5.9	GOM07	Darksignal	Measure stability of Darksignal corrections • Offset • Leakage • Noise	GREEN	⇒	Channel 2B data missing, requires L0-1B reprocessing. Separation of Offset and leakage not available Some seasonal variation in mean dark signal evident.

Table 5-1: Physical Signatures Synopsis. See also the legend on the following page.

Status definition

Status Colour	Status Meaning
BRIGHT GREEN	Fully Operational
LIGHT GREEN	Fully Operational, but not in use, redundancy available
YELLOW	Operational with Limitations
ORANGE	Operational with Degraded Performance
LIGHT ORANGE	Not Operational with Degraded Performance
RED	Not Operational
GREY	Not applicable
BLANK	No status reported

Trend arrow definition

Trend Arrow	Trend Meaning (trend, not the consequences)
⇒	no negative trend, i.e. stable
⇘	negative trend within expectations
⇗	positive trend within expectations
⇓	negative trend above expectations
⇑	positive trend above expectations
	no trend reported

Trend definition

Trend Colour	Trend Meaning
GREEN	any trend (if there is any) will have no impact before end of assumed mission life at current rates
YELLOW	any trend will lead to a change of status before the end of assumed mission life at current rates
ORANGE	any trend will lead to a change of status within the next year at the current rates
RED	any trend will impact ability to perform EOL operations within the next year at the current rates
BLANK	No trend reported

5.3 GOM01: HKTM Stability

5.3.1 Description

This physical signature reflects the main housekeeping functions of the instrument, i.e.:

- FPA, PMDs thermal management;
- Power conditioning;
- Housekeeping and science data management;
- The optical bench structure.

The health assessment of GPDU, CDHU electronics is performed by measuring voltage, current, power according to status of equipment. To assess the health of detector coolers the following temperatures are monitored:

- FPA temps should be within 0.2 degrees of target temp and vary less than 0.25 degrees per orbit.
- PMD temps should be around 230 K on the flight line, varying with Pre-disperser Prism Temp.
- PMD s/p temperature gradient must be monitored since the signal ratio is used in the derivation of polarisation correction for the main channels.

The monitoring of equipment, e.g., problems with switching failures, latch-ups etc is detected through the Type 14 Entries. The trending is performed through evolution of consumed power, considering the ageing and seasonal evolution

5.3.2 Analysis

The long term behaviour of several HK parameters has been analyzed in order to identify and justify:

- Expected transients and discontinuities correlated to instrument /satellite and external events or operations.
- Trends or evolutions that can be correlated to other parameters/phenomena discovered on-board or on-ground, and that can be used as input for the discussion regarding the durability (or residual reliability) of the instrument with regard to the planned operational life.
- Any kind of unexpected behaviour and its correlation with regard to other parameters/phenomena.

Hereafter we report a summary of the observations made and a selection of the plots where the evidences of such phenomena are evident and from which such features can be completely described and discussed.

Furthermore, plots indicating HK Stability are presented in weekly extranet reports, so only some representative examples are included here.

The orbital averages are used to generate statistics on the min, mean and max where valid HKT is available.

1. The correlation between mean temperature values across the instrument is checked.
2. Unusual behaviour is cross checked against instrument/satellite events

3. The overall trend of the temperatures and voltages across the reporting period is considered in order to decide whether or not the temperature is likely to exceed the parameter limits in the next five years.

5.3.3 Interpretation

All the observed parameters show a good stability over the reported period.
The only noticeable variations are those due to seasonal effects and to specific events as marked on the plots.

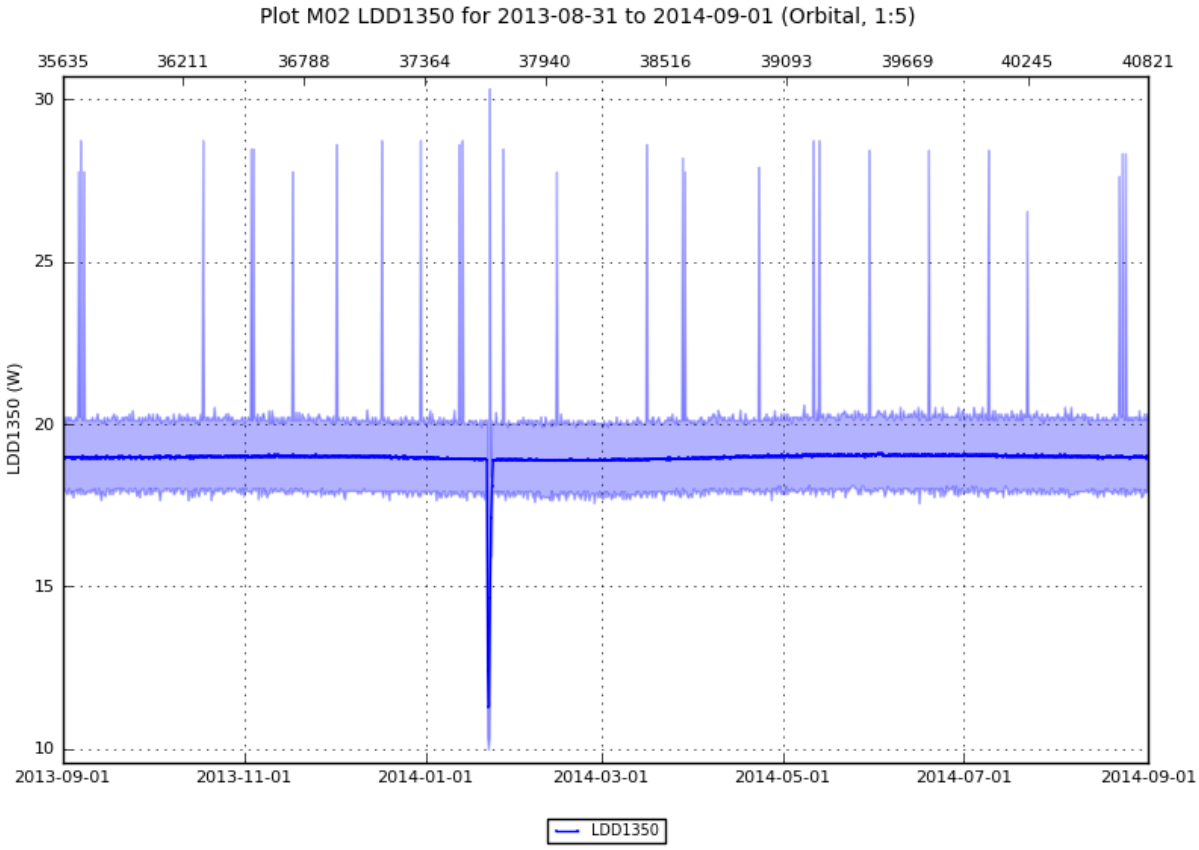

Figure 5-2 GOME ICU Power During the Reporting Period

Figure 5-2 shows stable ICU Power consumption during the reporting period. Spikes in the ICU Power are due to Telemetry sampling being coincident with shutter movements, which are powered by the ICU. The drop in January marks the HDM Latch-up anomaly.

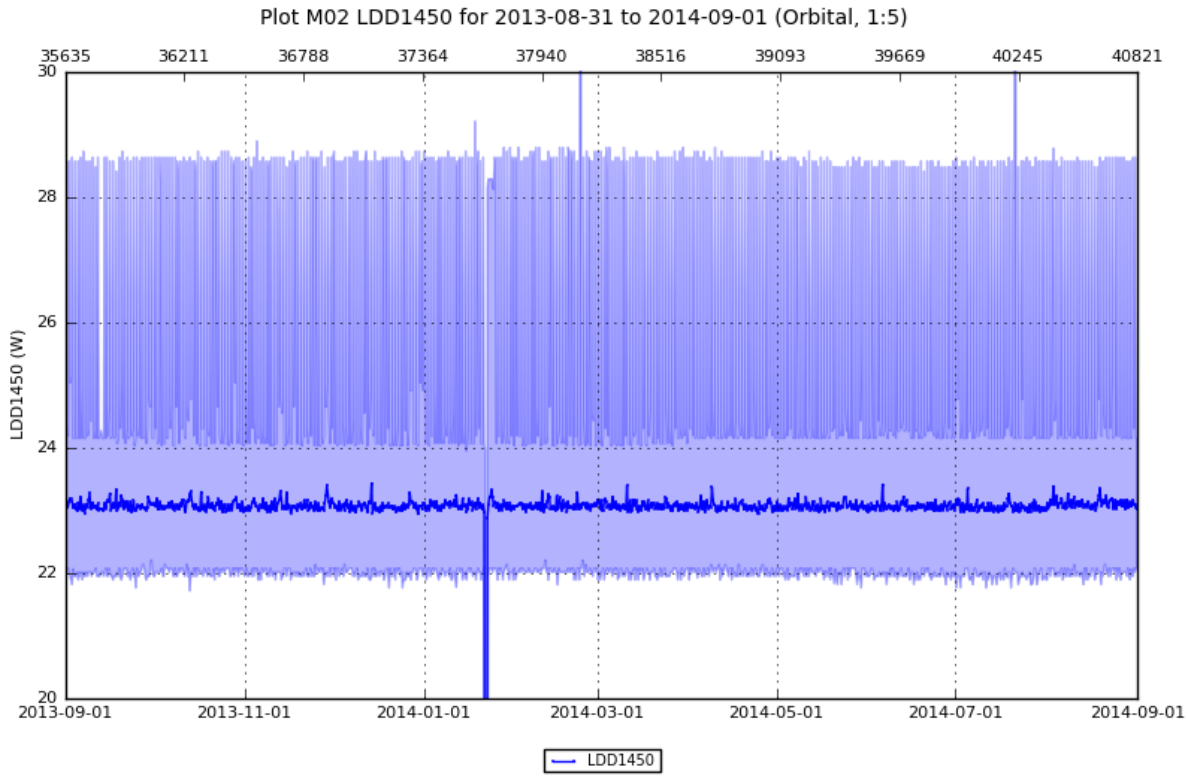

Figure 5-3 GOME EQ Power During the Reporting Period

Figure 5-3 shows that the EQ Power has been relatively stable during the reporting period with the exception of two peaks. The first peak, on 23 Feb 2014, was at the start of the daily SPECTCAL operation and was concluded as being due to sampling of the GPDU inrush current. The second peak was on 21 July 2014, again at the start of the daily SPECTCAL. Neither is considered to be anomalous. Similar peaks have been seen in previous years, associated with the inrush current of the QTH lamp.

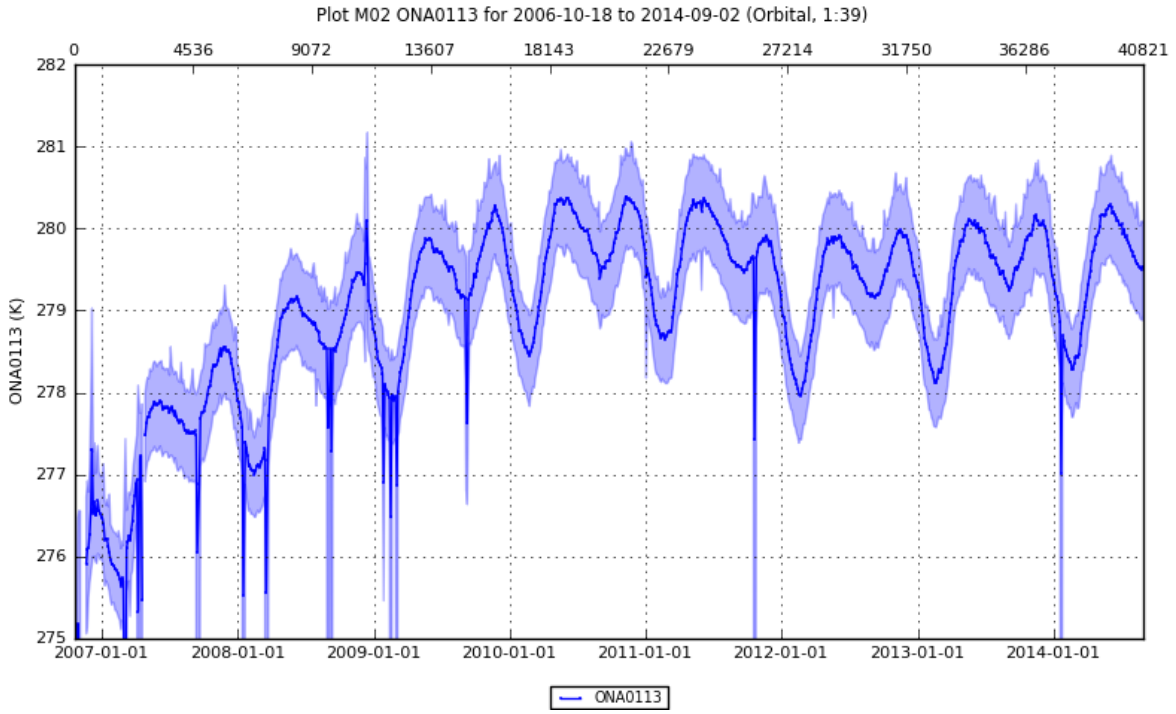

Figure 5-4 GOME Optical Bench Temperature Since Launch

Figure 5-4 shows that the Optical Bench Temperature has been following the expected seasonal trend during the reporting period. All deviations from this trend are explained by known events. The reduction in temperatures since 2011 are due to an increase in solar activity which has raised levels of atomic oxygen which restores reflectivity to the MLI outer layer.

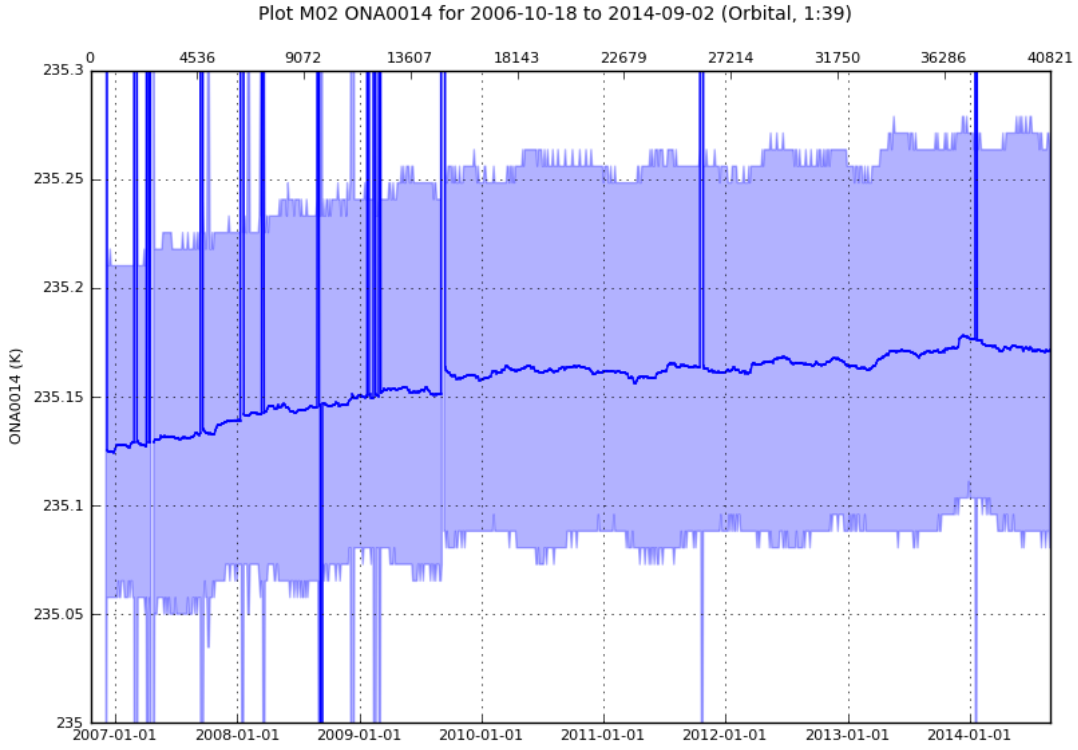

Figure 5-5 GOME FPA Detector Temperatures Since Launch

Figure 5-5 shows FPA 1 detector Temperature 1, which is representative of the other FPA thermistors. From this figure, it can be seen that the temperatures are stable under nominal conditions. All deviations from 235.3 ± 1K are well understood and due to known events.

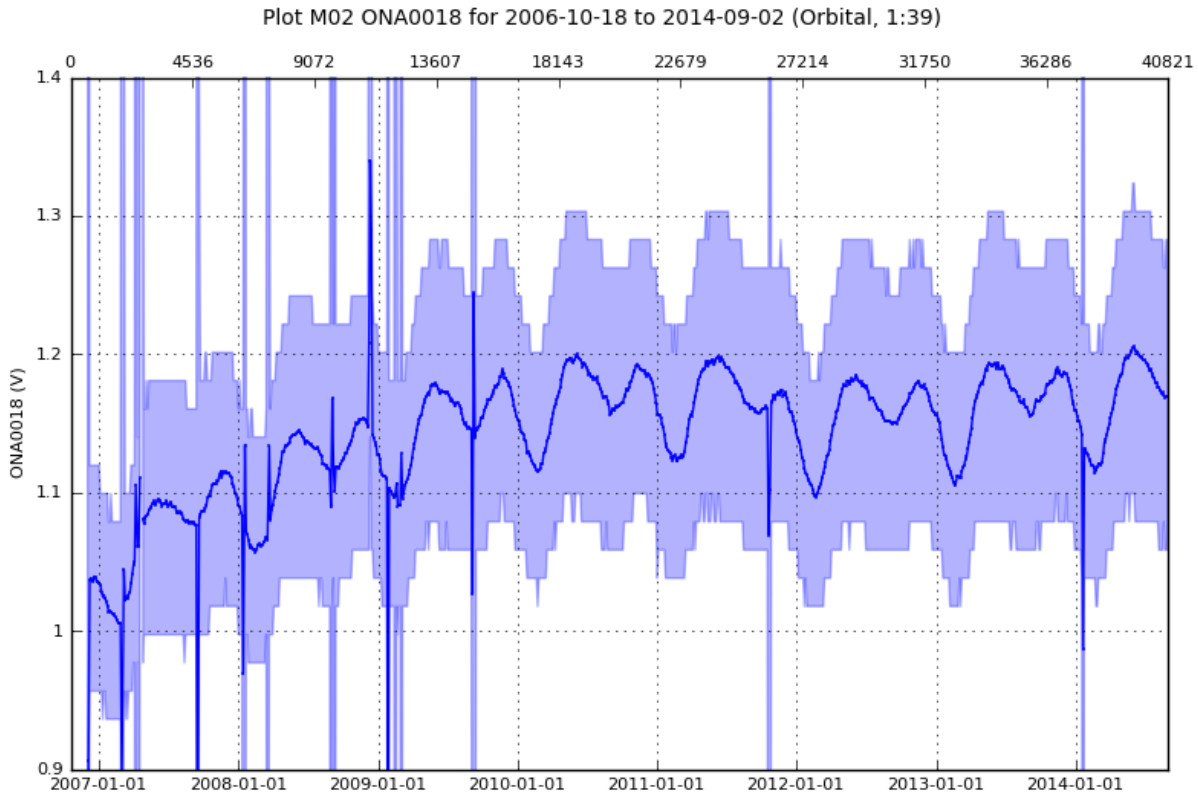

Figure 5-6 GOME FPA Peltier Output Since Launch

Figure 5-6 shows FPA 1 Peltier Output, which is representative of the output of the other FPA Peltier Loops. From this figure, it can be seen that the output is consistent with other GOME temperatures and all deviations are due to well known and understood phenomena.

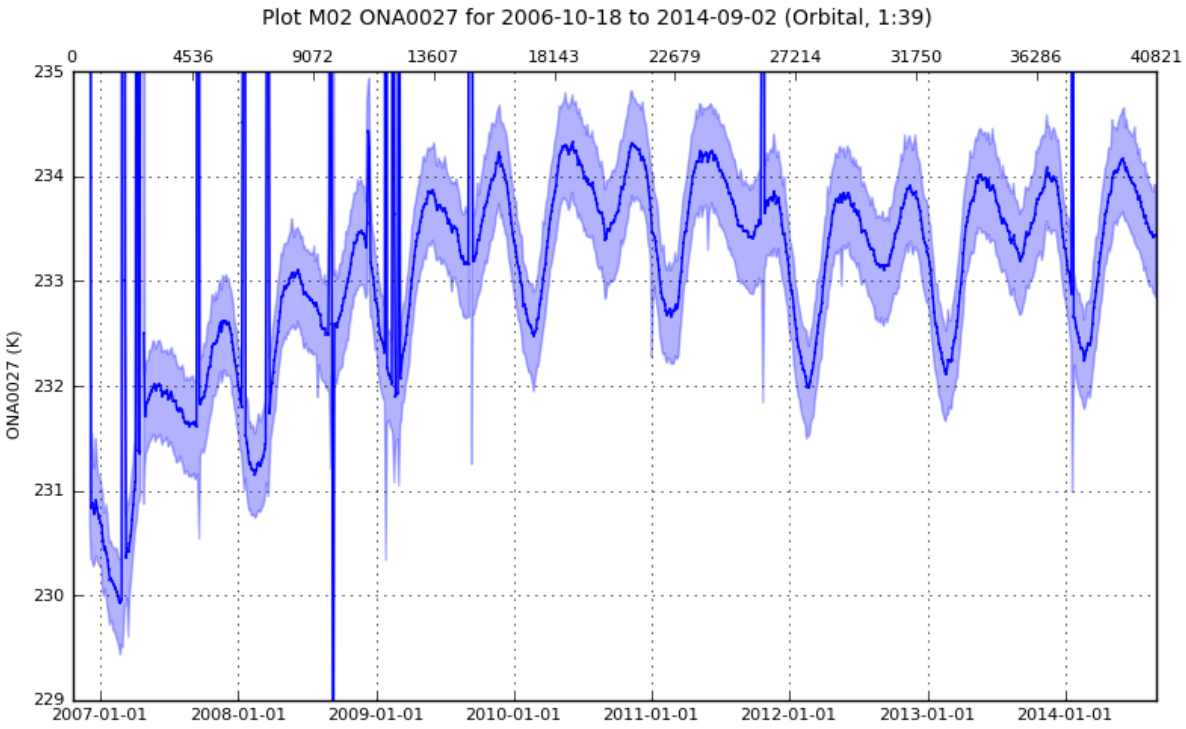

Figure 5-7 GOME PMD-s Temperature since Launch

Figure 5-7 shows PMD-s temperature, which is close to that of the PMD-p temperature. From this figure, it can be seen that the trend is consistent with other GOME temperatures and all deviations are due to well known and understood phenomena.

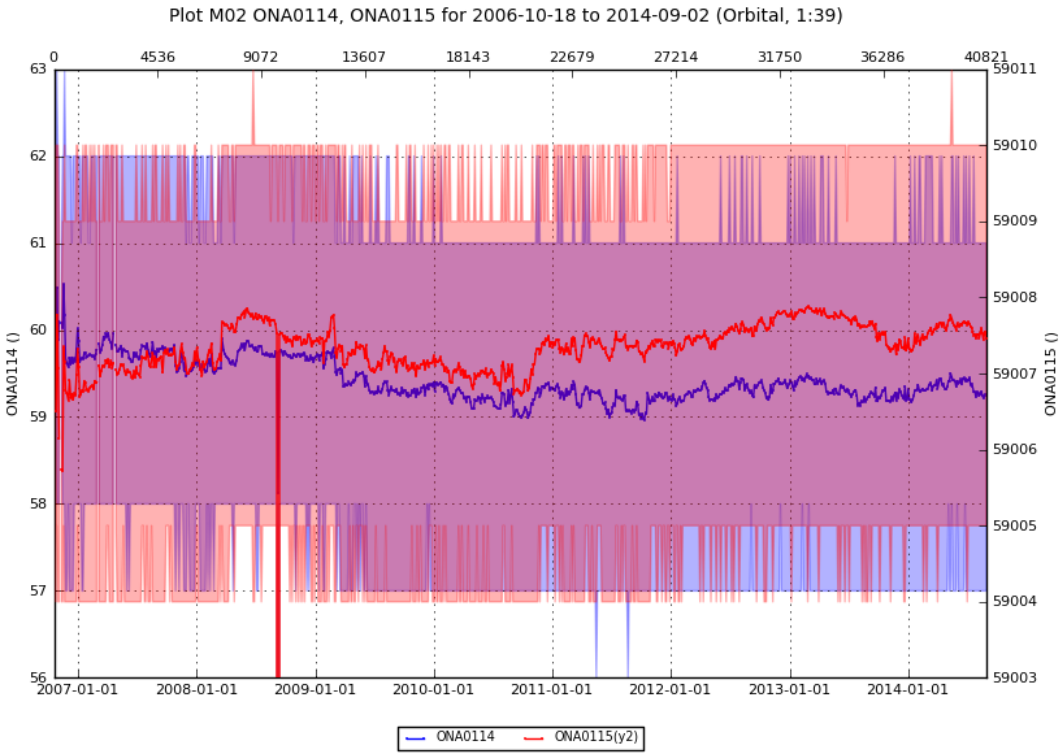

Figure 5-8 GOME Analogue Board Offset (blue) and Gain Value (red) Since Launch

Figure 5-8 shows the Analogue Offset and Gain Value. From this figure, it can be seen that the offset value is stable. The only significant feature is the Scientific Processor Crash due to the incorrect loading of software version 2.6.1 in 2008.

5.3.4 Assessment

All the observed parameters are well within specification range. This clearly shows that the functional performances status of the instrument does not raise any particular concern to date.
Temperatures are behaving in line with those over the satellite as a whole showing seasonal, diurnal and orbital variations. There are no indications of any trends which may limit the lifetime of the instrument within the timeframe of 2018.

5.4 GOM02: SU Bearings Monitoring

5.4.1 Description

During scanning, the GOME Scan Mirror is controlled by means of on-board lookup tables to achieve an Earth Curvature Corrected scan of one of five swath widths. This was nominally 1920 km until the start of Tandem operations on 15 July 2013, when it was changed to 960 km. These lookup tables contain a list of target positions at certain intervals within the scan profile. The Mirror position is measured and control loops calculate the required motor drive current based on the difference between the target and actual mirror positions. The motor drive current is what is actually being measured during torque monitoring.

The Scan Unit bearings and races are lead lubricated. It is known that constant forwards and backwards scanning without making complete rotations can result in this lubricant becoming unevenly distributed along the races. This can lead to large position errors due to accumulation of lead hills on some parts of the races and depletion on other parts of the races. This can ultimately result in the mirror occasionally sticking and even damage to the races and bearings. Permanent failure of the scanning mechanism would result in a loss of the mission, so monitoring the health of the bearings is essential.

This Physical Signature is intended to measure the performance of the GOME Scan Unit in terms of pointing accuracy and the torque required to drive the mirror.

5.4.2 Analysis

The GOME Scan Mirror Torque is telemetered in such a way in Science Data Packets that after 16 complete scans, it is possible to construct a single pseudo 171Hz sampling torque profile. By constructing a torque profile of a scan from near BOL and using this as a reference, it is possible to compare all subsequent scan torque profiles and thus monitor the evolution of the torque profile.

The absolute difference between each point on the torque profile being measured and the reference profile is calculated and averaged over the whole profile. This is repeated for all swath profiles in a day and then the average result determined. Note that scans of different swath widths cannot be meaningfully compared to each other, and are therefore shown in separate plots. The 1920km swath width data is provided for historical completeness, but does not extend into the current reporting period.

By looking at individual torque profiles, it was noticed that the evolution of the torque profile at the extremities of the scan was different to that of the main part of the forward scan and fly-back, so these have been separated as illustrated in Figure 5-9

Scan mirror position is monitored in exactly the same way, although with less temporal resolution since it is only possible to construct position profiles at 10.66 Hz resolution.
To capture the maximum errors in position and torque, the orbital maximum torque is presented; this is assumed to be a spike at one of the scan cycle extremities. For position, the daily maximum deviation from the reference is displayed.

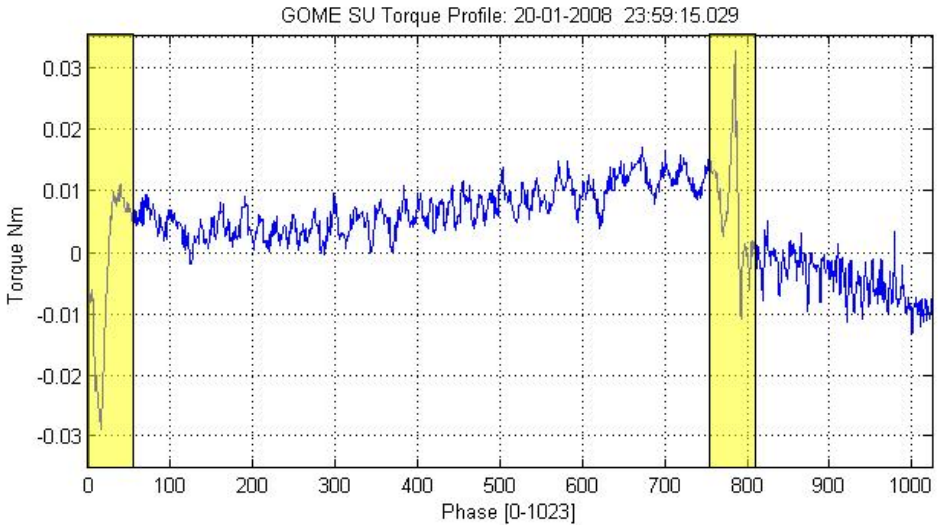

Figure 5-9: Typical GOME SU Torque Profile over a 6s 1920km swath scan cycle. Areas in yellow are considered scan extremities and are assessed separately.

Due to the fact that the Scan Unit mechanism has exhibited a worsening trend in the past for which mitigating action was taken to rectify, a complete history of the evolution is presented here.

5.4.3 Interpretation

Figure 5-10 below shows the position error evolution. The blue line is the average error in position (compared with reference profile) over the entire scan cycle (left axis) and the red line represents the maximum position error (right axis). Both errors are in degrees.

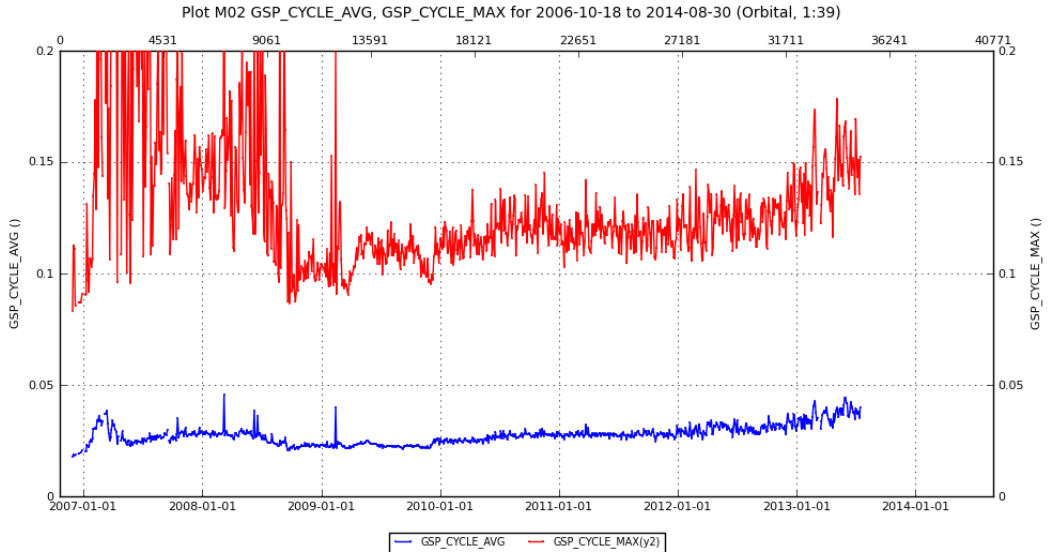

Figure 5-10: GOME SU Position Error Evolution Since Launch (1920km swath width) / °.

From Figure 5-10, it can be seen that the SU position error has been stable since daily spinning started, however a worsening trend was starting to become apparent in the average error over the cycle by the end of 2011. This trend was not apparent in the maximum error over the cycle which was still very stable until mid 2012. Figure 5-11 below shows the average deviation of SU torque from the reference profile over the entire cycle, for the 1920km scan width. It can be seen that there was a clear worsening trend in this plot from 2010. Similarly, Figure 5-12 shows the corresponding plots for the 960km scan width since 2013. No worsening trend is visible in this plot, in which both measures appear to be stable.

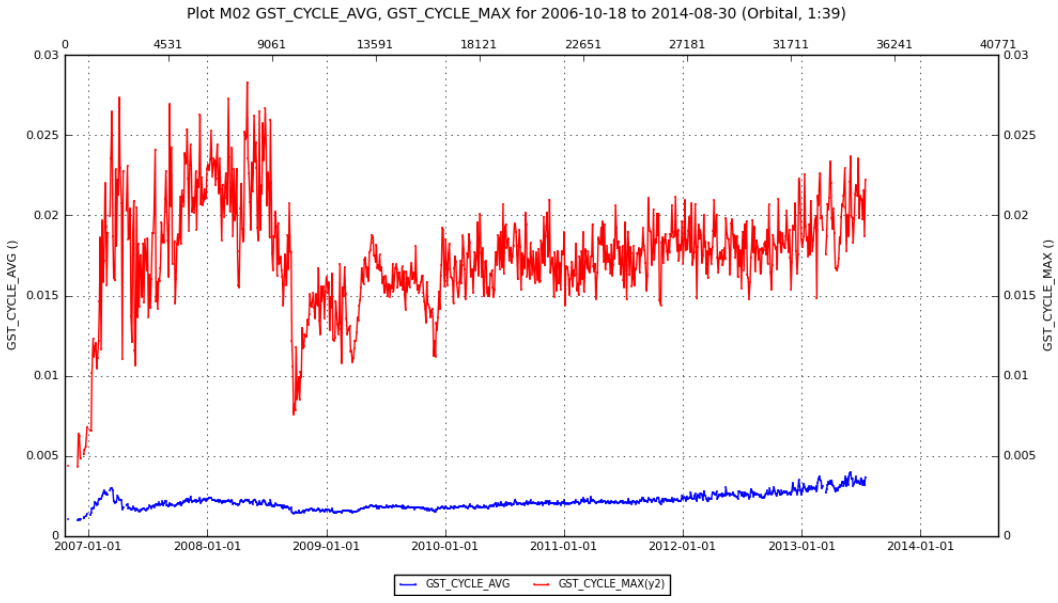

Figure 5-11: GOME SU Torque Evolution – difference from reference profile for 1920 km swath width.

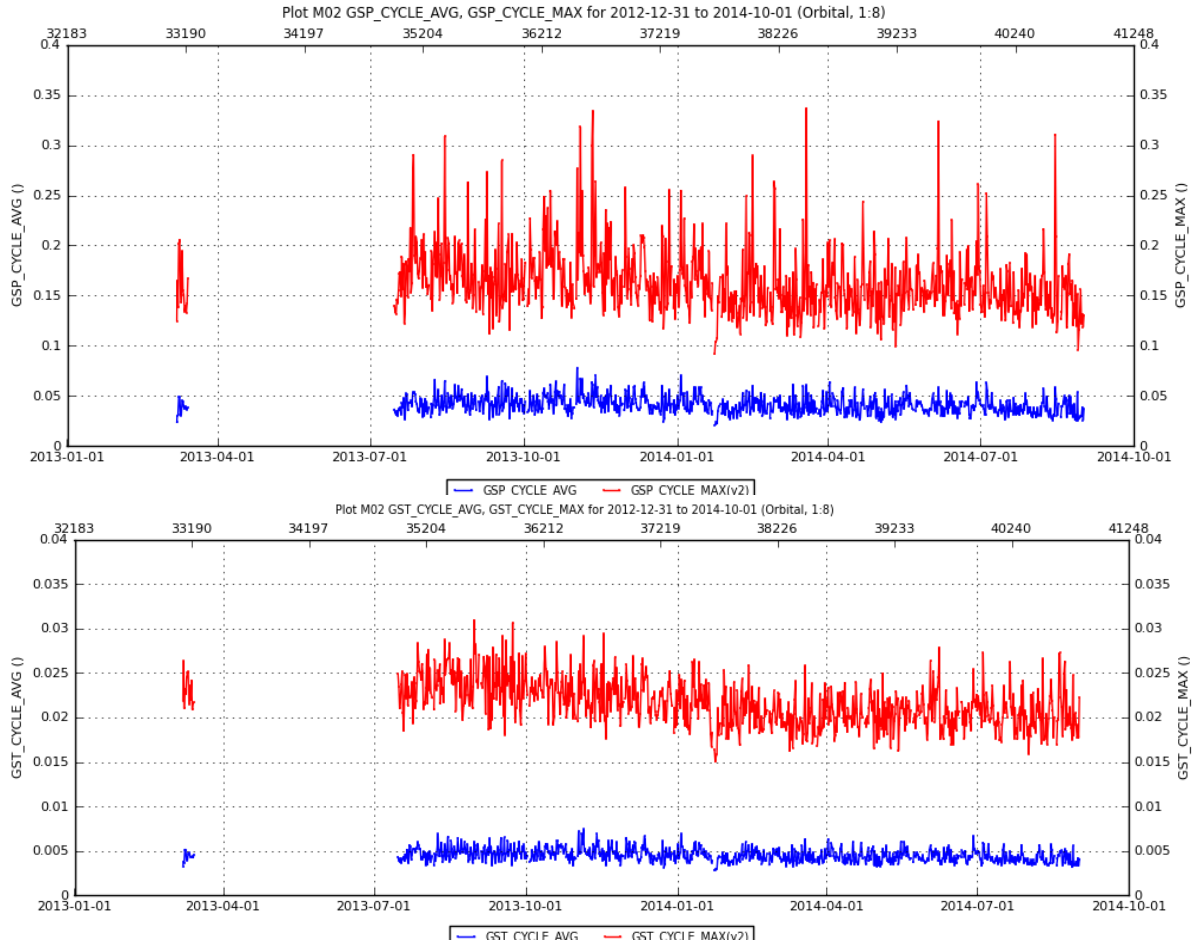

Figure 5-12: GOME SU Evolution - difference from reference profile by position (top) and torque (bottom) for 960km swath width.

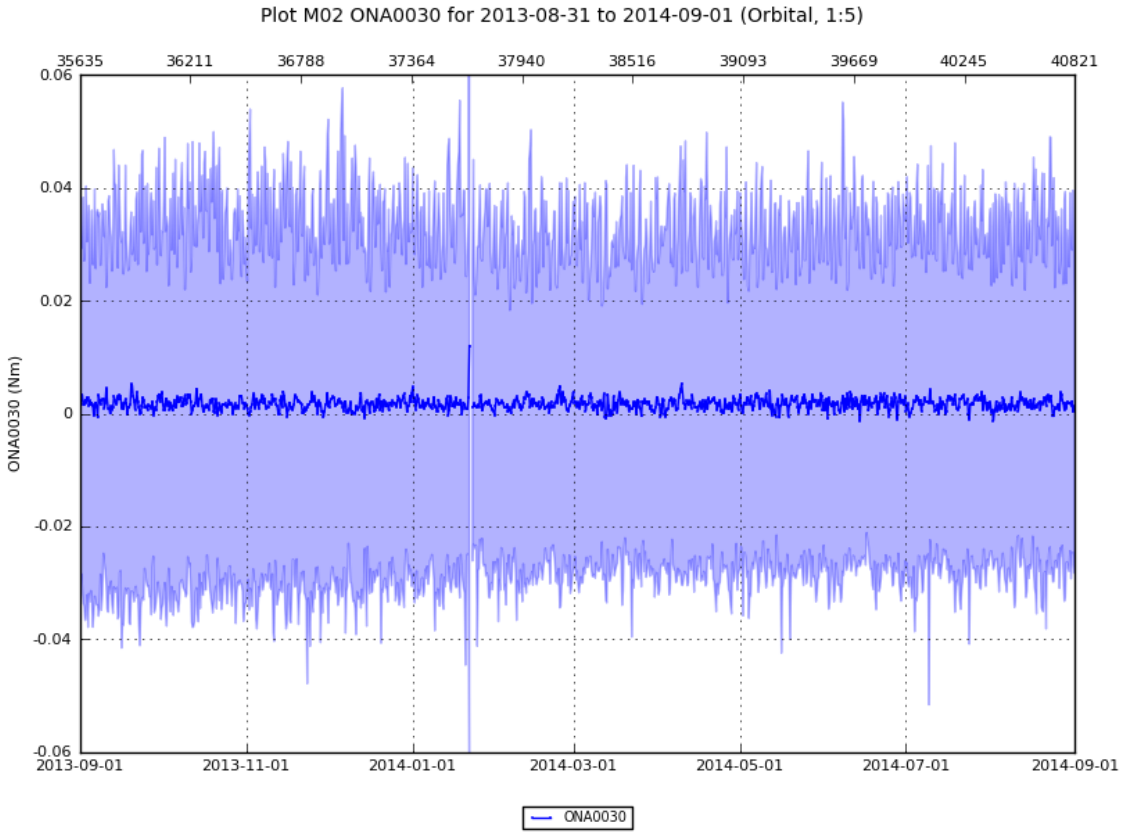

Figure 5-13: GOME SU Torque during reporting period

Figure 5-13 shows the min/max and average SU torque throughout the reporting period (TLM point ONA0030). The spike in Jan 2014 is an artefact of the HDM latchup event.

During the daily spinning activity, it is not uncommon to have one or more values beyond 0.02Nm in either direction. Figure 5-14 tracks the total number of TLM points reported beyond a ±0.02Nm threshold during the start of the daily spin cycle, and Figure 5-15 shows the maximum torque value reported in the same period. These figures show that the maximum torque typically experienced at the start of spinning rose steadily throughout 2012 and levelled off in 2013, corresponding with the increase in deviations from the average torque and position reference profiles above. This was followed by an increase in the number of values breaching the 20mNm threshold during 2013. The max values stabilised in July 2014, around the time the scan swath was reduced to 960km, and the count of high values dropped at the same time. The start of Tandem operations, which reduced the nominal scan width, is denoted in both graphs by a vertical line.

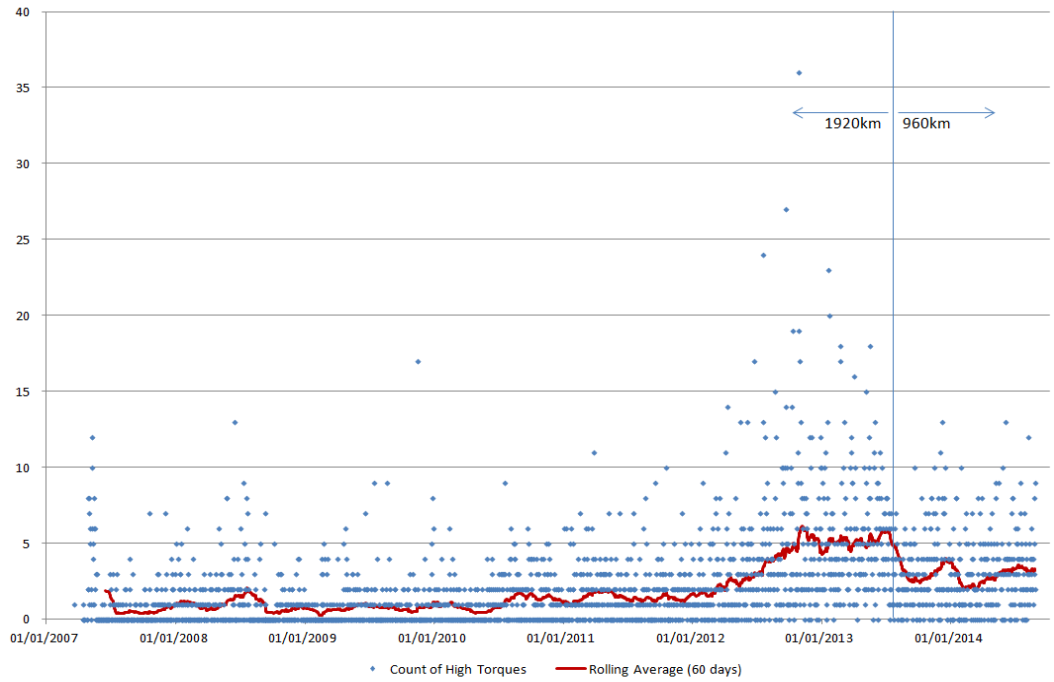

Figure 5-14: Count of GOME SU Torque values >20mNm at the start of daily spinning.

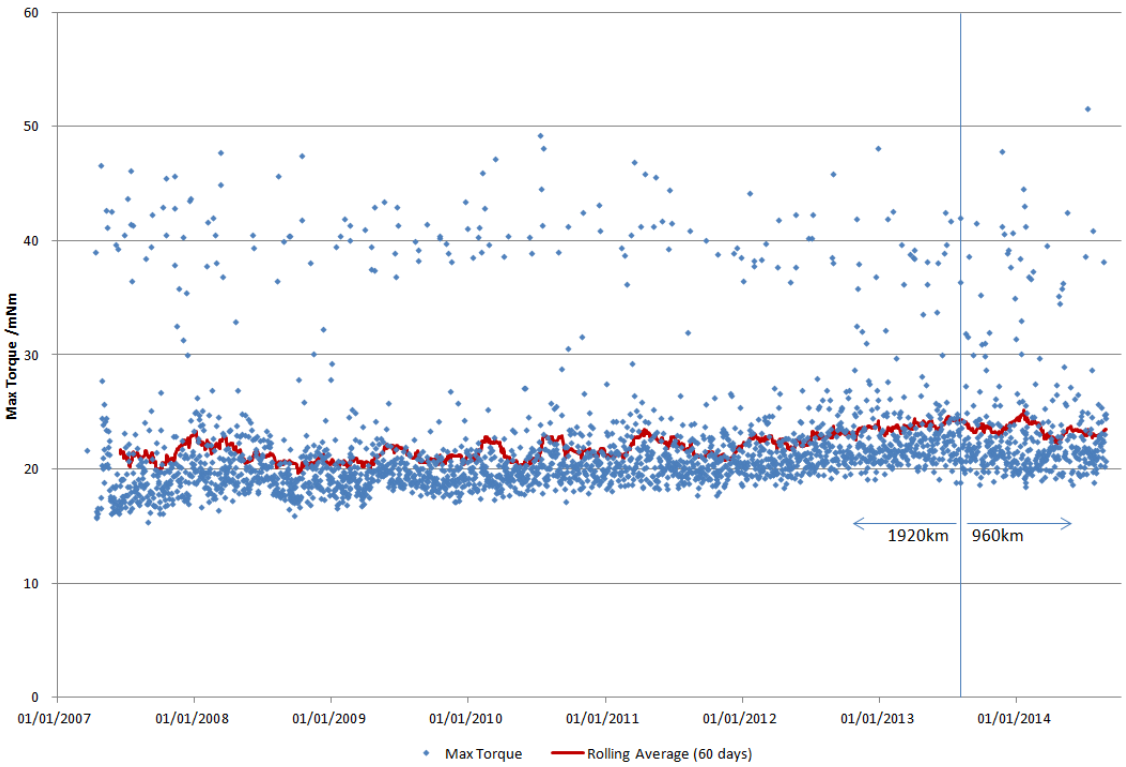

Figure 5-15: Maximum Torque reported at the start of daily spinning activities /mNm.

It has also been noted that of the seven scenarios in which the mirror is stationary (DarkCal, SpectCal, SunCal, RadCal, manoevre/launch, TML start & MoonCal), only RadCal shows torque values ~0 as might be expected (AR15517). The most significant of these is the TML start position, which contributed to AR15102. An investigation to explain the mechanism behind this behaviour is ongoing.

5.4.4 Assessment

From the attached plots, it can be seen that the regular daily spinning implemented in reaction to AR.7446 has had a beneficial effect on the noise in the position and torque. Since regular spinning, the noises in the torque and position profiles have followed similar patterns.

In both cases, the profiles during the main part of the scan and flyback have been reasonably stable. There is still plenty of torque margin and the Line of Sight Requirement of +/-0.0645 degrees is only breached at the turn-around points. There is plenty of margin for the main part of the profile, however the trend needs to be closely monitored as it may be very non-linear.

It is assumed that the high values at the start of the daily spinning activity are caused by the intentional redistribution of lubricant which has built up at the extremes of the mirror's nominal scan swath. It would thus be a logical prediction that reducing the scan swath should have lead to a reduction in this buildup. An investigation is ongoing, but the results presented here are in line with this prediction.ESA tribology experts will perform a deeper analysis of these results to determine whether it is possible to make any predictions on evolution or recommend a different spinning strategy.

5.5 GOM03: HCL and QTH Lamps Monitoring

5.5.1 Description

The HCL lamp can be monitored for changes in ignition time by taking the difference between the time at which the voltage ramp begins and the time that current begins to flow for each lamp ignition. During each lamp ignition, the voltage profile can also be monitored to look for signs of unusual behaviour. The throughput as monitored by HCL lamp measurements when compared to SMR measurements can also act as an indicator of lamp health.

QTH Lamp voltage monitoring can show signs of filament thinning. Also, throughput of the lamp compared to that of SMR can reveal blackening of the QTH bulb wall. The function of the halogen is to set up a reversible chemical reaction with the tungsten evaporating from the filament. In ordinary incandescent lamps, this tungsten is mostly deposited on the bulb. The tungsten-halogen cycle keeps the bulb clean and the light output constant throughout life. At moderate temperatures the halogen reacts with the evaporating tungsten, the halide formed being moved around in the inert gas filling. At some time, it will reach higher temperature regions, where it dissociates, releasing tungsten and freeing the halogen to repeat the process. In order for the reaction to operate, the overall bulb temperature must be high. Blackening, or a loss of throughput measured by the QTH Lamp can indicate that the bulb wall is not reaching a high enough temperature and that the tungsten-halogen mix is condensing on the bulb wall.

5.5.2 Analysis

HCL Ignition time is monitored using telemetry from science data packets. For each HCL ignition, the time difference between the leading edge of the voltage ramp and the flow of current is noted. Since HCL voltage and current are sampled at 375 ms rate, and the measured ignition time is on the order of a second. HCL Running voltage is monitored by plotting the voltage over a narrow range to highlight differences in each ignition. This can also be correlated to the lamp throughput. For the QTH lamp, throughput monitoring can be used to look for signs of lamp blackening. Also, voltage can be monitored as a sign of filament thinning.

5.5.3 Interpretation

5.5.3.1 HCL / Spectral Lamp

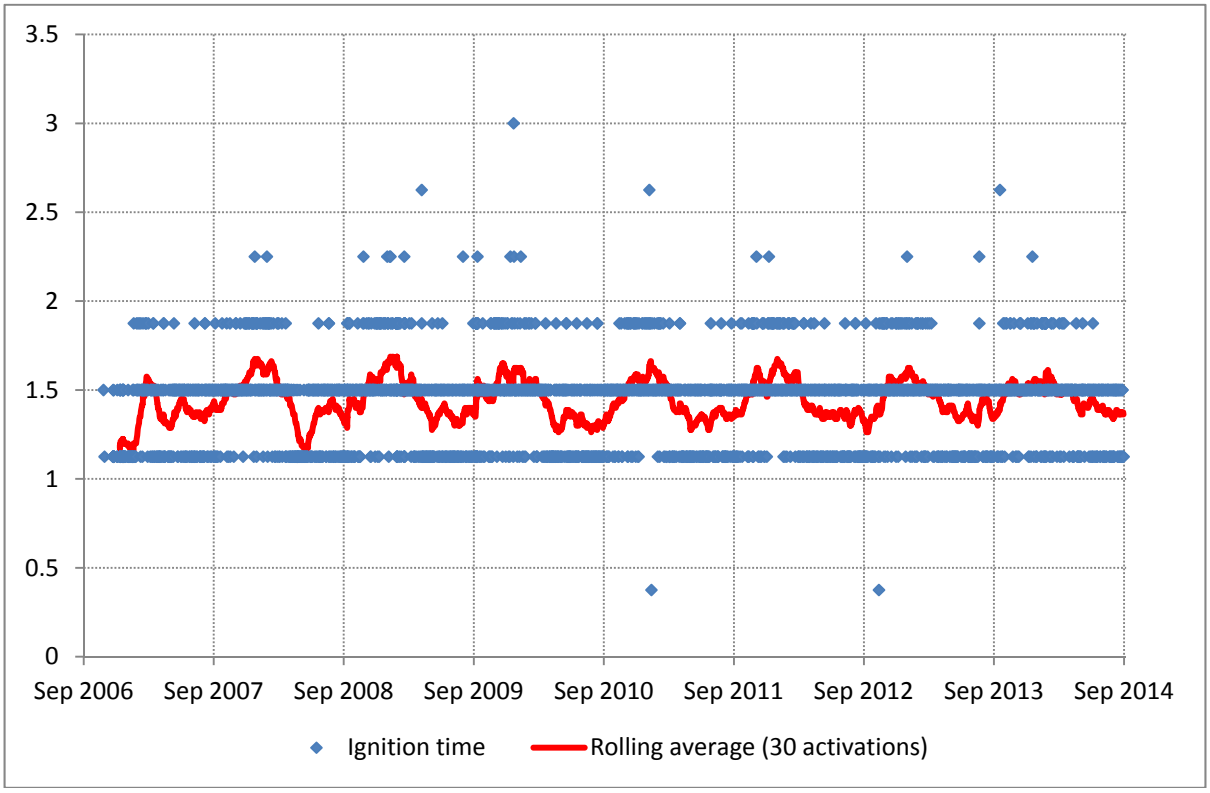

Figure 5-16: GOME HCL Ignition Time

As shown in Figure 5-16, it can be seen that the HCL Ignition time appears to follow a cyclic trend, matching the temperature of the instrument.

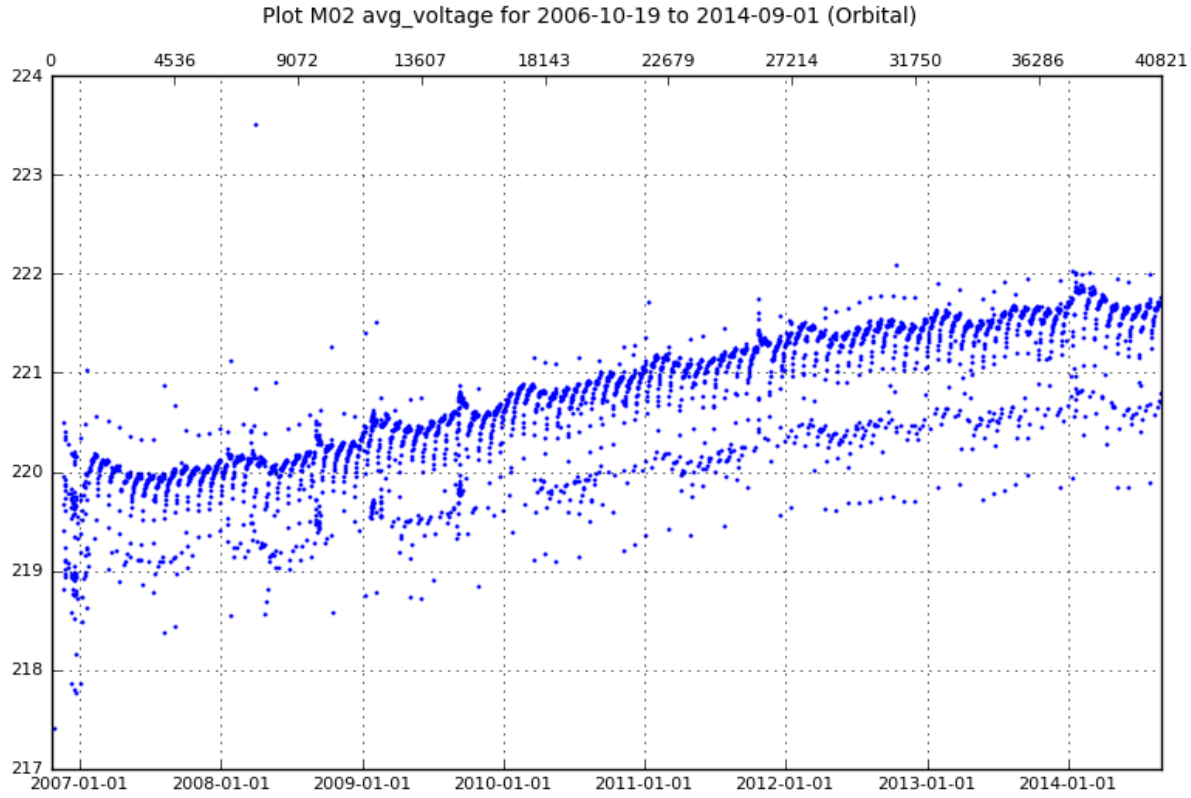

Figure 5-17: GOME HCL Voltages

The 29-day cycle is apparent in the HCL Voltage which is caused by the long DIFCAL (HCL Lamp over diffuser) during the CAL5 timeline.

Figure 5-18 also highlights the 29 day cycle in HCL Lamp throughput. This does not cause a problem for the quality of the spectral calibration. However, it does raise some concerns about the quality of the SLS over Diffuser measurements (DIFCAL) used to measure throughput loss of the diffuser. From Figure 5-17 and Figure 5-18, there appears to be some relationship between HCL Voltage and HCL output, however the correlation is too weak to be isolated analytically.

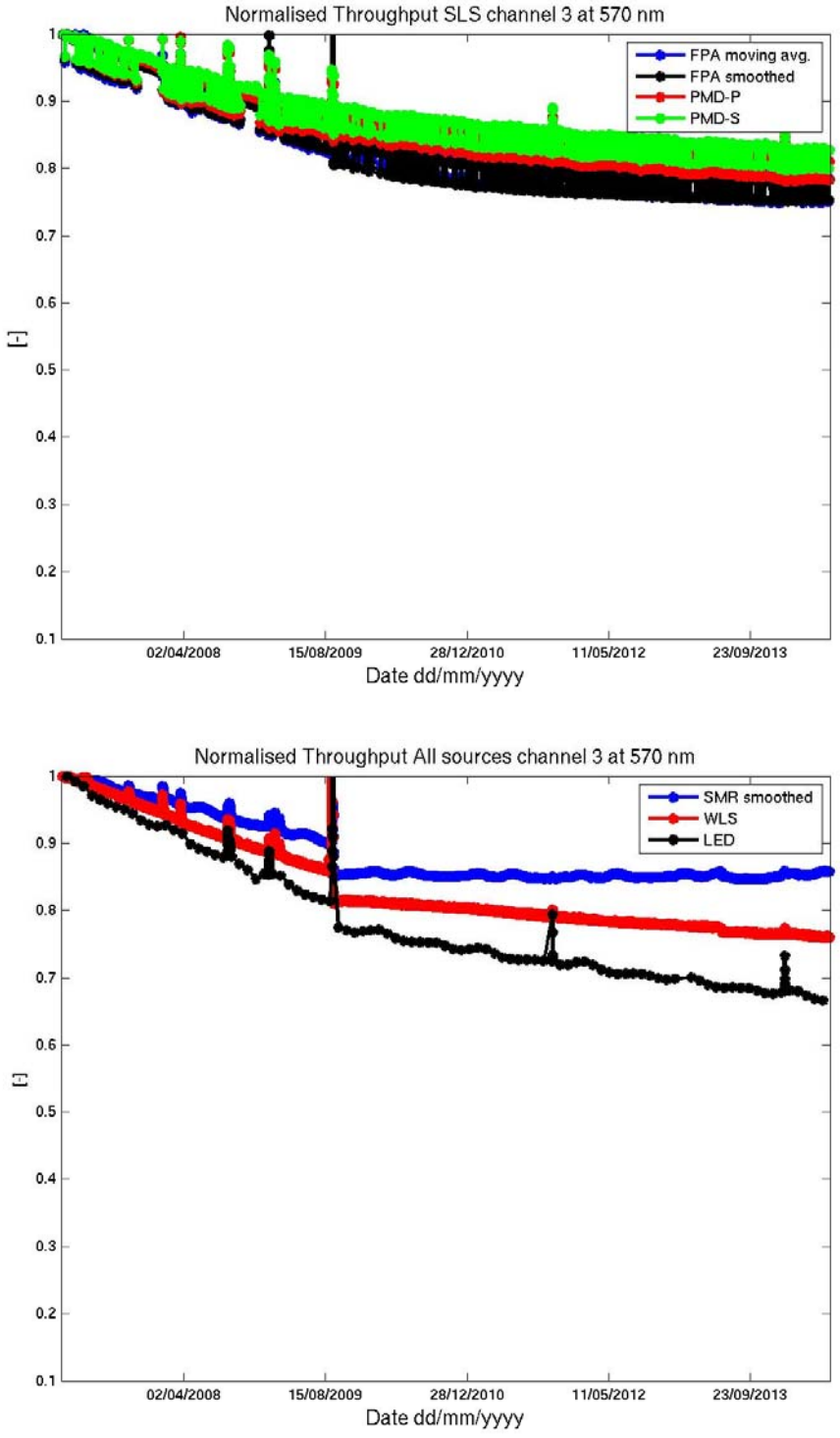

Figure 5-18: Upper panel: Change in instrument throughput around 570 nm for SLS. The SLS signal is smoothed with the spectral response function of PMDs in black and with a moving average in blue for main channel data. SLS data for PMD P and S are plotted in red and green respectively. Lower panel: Same as upper panel but for SMR, WLS and LED and for main channel data.

Ground analysis confirms these observations and also that this instability of the Spectral Lamp voltage can increase or decrease the signal strength of different lines. This means that the DIFCAL can only be used to monitor the diffuser with careful use of the HCL Lamp.

In order to be able to use the DIFCAL effectively, timelines would have to be updated to provide SLS, SLS over Diffuser, SLS, SLS over Diffuser in one single eclipse.

5.5.3.2 WLS / QTH Lamp

Figure 5-19 shows a continuing increase in the QTH Voltage during operation. This is due to a thinning of the filament. The small clustering of points with a slightly lower voltage in Jan 2014 were a part of the recovery operations immediately following the HDM latchup anomaly; all activations prior to the toggling of the DALE resistor to open and switching PMD cooler to FLIGHT line are approx 0.01V lower than the nominal series.

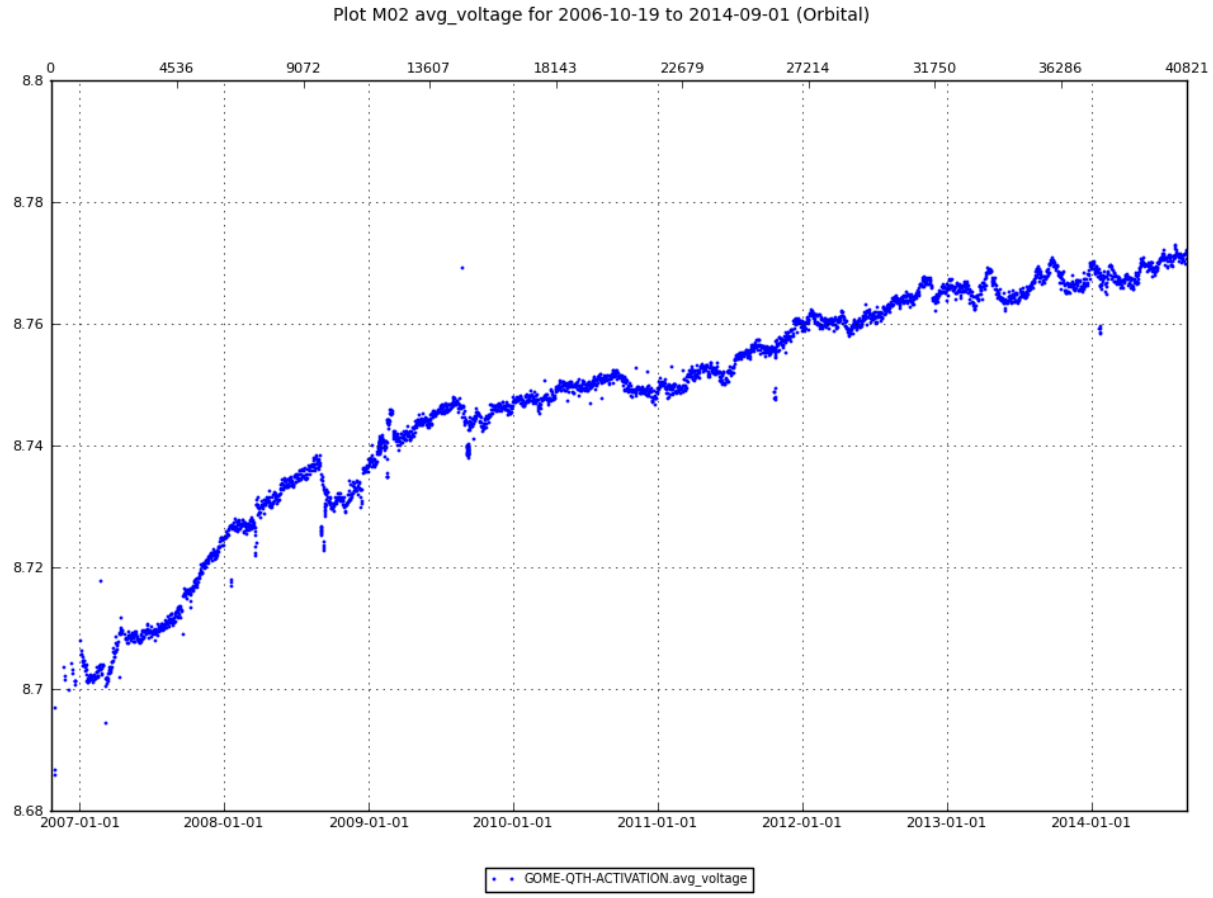

Figure 5-19 GOME QTH Voltage since launch

Figure 5-18 also shows throughput at 570 nm (Channel 3), normalised to 28 Jan 2007. This is approximately the wavelength of light emitted by the LEDs, so puts all sources on a level playing field. From Figure 5-18, it can be seen that throughput as measured by the QTH Lamp is falling more rapidly than that of the SMR measurements, implying there is some lamp blackening. However, for a full picture all wavelengths should be considered.

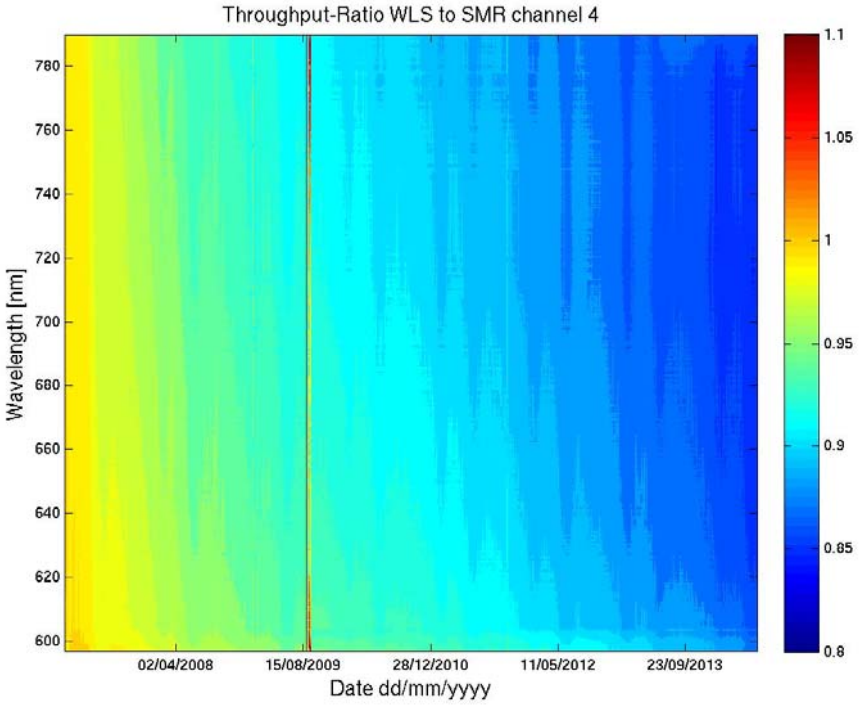
Throughput-Ratio WLS to SMR channel 4
Wavelength [nm]
780
760
740
720
700
680
660
640
620
600
02/04/2008
15/08/2009
28/12/2010
11/05/2012
23/09/2013
Date dd/mm/yyyy
1.1
1.05
1
0.95
0.9
0.85
0.8

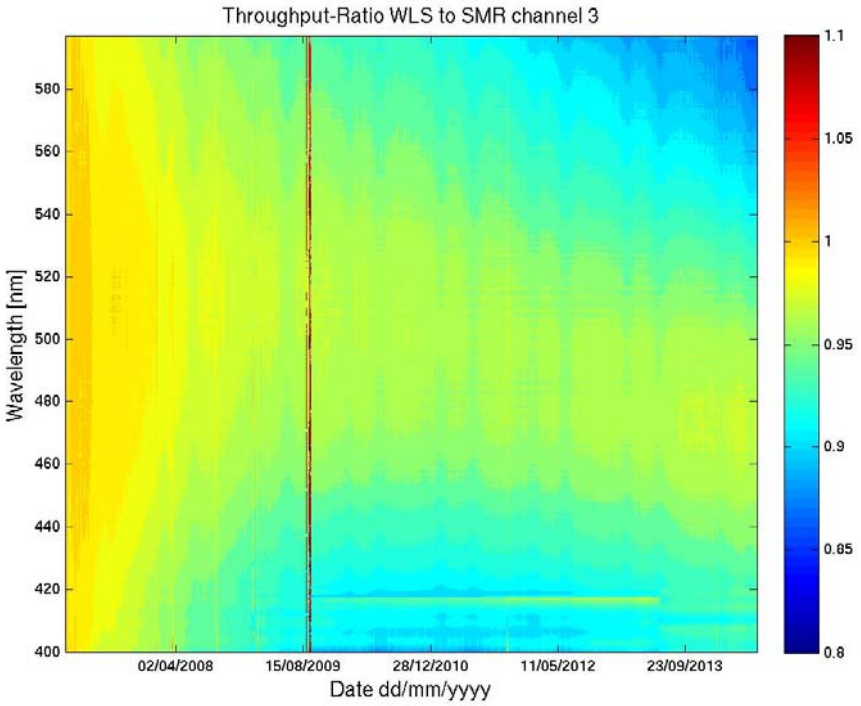
Throughput-Ratio WLS to SMR channel 3
Wavelength [nm]
580
560
540
520
500
480
460
440
420
400
02/04/2008
15/08/2009
28/12/2010
11/05/2012
23/09/2013
Date dd/mm/yyyy
1.1
1.05
1
0.95
0.9
0.85
0.8

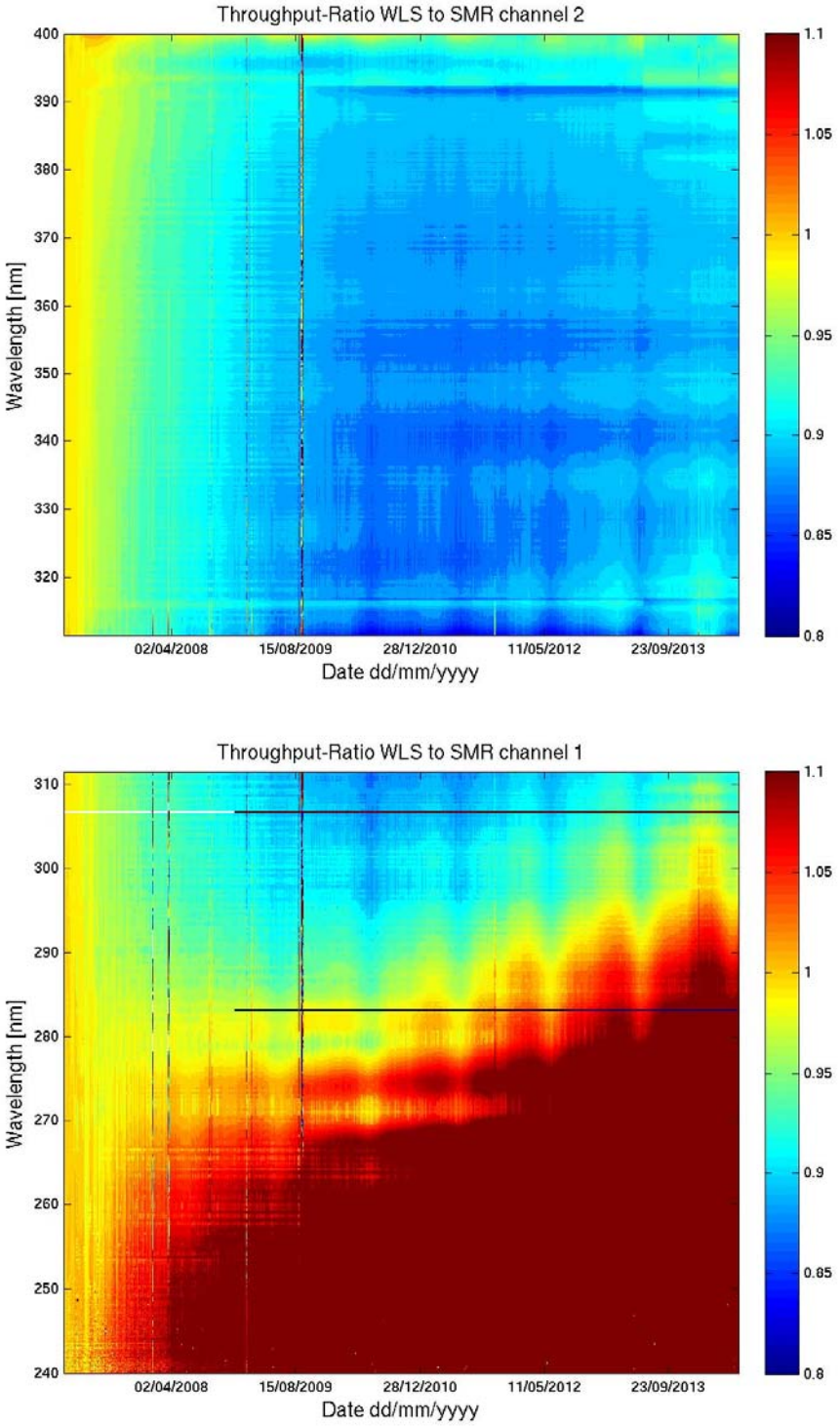

Figure 5-20: GOME WLS to SMR ratio normalised to January 2007 for all Main Channels.

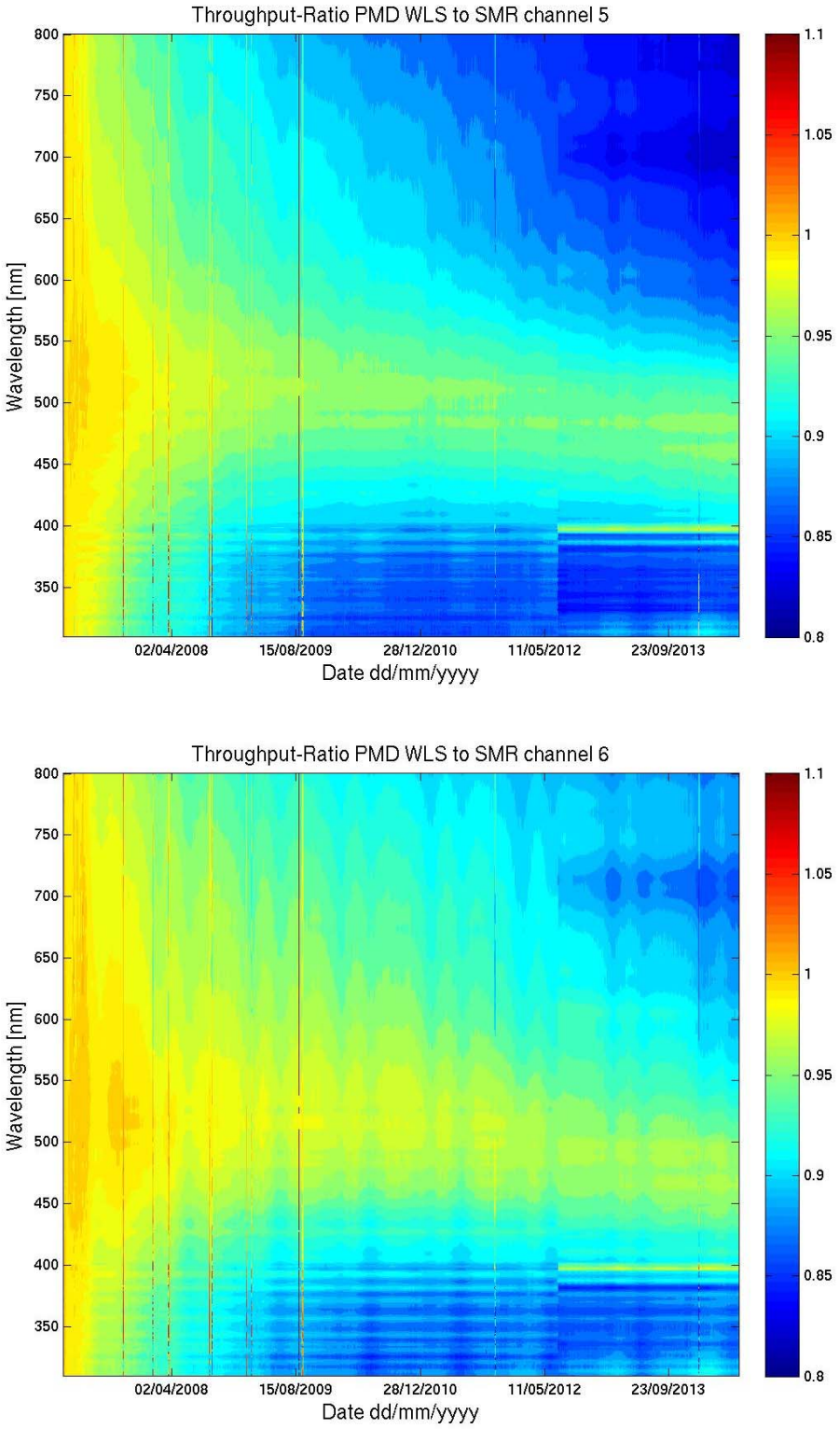

Figure 5-21: GOME WLS v SMR Throughput for PMD Channels (Upper pane PMD-P, lower panel PMD-S).

From Figure 5-20 and Figure 5-21, it can be seen that there is a strong wavelength dependency for the WLS v SMR throughput. In the wavelength range 300-400 nm and 700 + nm, the throughput as measured by WLS is as much as 15% lower than that of SMR at an increasing rate. The throughput loss is similar only in the region of 500 nm. In the UV (below 290 nm) the output levels of the WLS are too low with respect to the solar measurements to provide reliable results.

The extra loss of throughput as measured by the QTH Lamp could either be due to some mirror angle / wavelength cross coupling if the source of the throughput loss is the scan mirror surface. However, since the WLS throughput has fallen at the same rate as SMR or quicker (depending on wavelength) it is more likely that the absorption spectra of the tungsten-halide soot is being observed.

The QTH test was performed in August 2009 without conclusive results – i.e. there was no increase in throughput. It is now understood that the OMI QTH lamp is operated at 408mA and powered at a higher voltage, consuming 5.32W, much higher than can be achieved on GOME-2.

Signal degradation in itself is not an issue for the instrument since an etalon correction can still be produced in the UV. If the SNR gets too low, options are to increase the integration times or run the lamp at 380mA, however these will only be revisited if and when needed. Health of the QTH lamp is also confirmed by the Life limited item usage and the very small voltage increase (caused by filament thinning)

5.5.4 Assessment

From analysis of this physical signature, both Lamps appear to be healthy. The HCL ignition time appears to be related to temperature and does not exhibit any additional trend over and above this. There are also no further signs of unusual ignition behaviour as observed in AR.9559.

The HCL Voltage and output instability mean that measurements of the diffuser throughput stability are “noisy” and can only be meaningfully interpreted after a couple of years. For details, see Section 5.8.3.

The throughput of the QTH Lamp does appear to be falling faster than that of SMR measurements, indicating Lamp Blackening which is confirmed by the increasing lamp voltage during operation and OMI experience. A lamp cleaning test was unsuccessful, so this situation can only be monitored for further degradation. The extent of blackening which is currently evident is not believed to be a concern for lamp life and in the worst case scenario, longer integration times can be used for Radiometric calibrations.

5.6 GOM04: Detector response stability

5.6.1 Description

LEDs can be used to monitor Pixel to Pixel gain which is used to correct for the pixel to pixel variation of quantum efficiency of the detectors, as well as for identification of hot or dead pixels. Pixel to Pixel gain is measured by using the LEDs mounted directly in front of each detector.

5.6.2 List of Correlated Events

N/A

5.6.3 Analysis

LEDs illuminate the detectors uniformly with green light (ca 550 nm). By comparing the LED measurements with an LED spectrum smoothed over ~5 pixels, an estimate of the pixel-to-pixel gain can be made. By monitoring changes in pixel-to-pixel gain changes in the relative behaviour of the quantum efficiency of the detectors can be observed. This is a result must be fed back into other throughput monitoring so that relative changes in pixel performance do not appear as pixel dependent signatures.

5.6.4 Interpretation

From Figure 5-22, the time series of the Pixel to Pixel gain (PPG) standard deviation of the PPG averaged signal over the channel for both the FPA and PMD detectors remain fairly constant in all main channels and well within expectations. There is only a small increase visible over the whole time of the mission, which is on the order of 10^{-5} BU.

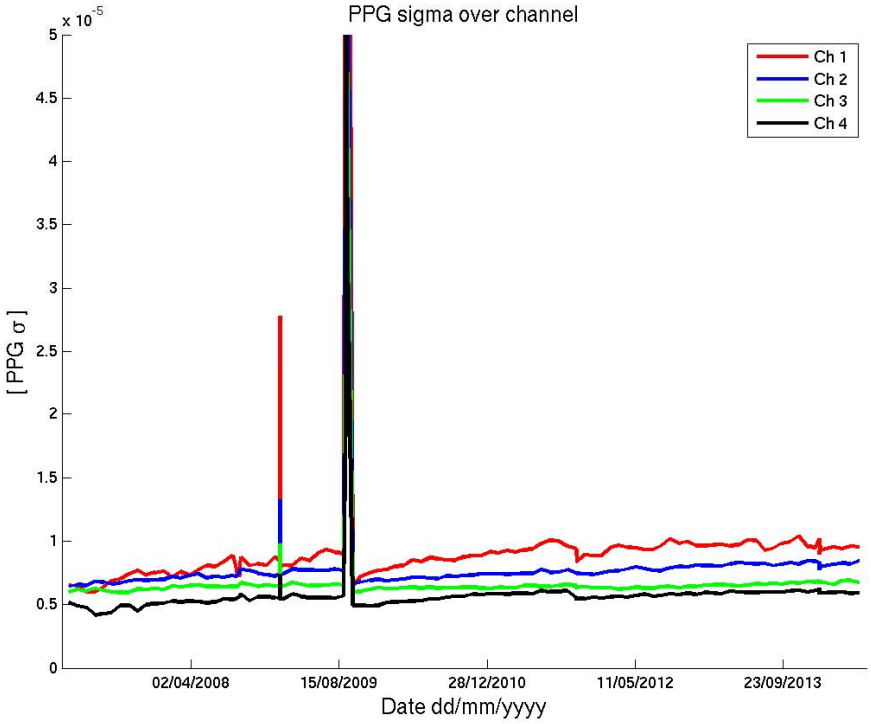

Figure 5-22: Time series of of the channel average standard deviation of the PPG correction in all four main channels (red: channel 1, blue: channel 2, green: channel 3, yellow: channel 4)

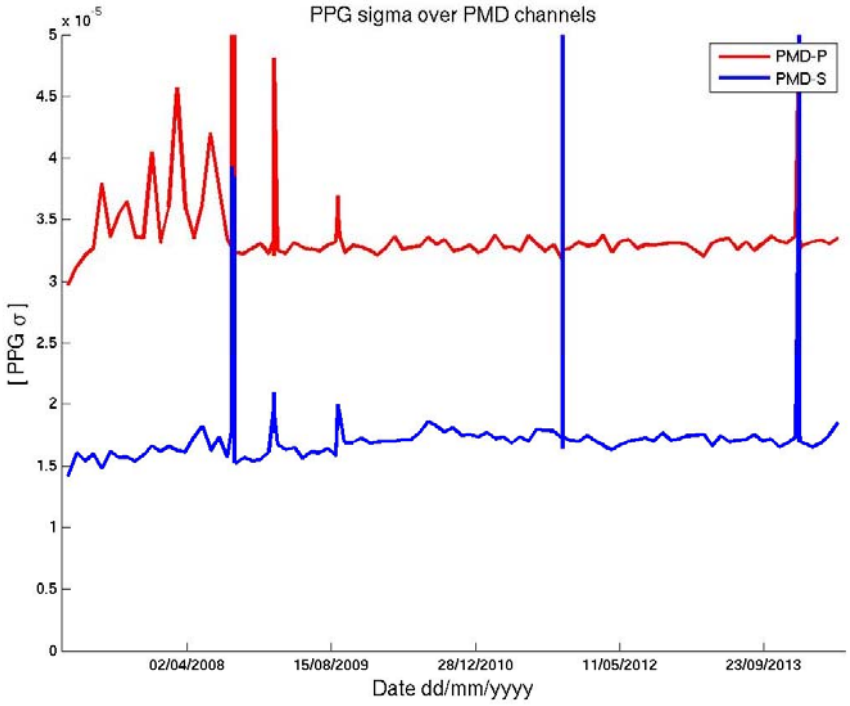

Figure 5-23: Time series of the channel average standard deviation of the PPG correction for PMD channels (red: PMD-P, blue: PMD-S)

5.6.5 Assessment

The pixel to pixel gain appears to be quite stable in all channels. (The impact of degradation is only slightly different for LED in all 6 channels). Vertical lines in the plots are the results of non-nominal operations conditions like PMD band setting and FPA detector throughput tests.

5.7 GOM05: Spectral Stability

5.7.1 Description

SLS measurements are primarily used for pixel to wavelength mapping and also to monitor the spectral stability of the instrument which is important for the maintenance of product quality. The strength of the measured SLS lines is also an important result that must be used in the throughput monitoring. When the intensity of individual lines falls below specified thresholds they are no longer deemed reliable for use in spectral calibration. SLS measurements are made daily and the positions of spectral lines on the detectors are monitored.

5.7.2 List of Correlated Events

ID	*Date*	*Description*	*Justification*
G2	2008-09-02		GOME Off for OBSWM
G3	2008-09-10		GOME Off for OBSWM + SCI Proc Crash (Analogue TLM to 0x0000)
G4	2008-12-10		Update of FPA Band + Dale Resistor Relay left closed
G5	2009-01-27		GOME Throughput Test
G7	2009-02-16		GOME EQSOL/Suspend (AR.10874
G8	2009-03-03		GOME Off for OBSWM
G9	2011-10-24	PL-SOL #6	GOME off due to PLSOL

Table 5-2: List of Correlated Events

5.7.3 Analysis

The following plots show the results derived from maximum spectral line signals and daily spectral calibrations at various wavelengths. The wavelength that is being measured by a particular pixel is calculated and that trend is displayed throughout the reporting period. The wavelength range covered per pixel is given in Figure 5-3 below.

Channel	*1*	*1*	*2*	*2*	*3*	*4*	*5/6*
Band	1A	1B	2A	2B	3	4	PMD P/S
Used Pixels	877/659[1]	147/365[2]	71	953	1024	1024	256
Spectral Range (nm)	240-307/283[2]	307/283-315[2]	290-300	300-412	401-600	590-790	290-790
nm/pixel	0.07	0.07	0.09	0.09	0.2	0.2	2
Predefined dark signal electronic offset (BU)	1501	1501	1503	1503	1495	1492	1503/1499

Table 5-3 GOME Wavelength Range per Pixel for all main channels

[1] Changed settings at 10 December 2008.

5.7.4 Interpretation

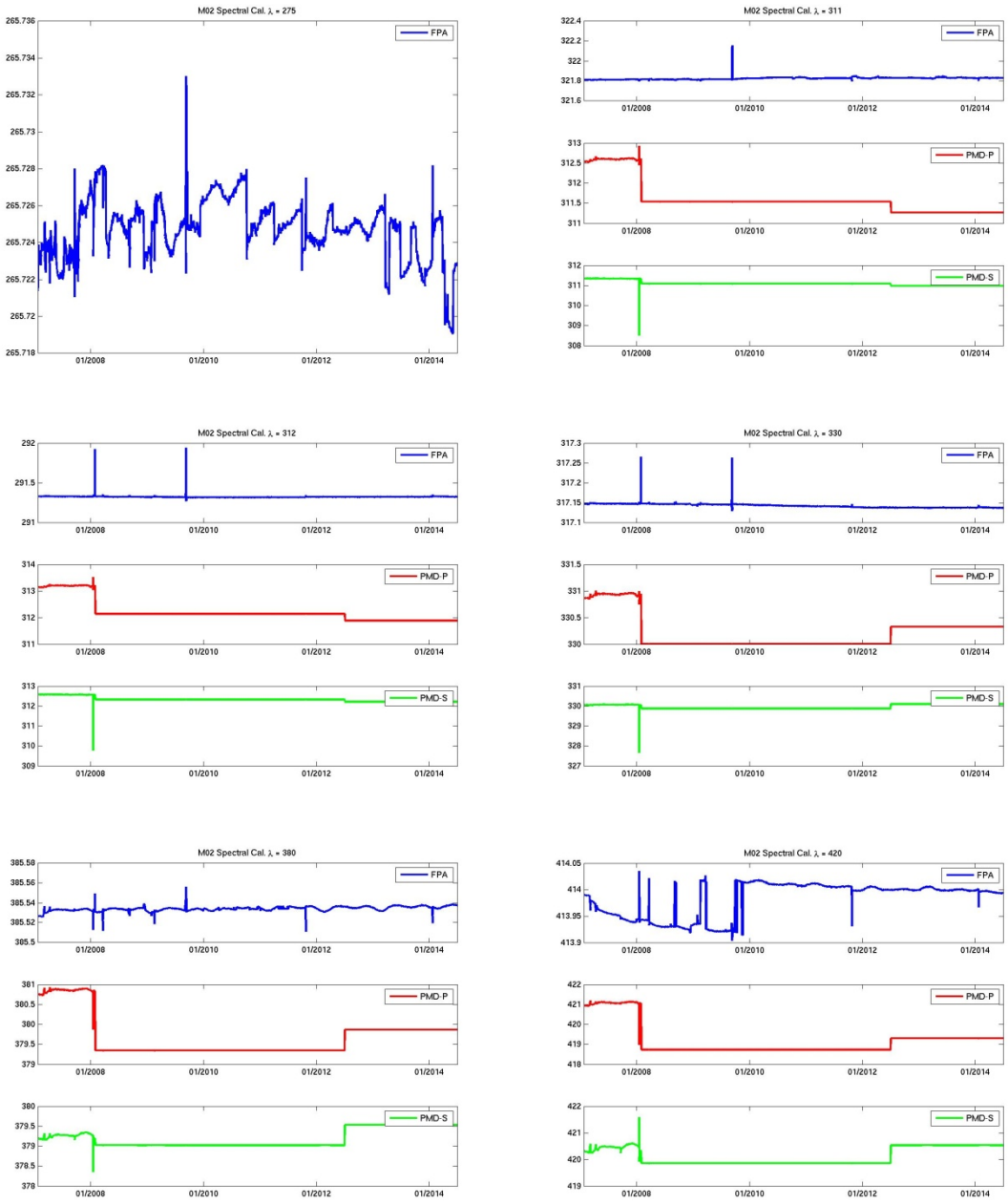

Figure 5-24: Spectral stability at various wavelengths between January 2007 and July 2014 and for main channels and PMD channels at 275, 311, 312, 330, 380 and 420 nm. The first step function is due to the on-board up-load of PMD band definitions 3.1 from the original pre-launch settings (1.0). The step function in PMD wavelentgh calibration is due to the adoption of the further improvedcross-corelation fitting windows as provided with FM3 re-analyzed key-data by TNO and implemented at 3 July 2012.

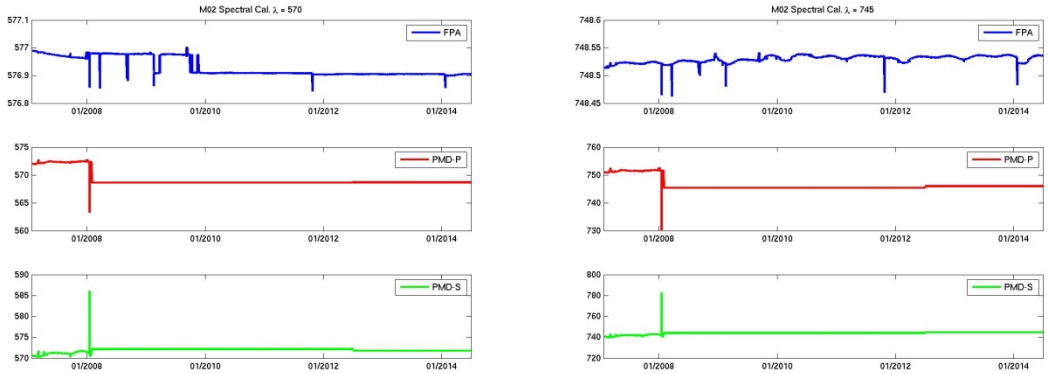

Figure 5-25: Spectral stability at various wavelengths between January 2007 and July 2014 and for main channels and PMD channels at 570 and 745 nm

From Figure 5-24, it can be seen that spectral stability is stable at all wavelengths. Features which can be attributed to the events listed before are evident in these plots. Figure 5-26 shows the stability of the spectral co-registration between PMD-P and S in per cent per detector pixel spectral width. The results demonstrate the strong stability of the co-registration outside the special events regime.

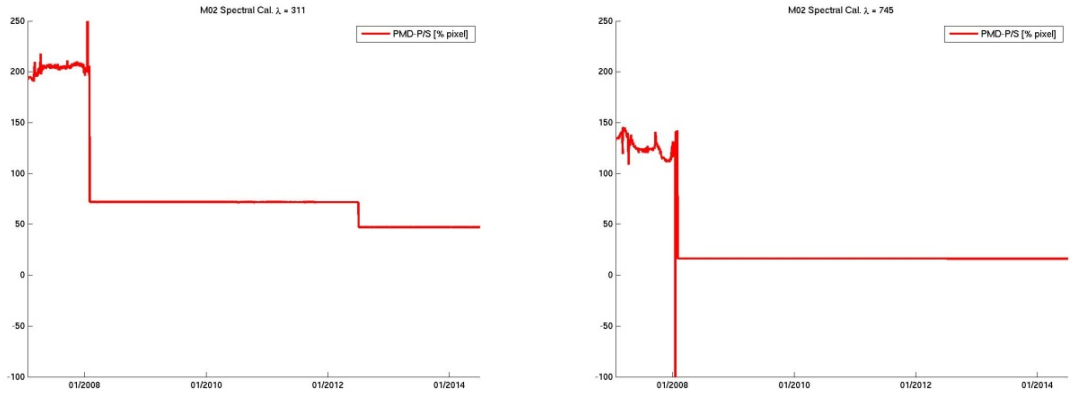

Figure 5-26. Spectral stability of the co-registration between PMD-P and S in percentage of fractional detector pixel around 311 and 745 nm. The first step function is due to the on-board up-load of PMD band definitions 3.1 from the original pre-launch settings (1.0). The second step function in relative PMD wavelentgh calibration is due to the adoption of the further improved cross-corelation fitting windows as provided with FM3 re-analyzed key-data by TNO and implemented on 3 July 2012.

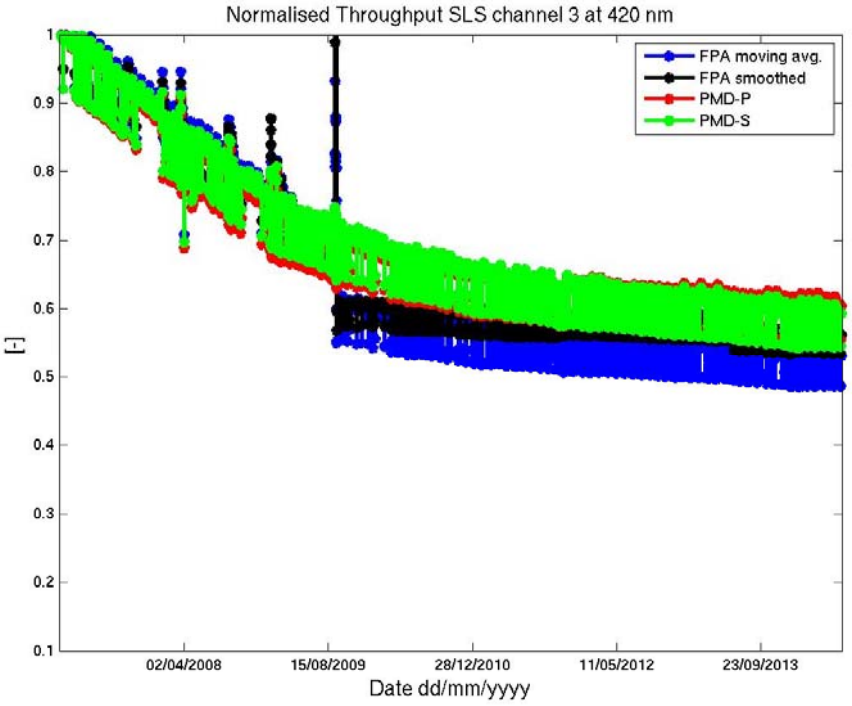

Figure 5-27: Signal strength around 420 nm spectral line.

Figure 5-27 shows the spectrally smoothed signal strength around the 420 nm spectral line - one of the weakest spectral lines used for spectral assignment of channel 3 radiances. There is the significant drop in throughput induced by the 2nd throughput test for the main channel, whereas the PMD throughput was not affected (because of no change of the PMD detectors). The throughput test caused a relative large shift (~0.05nm, i.e. ~25%/pixel) in the spectral assignment of channel three radiances in the blue part of the spectrum. This large but also smaller observed shifts may happen when the thermal environments changes and this part of the spectrum is particular vulnerable to such changes because of its relative sparseness in SLS lines.

Figure 5-28 shows the variation of the FWHM using a set of distinct SLS lines, which are well seperated from their neighbours in order to allow for a stable gaussian shape fitting. Note, that the applied gaussian shape is normal, and no distortion is applied, although the line shape is non to be assymetrical. Nevertheless, in case everything is stable, the derived FWHM should also be stable. However, it has been observed already a while ago that this is not the case and that the change in FWHM follows two patterns for FM3:

1) A spectrally well-ordered pattern (see Figure 5-28) resembling closely the timescale of the degradation during which the FWHM is continously decreasing especially for the lower wavelength range. A similar pattern has been observed by users of level-1 data using solar Fraunhofer lines. The long-term change is well anti-correalted with the optical bench temperature of the instrument over the same time range. See Figure 5-4.

2) On top of that, the FWHM varies significantly with the in-orbit change in the thermal environment and therefore following as seasonal pattern. The latter can easily be veryfied when comparing the seasonal signals with the OB temperature provided in Figure 5-4. The seasonal signal of FWHM changes is corelated with the OB temperature for channel 1, 3 and 4, while channel 2 is anti-corelated.

3) The FWHM also changes over the orbit as shown in Figure 5-29. The FWHM is here derived from Fraunhofer line fitting in the Earthshine spectrum (courtesy A. Richter, IUP Bremen). For the investigated case in channel 3 at 455 nm the signature is correlated with the OB temperatures.

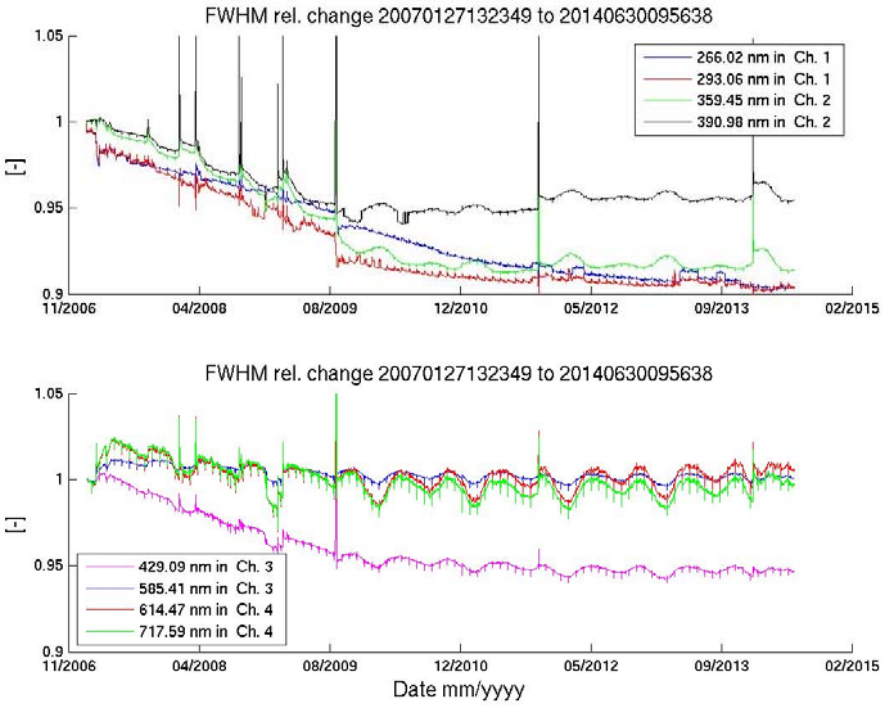

Figure 5-28: FWHM relative change with respect to January 2007 evaluated from a regular Gaussian fitting of well separated SLS lines. Upper panel shows the results in channel 1 and 2. The lower panel results for channel 3 and 4.

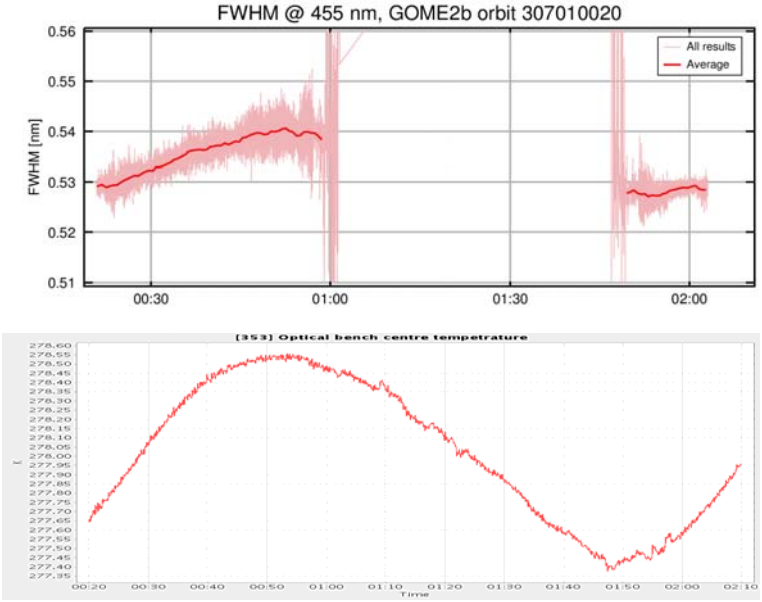

Figure 5-29: FWHM relative change over one orbit (upper panel) as derived from Fraunhofer-line fitting in the Earthshine spectrum in channel 3 at 455 nm (courtesy A. Richter, IUP Bremen). The lower panel shows the corresponding OB temperature.

A reanalysis of the TV test results provided as attachment in MO-NT-GAL-GO-0062 issue 1 and based on the original FM3 TV measurement documentation by Selex in MO-RP-GAL-GO-0006 from 2003 confirm these observations and identifies the origin of the behaviour in the introduced defocusing of the beams per channel and for all flight models in order to achieve a better oversampling (reduced spectral resolution).

Note: The latter design change has been introduced after the initial design phase and a detailed analysis of the consequences on the thermal behaviour has ***not*** been carried out at the time since it was not identified as a requirement.

Figure 5-30 to Figure 5-33 show the results of FWHM sensitivity to temperature change in the different channels as derived from the 2003 TV test of FM2. Results from FM3 are expected to follow the same rational.

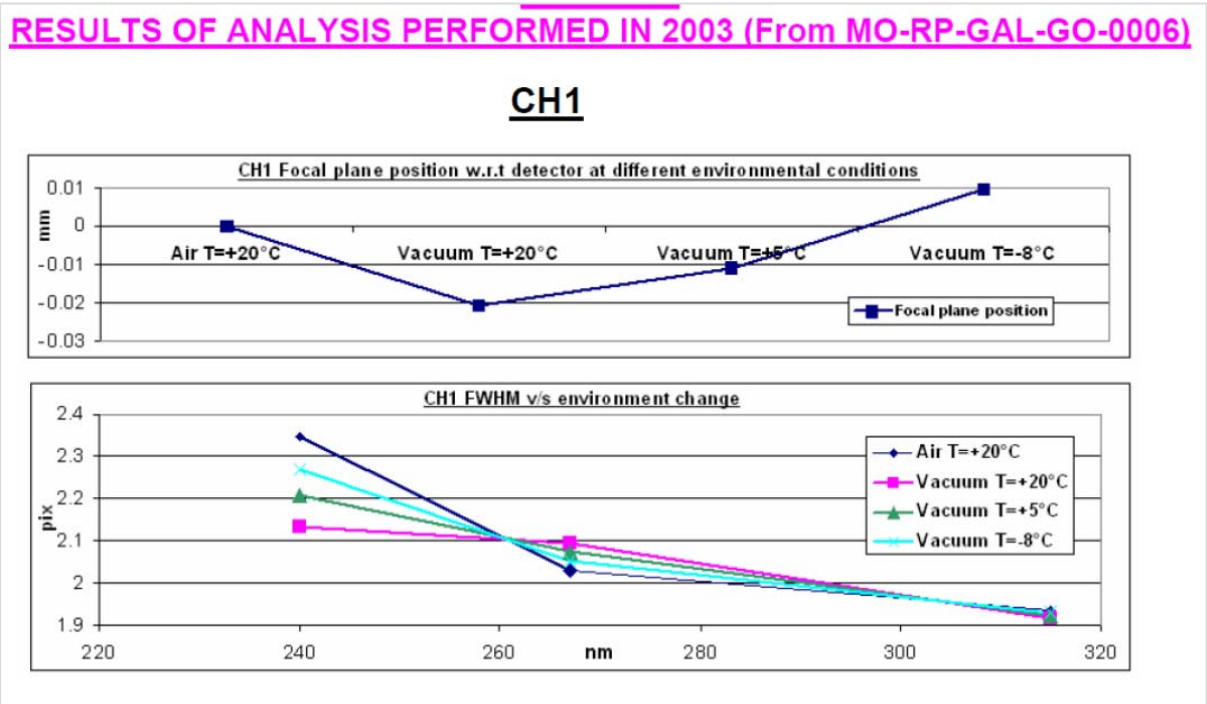

Figure 5-30: Upper panel: Focal plane position ("defocusing") in channel 1 for four different combinations of environmental (air/vacuum) and temperature conditions as evaluated during the TV test campaign in 2003. Lower panel: Associated FWHM changes.

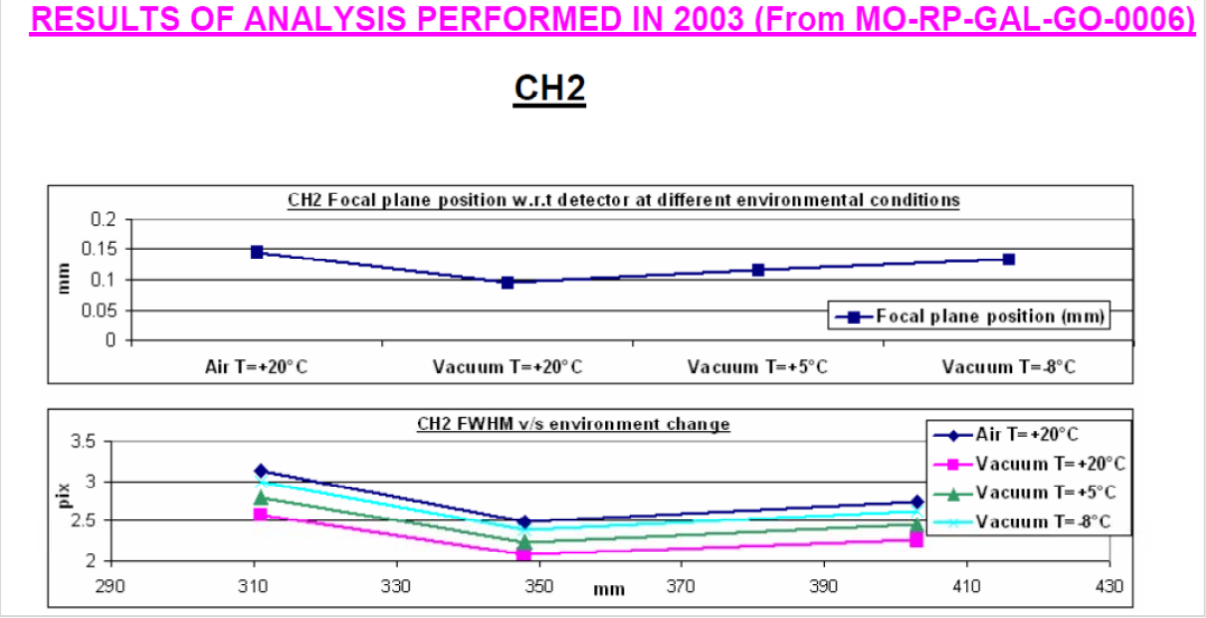

Figure 5-31: Upper panel: Focal plane position ("defocusing") in channel 2 for four different combinations of environmental (air/vacuum) and temperature conditions as evaluated during the TV test campaign in 2003. Lower panel: Associated FWHM changes.

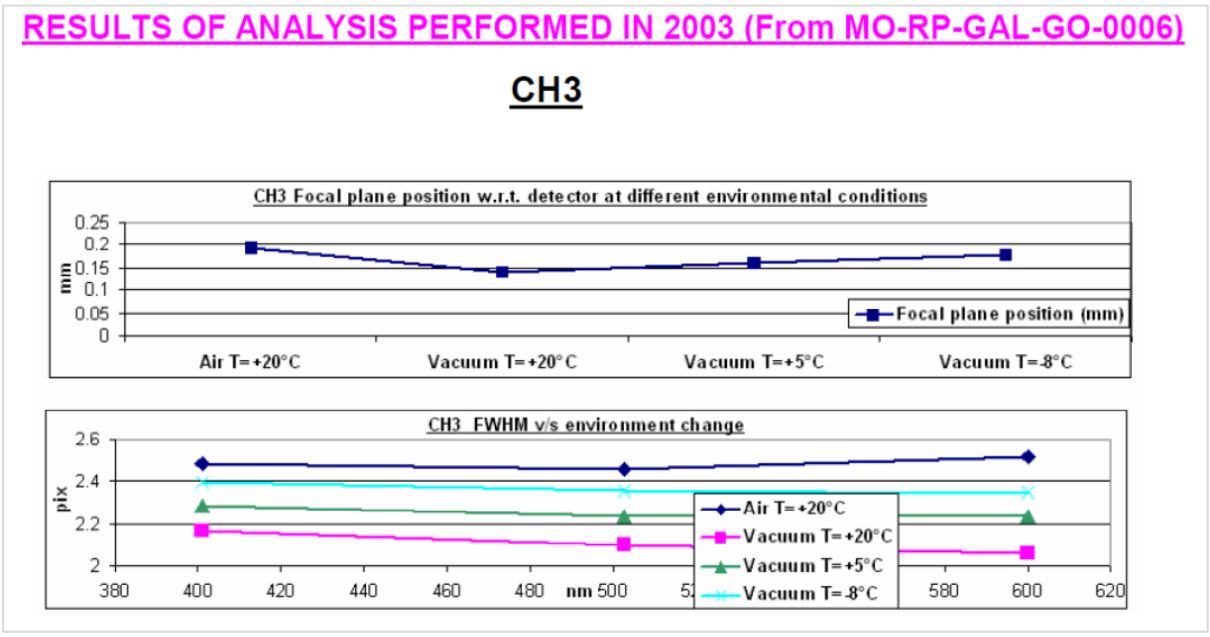

Figure 5-32: Upper panel: Focal plane position ("defocusing") in channel 3 for four different combinations of environmental (air/vacuum) and temperature conditions as evaluated during the TV test campaign in 2003. Lower panel: Associated FWHM changes

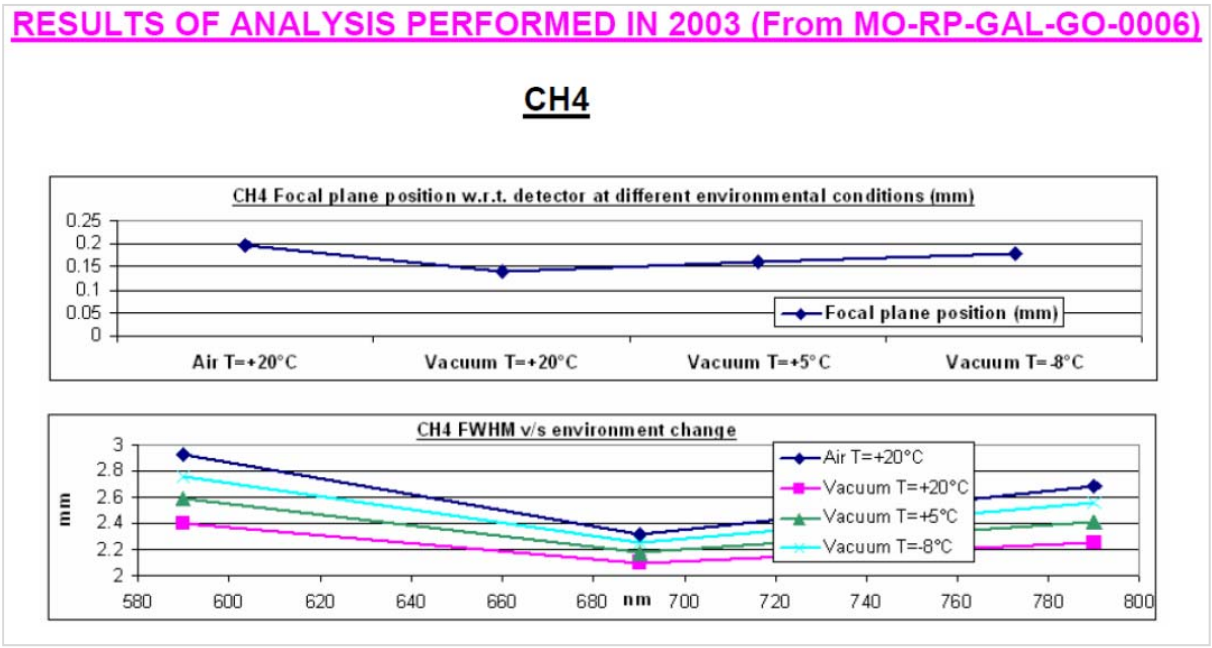

Figure 5-33: Upper panel: Focal plane position ("defocusing") in channel 4 for four different combinations of environmental (air/vacuum) and temperature conditions as evaluated during the TV test campaign in 2003. Lower panel: Associated FWHM changes

The results show that there is a) a wavelength dependence on the FWHM / OB temperature sensitivity, which is b) different for each channel. For channel 1 (Figure 5-30) there is a mixed sign of the correlation found in one direction for a negative defocusing direction (upper panel), however the sensitivity seems to be generally small especially for longer wavelength. This is consistent with the findings of Figure 5-28 showing a relatively weak signal in the seasonal variations for channel 1 wavelength (upper panel red and blue line). For channel 2 a consistent FWHM / OB temperature dependence is found over the whole channel (Figure 5-31) however for the same correlation sign with an opposite (!) shift (with respect to channel 1) of the defocusing direction. This is consistent with the observed anti-correlated and more significant seasonal signatures in FWHM changes with respect to temperature as observed in channel 2 of Figure 5-28 (green and black line). Finally channel 3 and 4 show the same consistent and significant FWHM/ OB temperature relationship (Figure 5-32 and Figure 5-33) for the same direction of the defocusing shift. Consequently the observed FWHM / OB temperature correlation is significant and has the same sign for both channels.

The long-term changes and the correlation in optical bench temperature with respect to FWHM changes is anti-correlated for all channels, and therefore more likely related to changes of the temperature gradients. One hypothesis is that a consistent shift of the defocusing in all channels induced by long term changes to the temperature or with respect to the temperature gradient distribution of the OB because of the satellite platform heat-up is consistently shifting the FWHM on these time scales. The upper panels of Figure 5-30 to Figure 5-33 show that an increase in OB temperature means a negative change of the defocusing consistently over all channels. See also Figure 5-34.

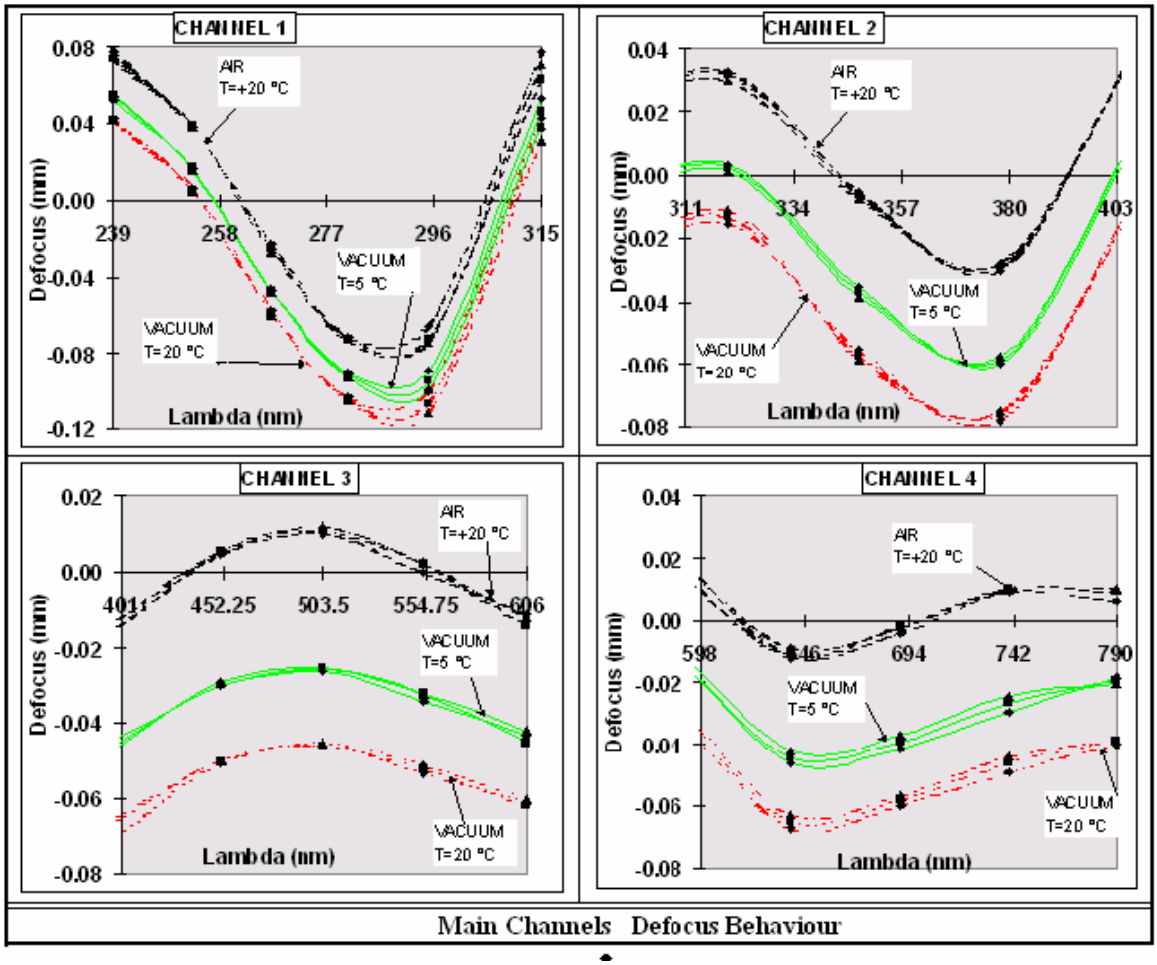

Figure 5-34: Defocusing of the individual channels 1 to 4 (upper left to lower right panel) before the additional defocusing has been introduced and in dependence of three combinations of environmental conditions and temperatures as taken from MO-NT-GAL-GO-0062 issue 1 and based on the original FM3 TV measurement documentation by Selex in MO-RP-GAL-GO-0006.

Figure 5-35 shows the difference in the centre line position with respect to November 2012. This variation basically reflects the origin of changes which translate into changes observed for the overall spectral calibration in Figure 5-24 and Figure 5-25. The change in the centre line position does not exhibit any long term tend and is predominatly correlated with seasonal changes (and orbital as known from level-2 retrievals) of the OB temperature.

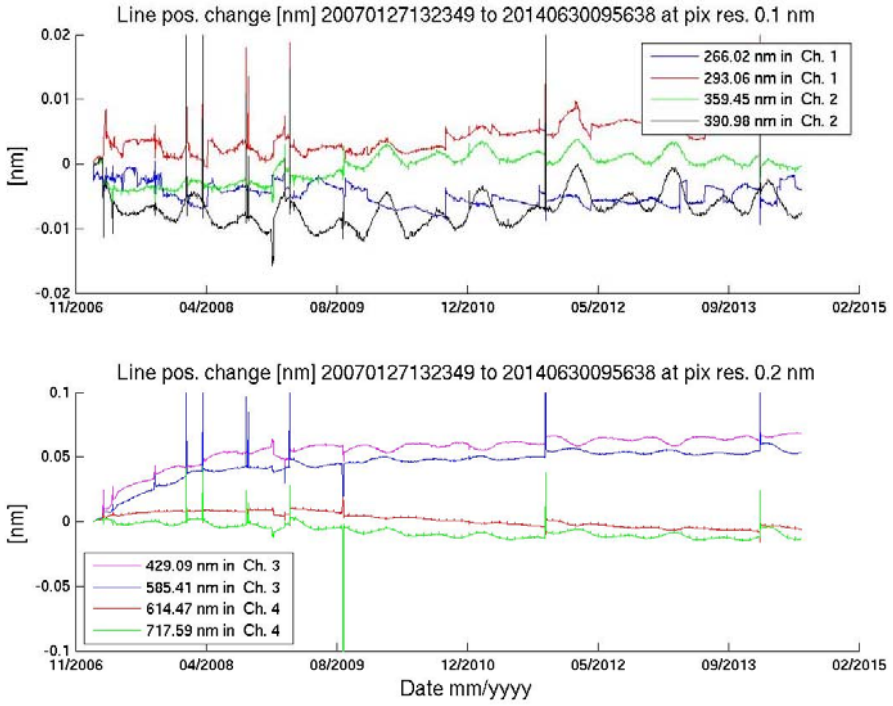

Figure 5-35: Difference of the centre line position with respect to January 2007 evaluated from a regular Gaussian fitting of well separated SLS lines. Upper panel shows the results in channel 1 and 2. The lower panel results for channel 3 and 4.

5.7.5 Assessment

Changes in the spectral stability of the instrument by changes in the thermal environment are to be expected since changes in temperature will cause slight movement of the optical components of the instrument. This is a clear deficiency in the overall optical design of the instrument which doesn't allow for a controlled temperature stabilized optical bench.

Apart from the seasonal variation in spectral stability, it is also possible to see changes on short timescales due to switch-off events. The very well known orbital variation in spectral assignment due to then orbital change of the optical bench temperature can however not be resolved.

Note: In addition, we observe a strong coupling between the FWHM and the OB temperature at all time-scales (long-term, seasonal and orbital) and with varying strength and different correlation signs per channel (for channel 1 also within the channel). This strong coupling is related to an increased FWHM to OB temperature sensitivity as a result of the on-ground defocusing of the instrument, which has been introduced during AIT in order to increase the spectral oversampling capabilities of the instrument.

Apart from the occasion of the mentioned events the overall spectral calibration of the instrument since Jan 2007 varies well within the sub-detector pixel range and the variation in the centre line position is translated in the change in spectral calibration, which in turn is known to be closely related to changes in the seasonal and orbital time-scales of the OB temperature.

5.8 GOM06: Throughput Stability

5.8.1 Description

Throughput measurements are made using a variety of techniques. The use of different techniques allows isolation of various components in the optical path.

5.8.2 List of Correlated Events

ID	*Date*	*Description*	*Justification*
G2	2008-09-02		GOME Off for OBSWM
G3	2008-09-10		GOME Off for OBSWM + SCI Proc Crash (Analogue TLM to 0x0000)
G4	2008-12-10		Update of FPA Band + Dale Resistor Relay left closed
G5	2009-01-27		GOME Throughput Test
G7	2009-02-16		GOME EQSOL/Suspend (AR.10874
G8	2009-03-03		GOME Off for OBSWM
G9	2011-10-24	PL-SOL #6	GOME off due to PLSOL

Table 5-4: List of Correlated Events

5.8.3 Analysis

Please note that the results and the impact of the observed long-term degradation and the first and second throughput test on instrument throughput performance are not discussed as part of the main body of this report. However we do note that the observed throughput degradation of FM3 is obviously an essential ‘feature’ of the instrument performance and will very likely continue to be so. In order to streamline the reporting on this issue to various parties and stake-holders we want to focus in the future on updating one dedicated report on the matter only. For earlier analysis of the throughput degradation and on the issuing of the throughput tests and their initial analysis, please see [AD 3] [AD 6] through [AD 7].

EUMETSAT GOME-2 instrument engineer documented throughput degradation analysis results in a dedicated report [AD.8], which was used as an input to the work of a dedicated tiger-team lead by ESA. The report of the tiger team is [AD.15]. For the analysis of the GOME-2 FM3 throughput degradation we therefore refer to these reports [AD.8] & [AD.15] and to the latest validation report of the reprocessed level 1 dataset release 2 (G2RP-R2). See [AD.9] and EUMETSAT document EUM/LEO/REP/09/0732. *Investigation on GOME-2 throughput degradation, v.2*.

In this section, we present initial results of version 0.9 of the empirically modelled “differential” (relative degradation of earthshine to solar signals is equal to reflectivity degradation) degradation matrix for FM3 removing seasonal and short time effects as well as high frequency spectral features. The results are presented for three different scan angle position:

- Pos. 1: most Easterly,
- Pos 17: same scan angle than the solar observations,
- Pos. 24: most Westerly viewing.

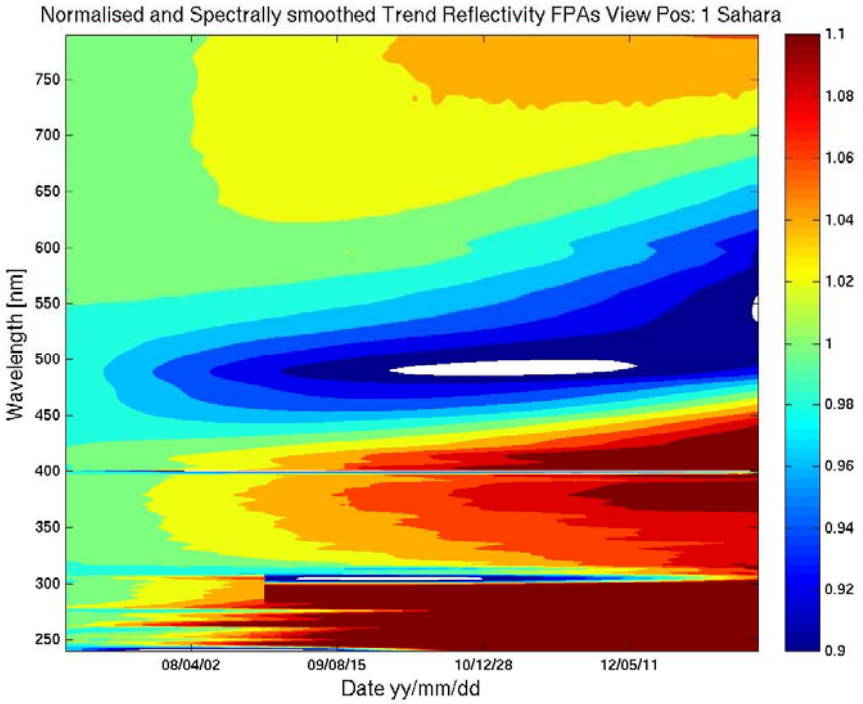
Normalised and Spectrally smoothed Trend Reflectivity FPAs View Pos: 1 Sahara
Wavelength [nm]
750
700
650
600
550
500
450
400
350
300
250
08/04/02
09/08/15
10/12/28
12/05/11
Date yy/mm/dd
1.1
1.08
1.06
1.04
1.02
1
0.98
0.96
0.94
0.92
0.9

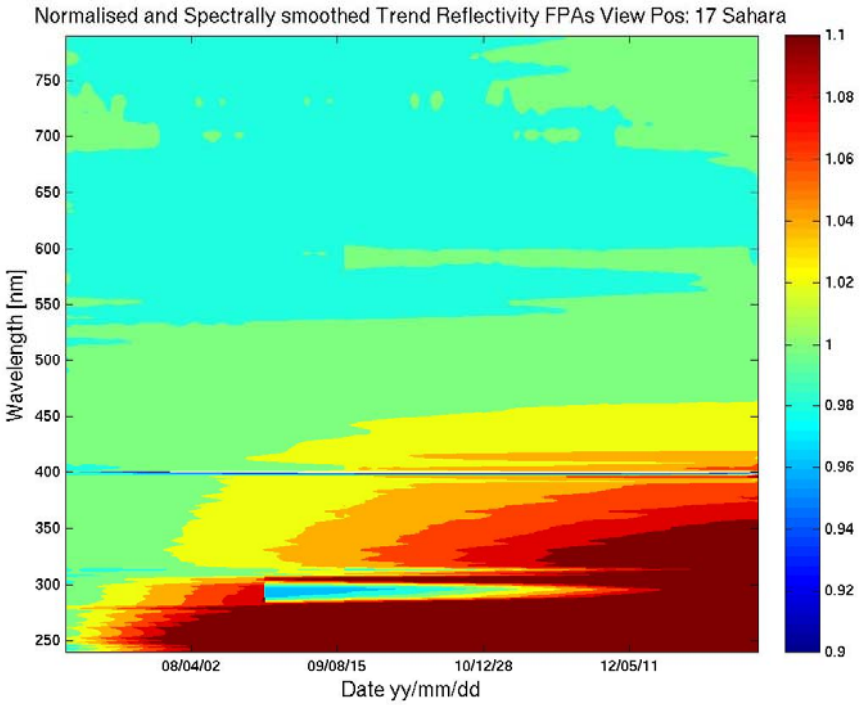
Normalised and Spectrally smoothed Trend Reflectivity FPAs View Pos: 17 Sahara
Wavelength [nm]
750
700
650
600
550
500
450
400
350
300
250
08/04/02
09/08/15
10/12/28
12/05/11
Date yy/mm/dd
1.1
1.08
1.06
1.04
1.02
1
0.98
0.96
0.94
0.92
0.9

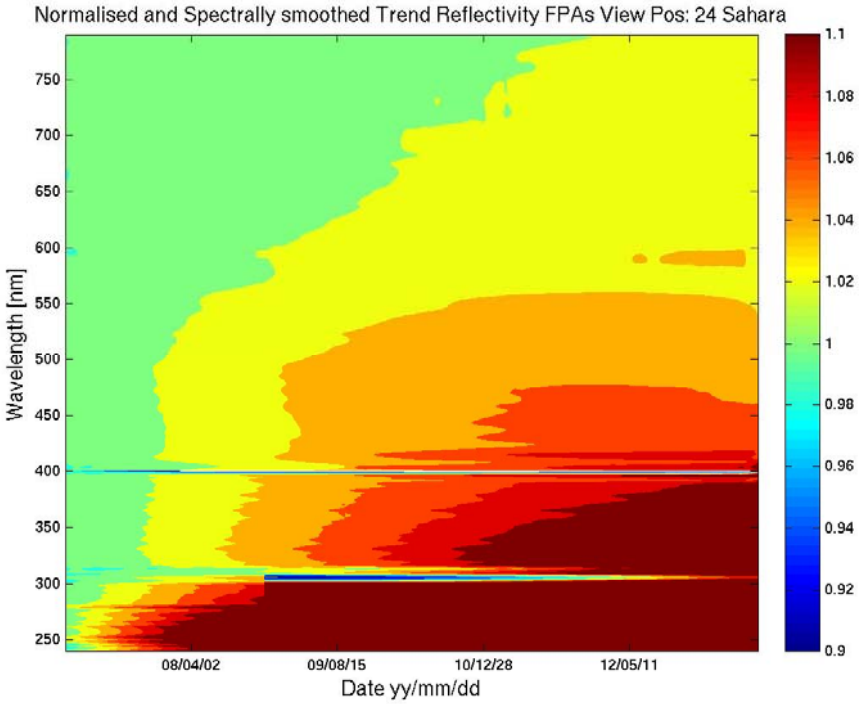

Figure 5-36: "Differential" (reflectivity) degradation over the full main channel spectral range (vertical axis) and the full FM3 in-orbit period starting 25th January 2007 (horizontal ais) for three different scan-angle positions: Pos. 1: most Easterly, Pos 17: same scan angle than the solar observations, Pos. 24: most Westerly viewing.

Figure 5-36 shows that for all viewing angle the solar path degrades faster than the earthshine path for the short wavelength probably due to diffuser degradation or additional contamination of surfaces / mirrors in the calibration unit. This effect is continuously decreasing towards longer wavelength. On top of this type of differential degradation we observe spectral structures changing over time and depending on the scan mirror position, especially around 500 nm and for the most Eastward looking directions. Such scan angle dependent features are known (from SCIAMACHY and GOME-1) to occur as a result of contamination layers on the scan-mirror developing over time and introducing different attenuation of the signal depending on its polarisation and the contamination layer thickness and properties (East looking light has the highest degrees of polarisation). This version 0.9 of the GOME-2 /Metop-A degradation model provides us with the possibility to forward project the signal evolution at various representative wavelength until the end of commissioning of GOME-2 / Metop-C (end of Metop-A/B and start of Metop-B/C tandem operations).

Figure 5-37 shows the evolution of the Earthshine signal averaged over all viewing angles for selected wavelengths in all channels. For Metop-A, the period after the second throughput test with much higher signal stability is used as basis for the projection (dashed line) until the 2018 time frame (launch of Metop-B). Next to the Earthshine degradation also the solar mean reference signal is shown using the same forecast method.

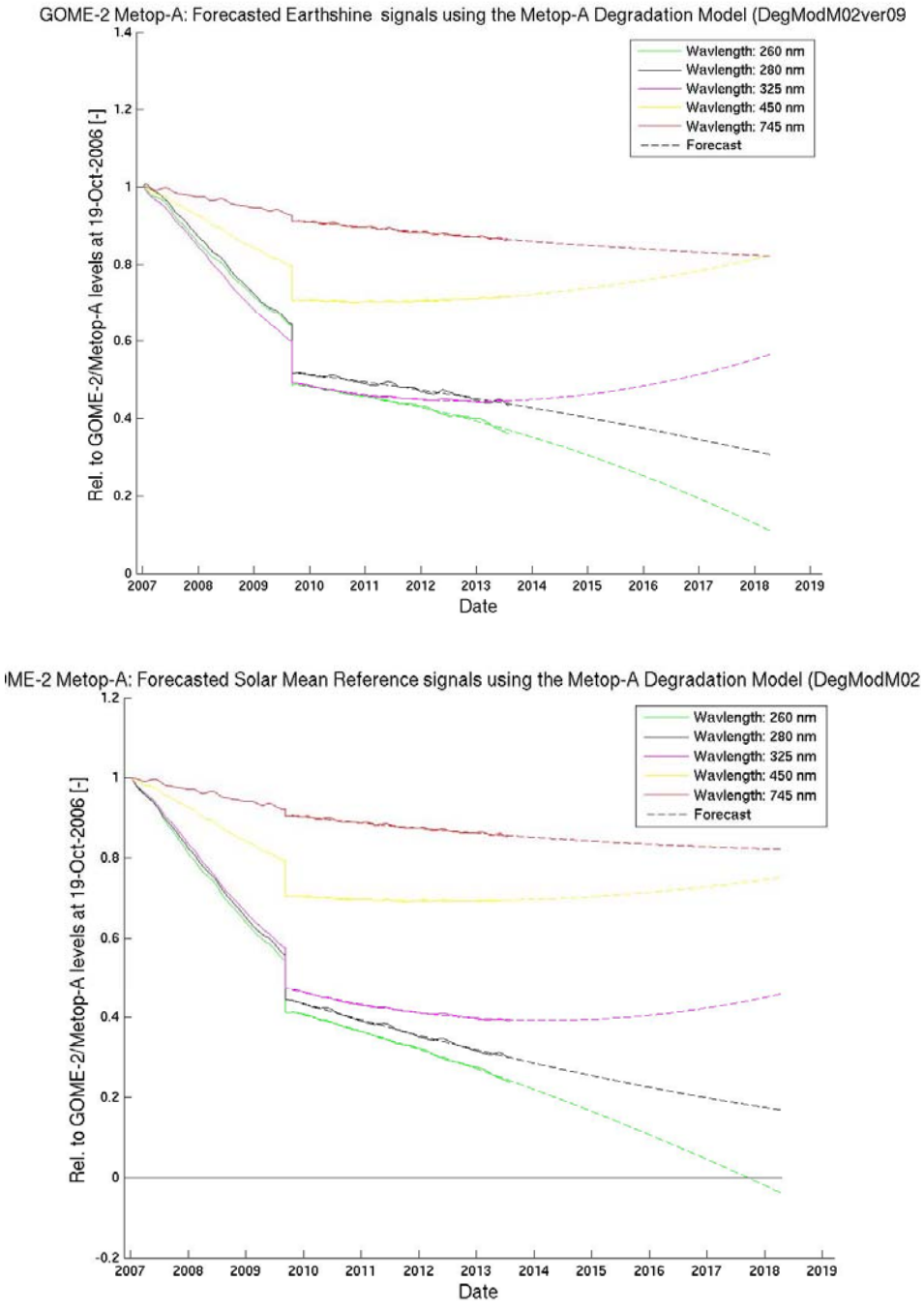

Figure 5-37: Signal evolution for selected wavelength for GOME-2 Metop-A based on version 0.9 of the signal degradation model. Dashed lines show the projection in the future based on the signal evolution of the post 2nd throughput test period. Upper panel: Earthshine signal averaged over all viewing directions. Lower panel: Solar mean reference signal.

Figure 5-38 shows the reflectivity evolution. The reflectivity is the quantity which is commonly used for level-2 retrievals. Since the solar path is degrading faster than the Earthshine path (as discussed in the assessment of the next section) the reflectivity is overall increasing. Decreasing signal levels of radiance and irradiance however lead to larger error bars on the reflectivity values and therefore to larger errors on the retrievals.

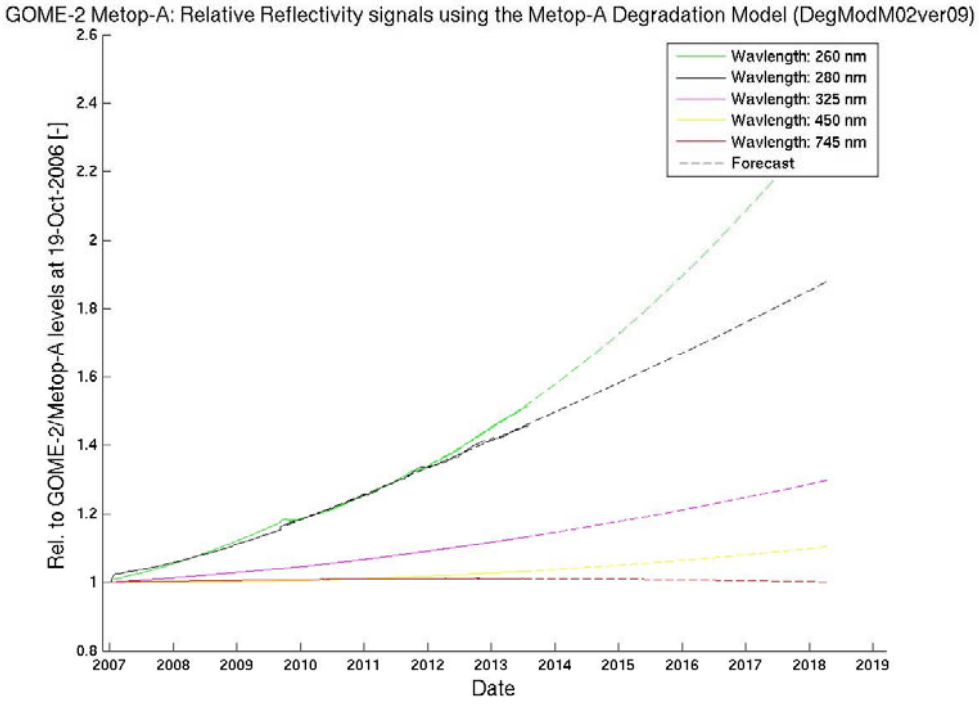

Figure 5-38: Same as Figure 5-37 but for the reflectivity. The dashed line shows the forecasted projection.

For a comparative assessment of the FM2 (Metop-B) and FM3 throughput, please see the corresponding Metop-B instrument report EUM/OPS-EPS/REP/14/771772

The monthly measurements of the diffuser signal using the HCL lamp are known to be "noisy" due to the instability of the lamp at long integration times (here 288/96 sec for DIFcal; see also Section 5.5). This instability hampers the interpretation of the signals of the SLS over the diffuser during the first years of the mission. Figure 5-39 shows the relative signal of the spectrally smoothed SLS (without diffuser in the light path) with respect to the diffuser measurements taken at the same day.

5.8.4 Assessment

After eight years in orbit, we may conclude that we are seeing only a slight degradation of the diffuser of maximal 5 to 10% over the whole period for wavelengths above 290 nm. Still there remains a significant uncertainty in this estimate because of the large scatter in the data. Version 0.9 of the degradation model seems to indicate that for the shorter wavelength up to 300 nm there is very likely a significant contribution of the calibration unit to the differential (reflectivity) degradation, whereas for the shorter wavelength the scan-mirror angle dependent features dominate, indicating a superimposed contribution of a scan-mirror contamination layer building up. The latter is expected from previous instrument (GOME-1 and SCIAMACHY) experience. The differential degradation leads to increased reflectivity values over time. Based on the post- 2nd throughput test signal evolution a projection of signal levels into the future reveals that we can expect still good overall performance of the instrument until the timeframe of Metop-C commissioning, with however continuous increase in retrieval errors as detailed in the dedicated study on signal level decrease on GOME-2 Metop-A level-2 product quality [RD 7].

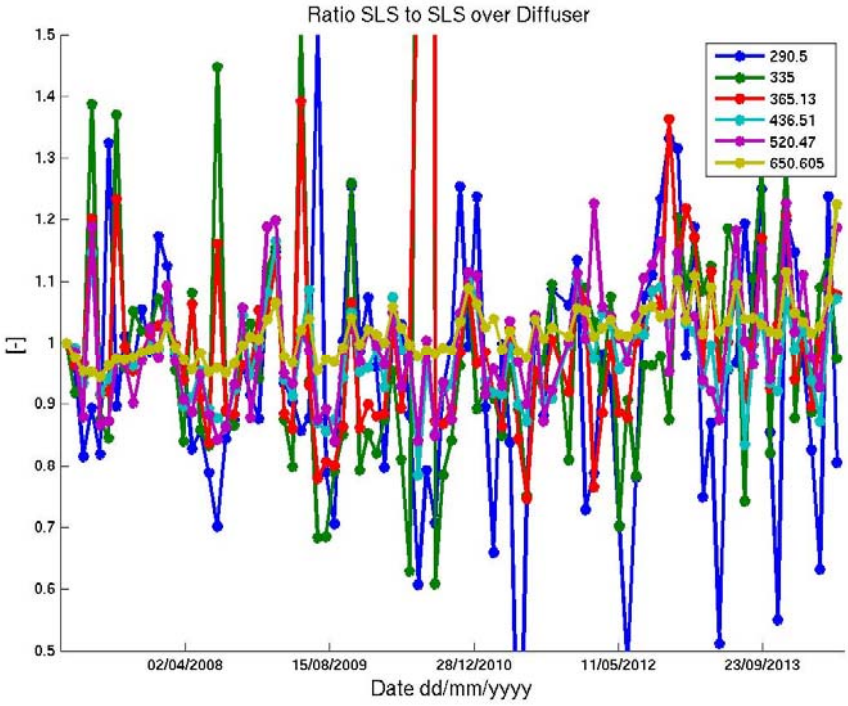

Figure 5-39: Ratio of signal from the nominal SLS measurements to the SLS measurements taken once per month over the diffuser. The measurements are taken during the same monthly calibration sequence. The observed scatter is due to the instability of the lamp at very long integration times as used for the diffuser measurements.

5.9 GOM07: Dark signal

5.9.1 Description

The dark signal noise, dark signal offset and leakage are evaluated from dedicated dark measurements at the dark side of the orbit. Dark measurements are taken for different integration times used during calibration and nominal earth scanning measurements and averaged over the valid integration period. The dark signal results are stored in the in-flight calibration file during processing for different temperatures and applied only for the relevant integration time and within a narrow range of the actual temperature.

The dark signal offset and leakage are specified in the PGS to be determined by the level 0 to 1b processor from mean dark signal readouts using a linear fit over integration time. During the analysis of data from the second throughput test, it has been found that this assumption on linearity is valid for the current operational temperatures of the main detectors, but breaks down at temperatures significantly above 280 K and for integration times longer than three seconds. To ensure a robust fit, the following analysis has been based on dark measurements with integration times shorter than three seconds. The post process of the results from data derived from the operational monitoring database makes sure that results are provided only if a significant amount of measurements is found to ensure a robust fitting result. For band 1A, during parts of the year not enough measurements for a certain integration time are available since they are taken outside of eclipse. Results close to these data gaps are therefore also not trustworthy (because the eclipse might be too shallow at this point in time).

Note: Based on these fitting criteria, the only other operations induced change visible in the data is the turning on and off of co-adding in channel. Co-adding has been re-introduced on 3 March 2009 with the introduction of new timelines. It had been turned-off earlier in March 2007 shortly after SIOV.

5.9.2 List of Correlated Events

5.9.3 Analysis

The following plots show band averaged results for dark signal electronic offset (blue-line) and leakage signal (green line). Note that the dark-signal measurements for different integration times per band are taken at a different part of the orbit and therefore at different SZAs. Even though all dark measurements have so far been assumed to be taken (tagged as "valid") well within eclipse, recent analysis of the timelines with the new GTL builder tool at EUMETSAT indicate that some of the dark measurements may suffer from (twilight) stray-light, especially when taking the variation of the "shallowness" of the eclipse over the seasonal cycle into account. The latter is likely to cause the observed seasonal cycle in the noise signals, which varies significantly with integration time (which are related to different SZA or positions within the eclipse).

The wavelength range covered per band is given in Figure 5-5 below.

Channel Number	1	1	2	2	3	4	5/6
Band Name	1A	1B	2A	2B	3	4	PMD P/S
Band Number	1	2	3	4	5	6	7/8
Used Pixels	877/659[2]	147/365[2]	71	953	1024	1024	256
Spectral Range (nm)	240-307/283[2]	307/283-315[2]	290-300	300-412	401-600	590-790	290-790
nm/pixel	0.07	0.07	0.09	0.09	0.2	0.2	2
Predefined dark signal electronic offset (BU)	1501	1501	1503	1503	1495	1492	1503/1499

Table 5-5 GOME Wavelength Range per Pixel for all main channels

5.9.4 Interpretation

In subsequent graphs, unless otherwise stated, data are presented as follows

- band averaged electronic offset signal in BU is in blue, on the left axis and leakage current in BU/sec in green, on the right axis.
- band averaged dark signals (for all operationally used integration times) is in blue in BU.

Note: Band 2A data are not reported because the data is outside the valid spectral range.

[2] Settings changed on 10 December 2008.

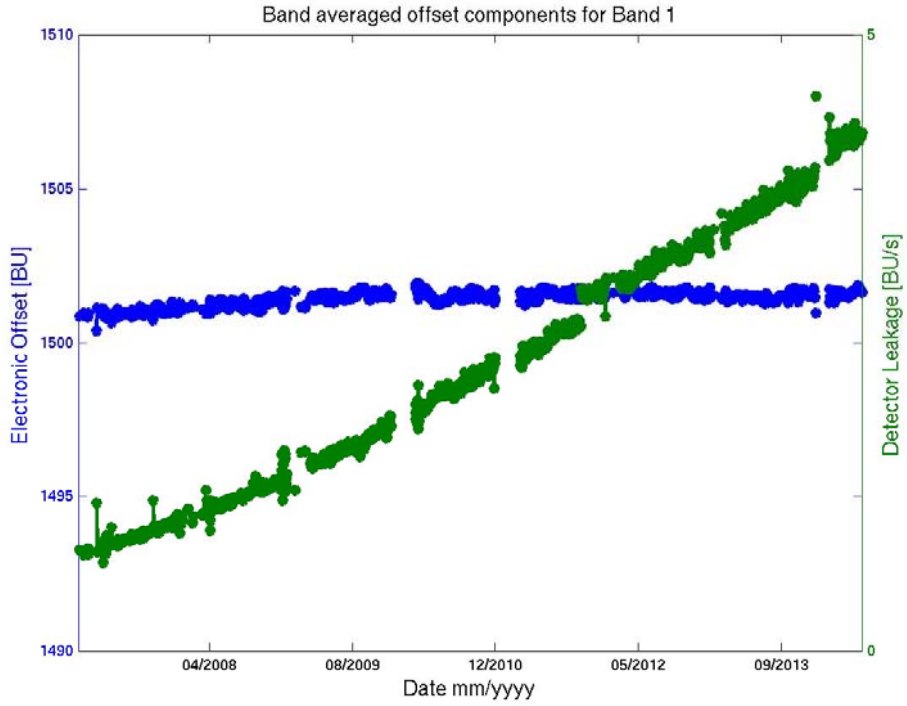

Figure 5-40: Band 1A averaged electronic offset (blue dots) and leakage current (green dots)

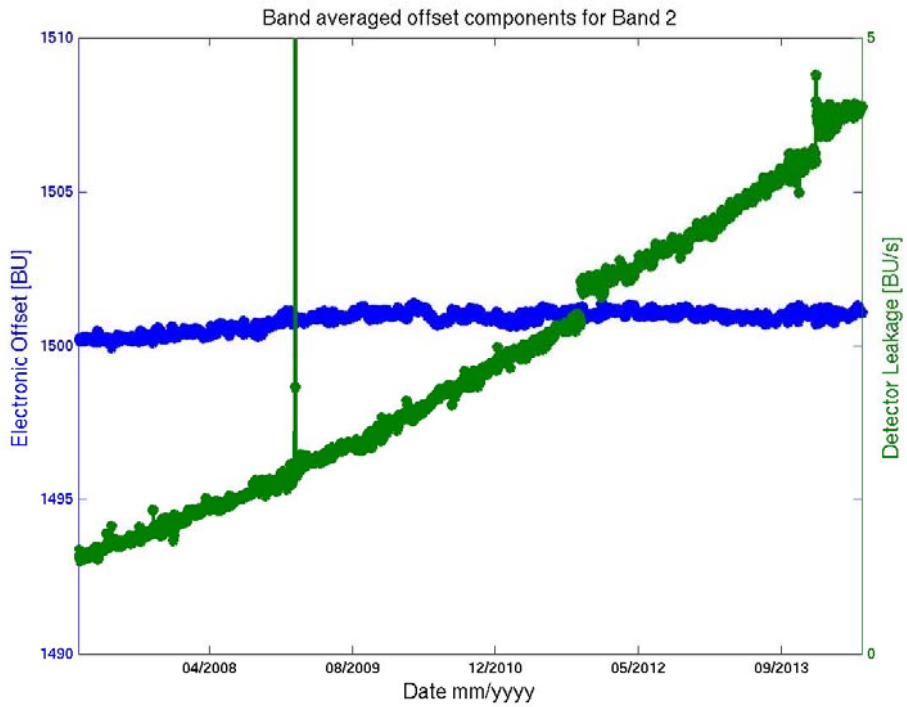

Figure 5-41: Band 1B averaged electronic offset (blue dots) and leakage current (green dots)

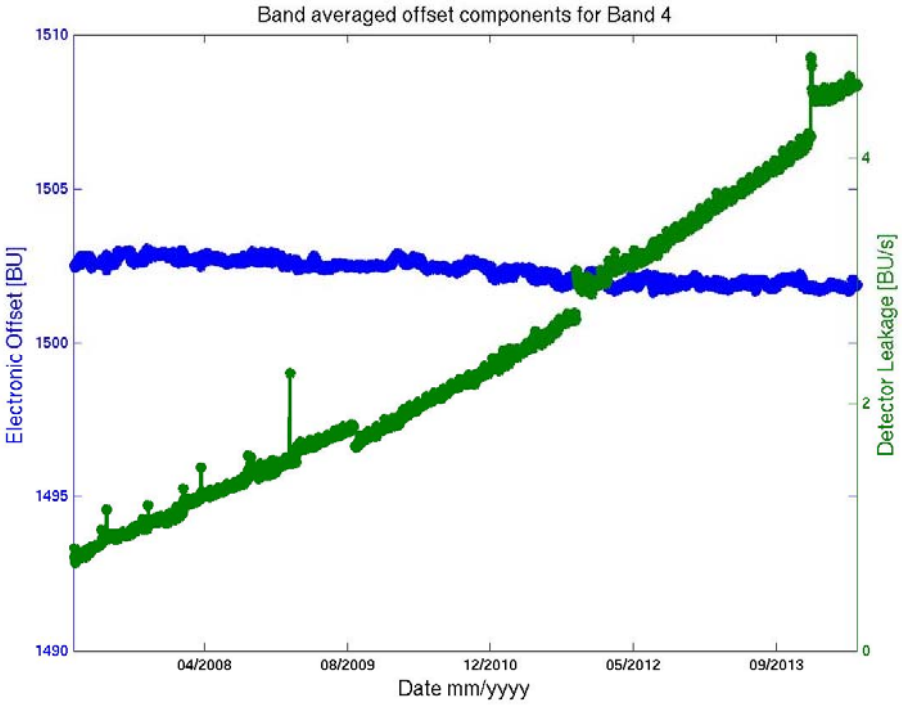

Figure 5-42: Band 2B averaged electronic offset (blue dots) and leakage current (green dots)

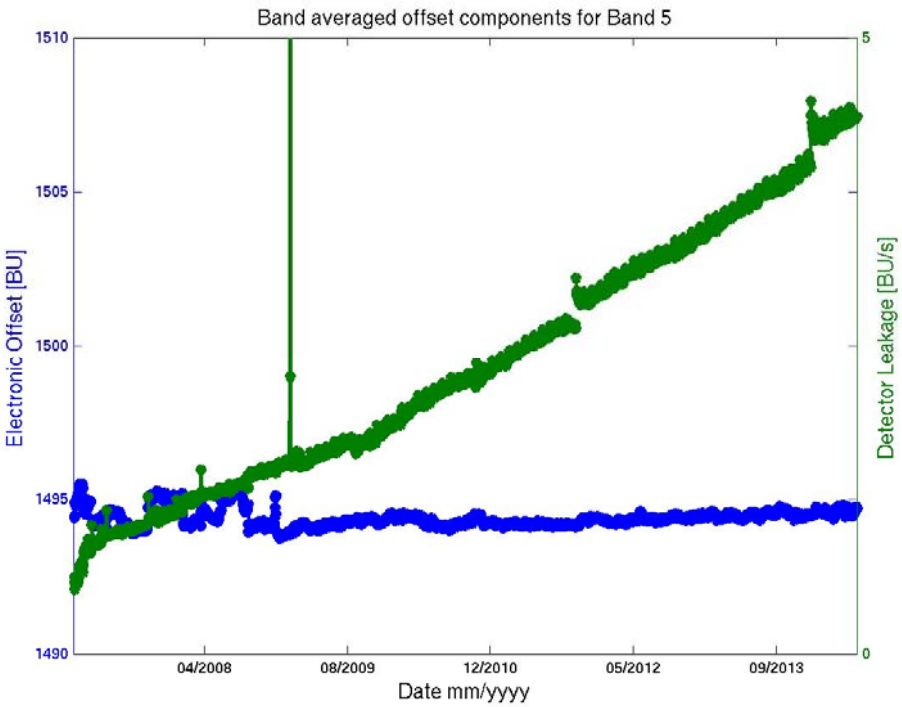

Figure 5-43: Band 3 averaged electronic offset (blue dots) and leakage current (green dots)

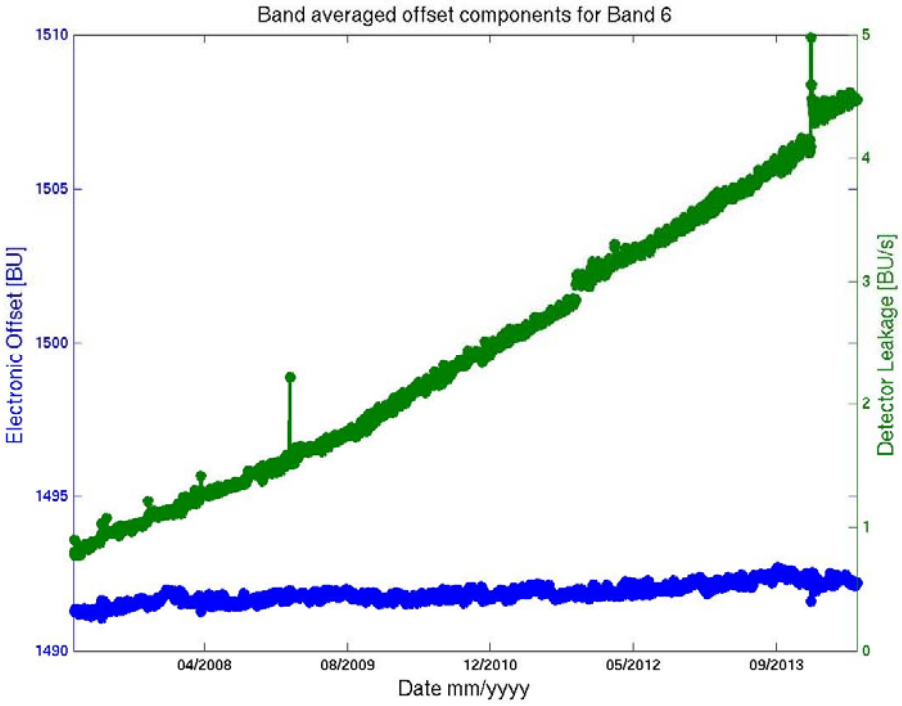

Figure 5-44: Band 4 averaged electronic offset (blue dots) and leakage current (green dots)

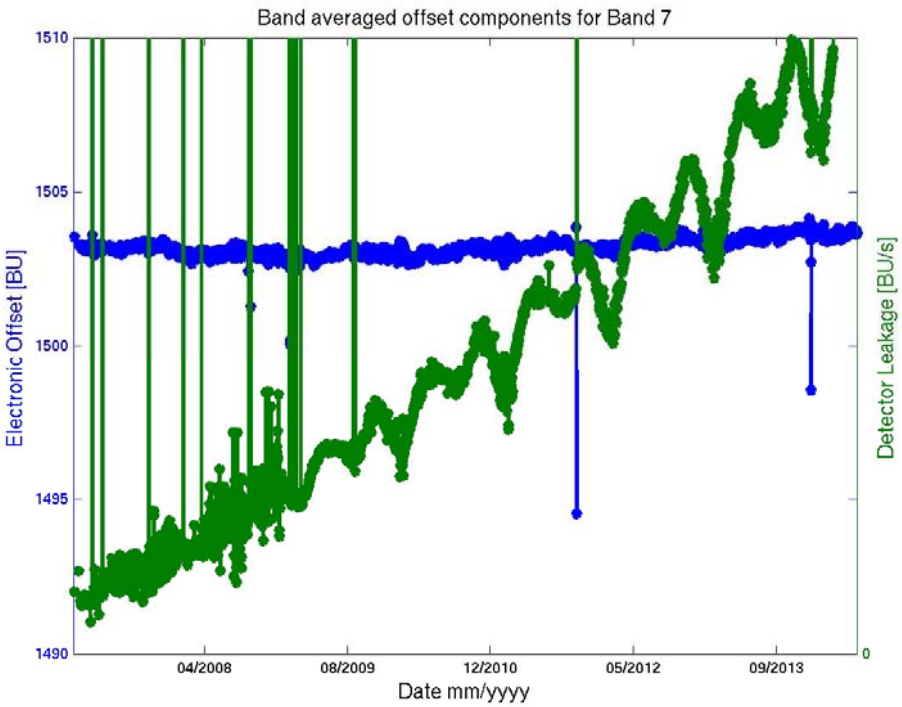

Figure 5-45: PMD-P averaged electronic offset (blue dots) and leakage current (green dots)

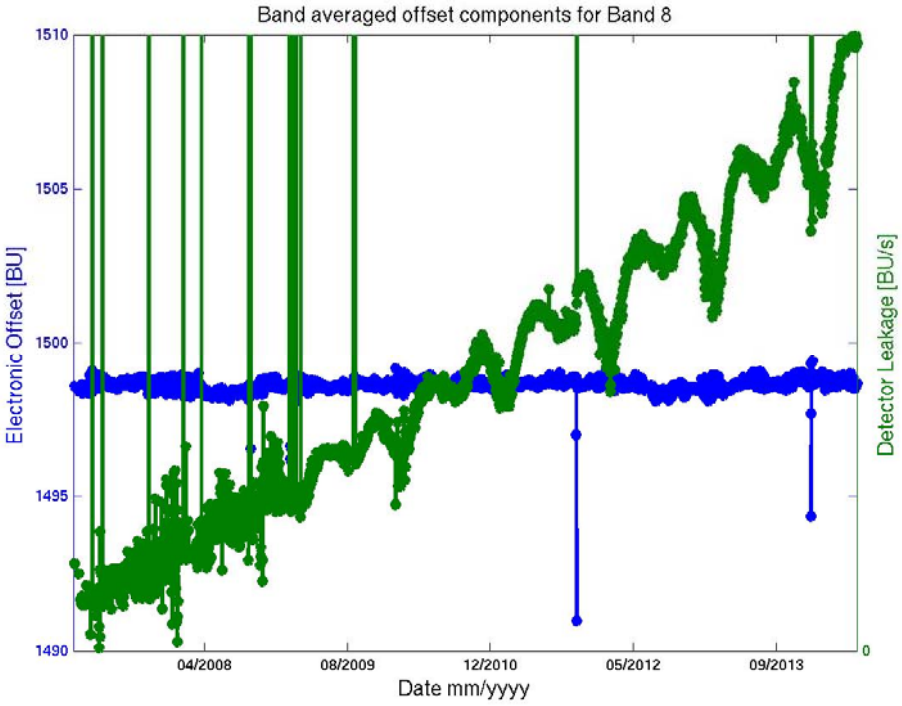

Figure 5-46: PMD-S averaged electronic offset (blue dots) and leakage current (green dots)

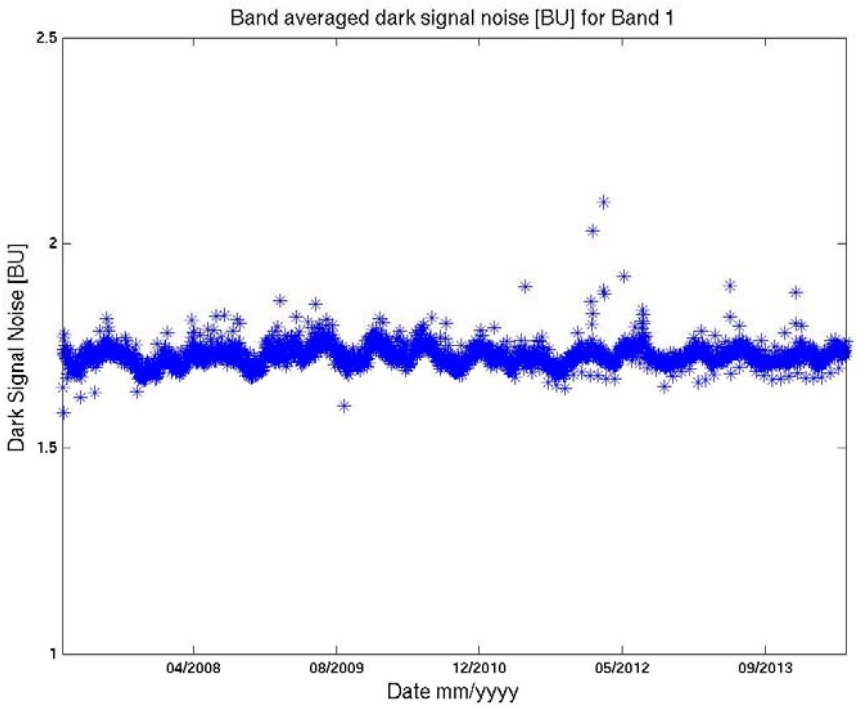

Figure 5-47: Band 1A averaged noise.

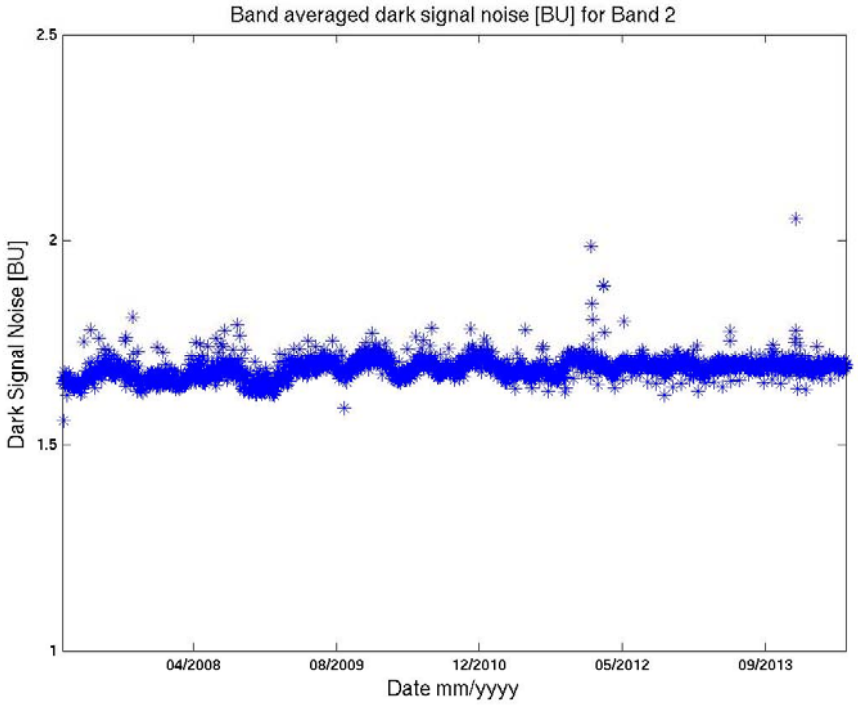

Figure 5-48: Band 1B averaged noise.

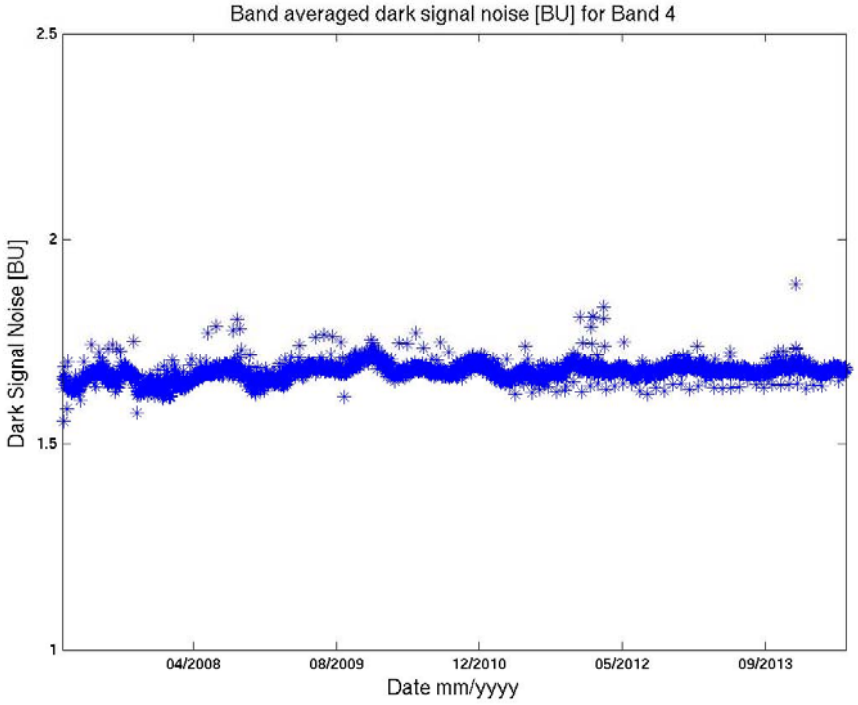

Figure 5-49: Band 2B averaged noise.

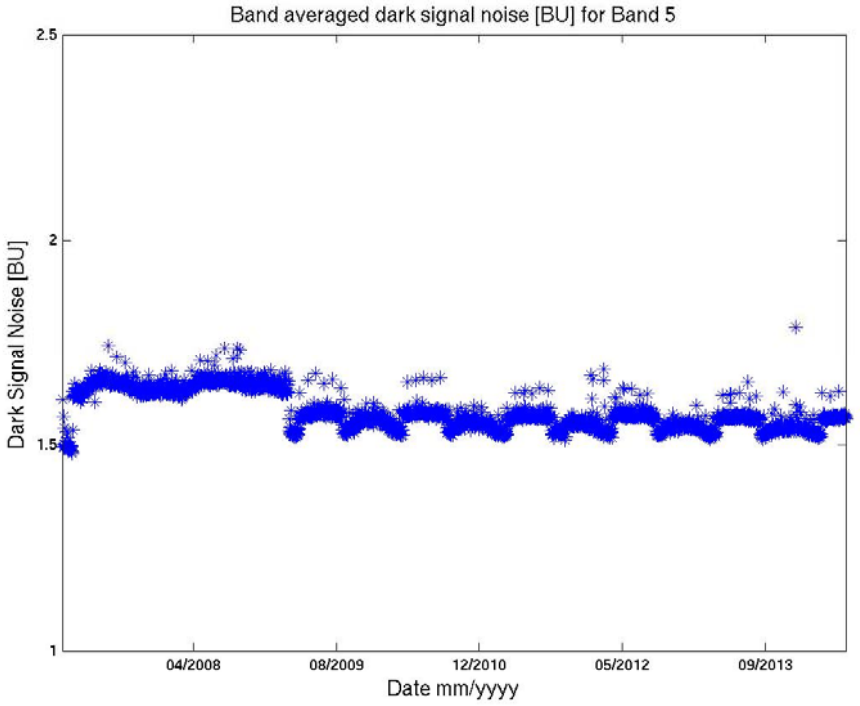

Figure 5-50: Band 3 averaged noise.

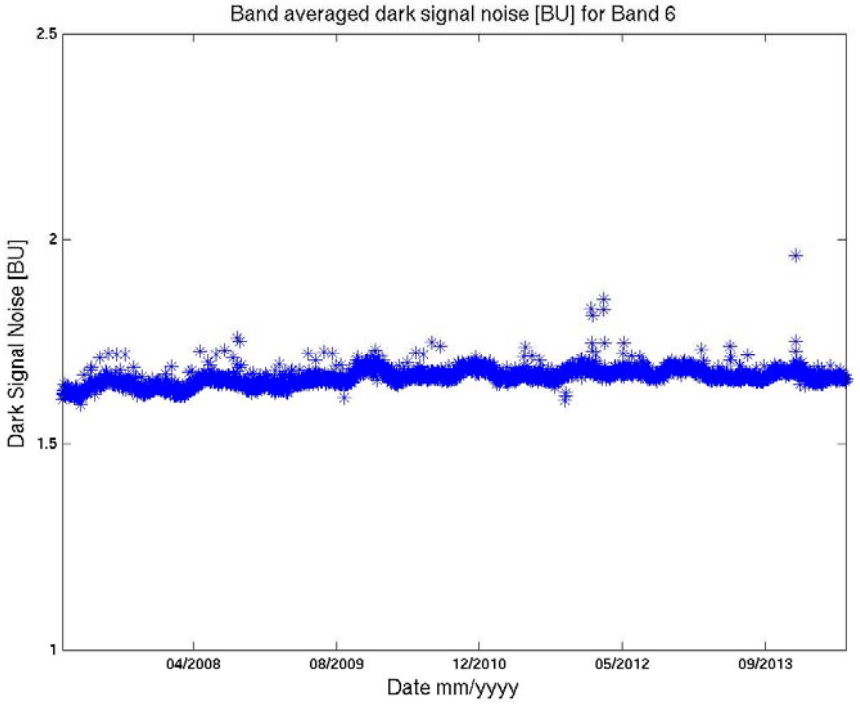

Figure 5-51: Band 4 averaged noise.

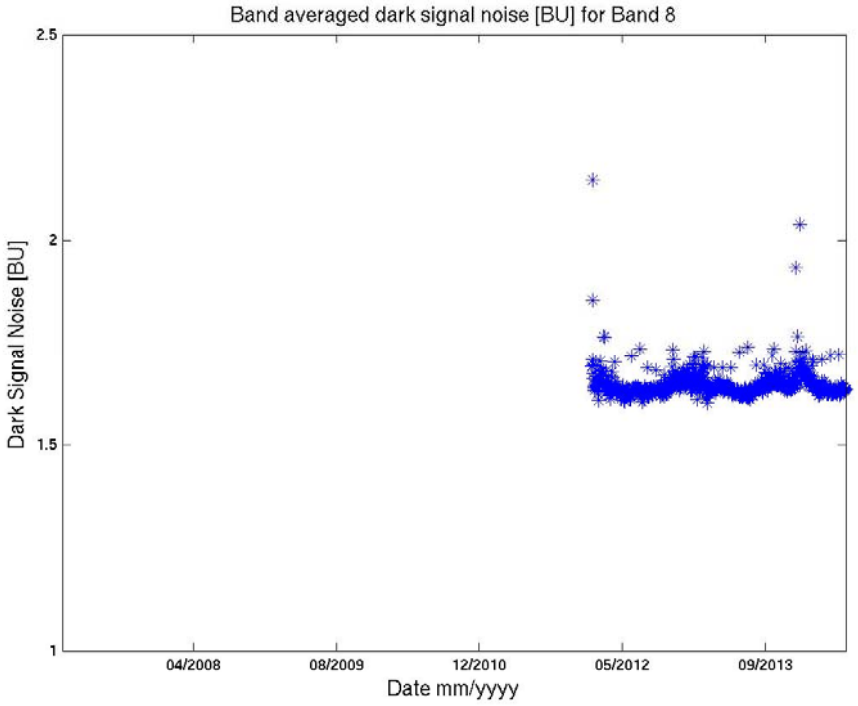

Figure 5-52: PMD-S averaged noise. (Data is missing in the reprocessed data base R2 (Jan 2007 to Jan 2012)

5.9.5 Assessment

The baseline for the electronic offset is stable for all bands. The leakage current is increasing moderately and at a level of less than 0.5 BU/s per year, which is not unexpected for this type of detectors. Generally, the leakage current contribution is sensitive to changes in the thermal environment. This is expected and is well visible from the step function introduced by the instrument switch off on 21 January 2014. See EUM/EPS/AR/15267 – Standby Refuse due to HDM Latchup.

Apart from the seasonal cycle contributions that depend on SZA (related to specific integration times) within eclipse, there is no significant other trending signal visible in the noise pattern. The seasonal cycle is related to the "shallowness" of the SZA within eclipse. The timelines have recently been optimised again in order to avoid intrusion of sun-light during dark-measurements. However, because of the complex nature of the timeline sequence the gains in reduction of stray-light were only small. Overall, the noise pattern is very stable and slightly below 2 BU, as expected from pre-flight calibrations.

There is no negative impact from the dark signal electronic offset expected for the near to medium term future, neither on instrument nor on processing level.

5.10 Physical Signatures Conclusion

Overall, the status of the GOME instrument can be considered healthy. Detailed analysis of each physical signature is given in each section. The main points raised by the analysis and subsequent discussions are these:

- HCL Lamp throughput needs to be assessed over a broad spectrum due to apparent instability in throughput which may be caused by a narrow spectral line hovering between two pixels for example. This is now handled in the stand-alone throughput document. [AD.8]

- Considering the relationship between HCL throughput, voltage and running time, getting useful data from DIFCAL measurements is extremely challenging. This is something that needs to be re-considered for Metop-C and/or future missions.
- QTH Lamp Blackening is considered to be a likely cause for differential WLS/SMR throughput loss, however test results and comparison with OMI indicate this is not likely to be curable on GOME-2. Mitigating actions such as increased integration time and running the lamp at a higher current may be considered in future. The impact on lamp life is not considered an issue.
- From the dark signal response measurements, there are some indications that some measurements are still affected by stray light. Timelines need to be reviewed to bring dark signal measurements deeper into eclipse, if possible.
- The FWHM is changing with OB temperature and potentially changing temperature gradients at long-term, seasonal and orbital time scales. The origin is the increased sensitivity of the instrument to thermal changes due to the "defocusing" of the instrument in order to improve spectral oversampling. This phenomenon has to be accepted as a design feature and is similar for FM2 and FM3 (and expected to be similar for FM1).
- The Leakage current has increased by 0.5 BU/s over the lifetime. The electronic offset has also increased by approx 2 binary units. The leakage current is as expected observed to be quite sensitive to the thermal environment.
- The signal is significantly more stable in channel 1 and 2 after the 2nd throughput test, though there remains a long-term impact on GOME-2 products. The throughput levels are stable in channel 3 and 4. In order to further assist the throughput investigation, use of the redundant LED chain is recommended.
- GOME Scan unit torque trend appears to have stabilised, and there is still plenty of torque margin. This will be further investigated by ESA triology experts. There is currently no frame of reference which can be used to judge whether the torque could cause problems within the time frame before 2018.

After eight years in orbit it can be concluded that a majority of anomalies and unexpected behaviour in the instrument performance is either influenced or can be in general referred to the instability of the thermal environment of the optical components of the instrument. This is due to a serious deficiency in the thermal design specifications of the instrument which was not required to be neither actively nor passively stabilized to sufficient levels across the whole optical bench and at each optical component. This is an important lesson learned for future instrumentation of this type.

The instrument performance with respect to level-2 products remains however at a very high quality level thanks to large efforts in compensating for effects of degradation, thermal instability and key-data deficiencies. This is expected to be true until the end of Metop-C commissioning.

6 OPERATIONAL CONFIGURATION AND EVOLUTION PLAN

6.1 HW Component Configuration

Component	*Description*	*Routine*	*Trending*	*Comments*
GEN	General Status	GREEN	→	
CDHU	Control and Data Handling Unit	GREEN	→	
GPDU	GOME Power Distribution Unit	GREEN	→	
CU	Calibration Unit (Including LED's)	GREEN	→	
SU	Scan Unit Electronics and Mechanism	GREEN	→	Torque
OPTICS	All Elements In Optical Path	GREEN	→	Throughput
PMD	PMD Detectors and Coolers	GREEN	→	
FPA	FPA Detectors and Coolers	GREEN	→	

Table 6-1: HW Component Performance and Configuration

Status Colour	*Meaning*
GREEN	Fully Operational (or capable of)
YELLOW	Operational with Limitations
ORANGE	Operational with Degraded Performance
RED	Not Operational
BLANK	No Status Reported

Trend Colour	*Meaning (with respect to expected behaviour)*
→	Stable
↘	Evolution in non-favourable direction
↗	Evolution in favourable direction
BLANK	No Trend Reported

6.2 Lifetime Limited Items

This section lists all those components that have a limited lifetime, indicating the predicted date when the lifetime will expire (e.g. a relay that has a limit to the number of on-off switches, a component that has a limited on/off time before expected failure etc.).

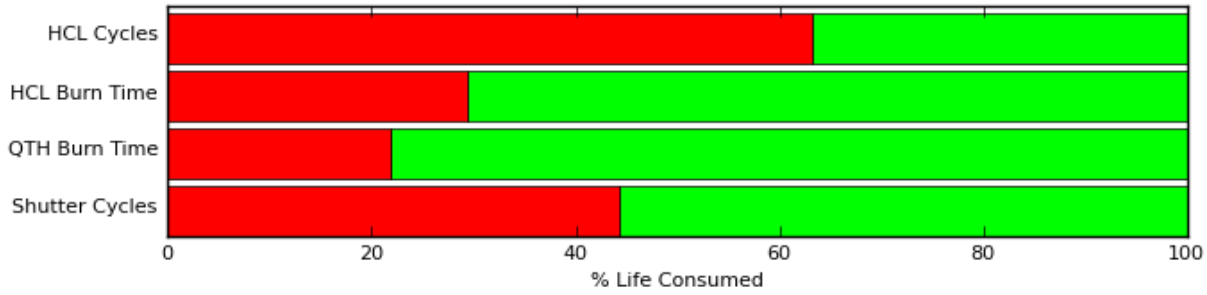

Figure 6-1: GOME-2 Life-limited Item Usage to September 2014

Figure 6-1 shows the GOME Life Limited Item usage to September 2014. These figures are derived from METOP HK data and are compared to the qualified ratings in section 9 of the GOME IOM.

The main concern is the continued use of the Spectral Lamp at the current rate – this number of cycles will be approaching the qualification limit close to 2018. However, the qualification limits are quite conservative and there is plenty of voltage margin, so this does not cause any concern at present.

6.3 SW Configuration and Evolution Plan

This section provides the current state of the on-board software and tables of the instrument, and any expected evolutions to that software that are expected in the future.

GOME-2 FM3 was launched with software version 2.5. Early on in the mission, two very small patches were identified to correct two anomalies, namely AR.6210 spurious EQSOL and AR.6674 Coffee Break. GOME software remained at version 2.5, with these two small patches bringing the software up to version 2.5.1

During early operations, it was also found that the co-adding function was not working correctly, resulting in geolocation shifts of co-added 93.75 ms data with respect to normal 187.5 ms data. The SCIuP software was completely re-written and recompiled and the ICUuP software untouched. This yielded software version 2.6. Software 2.6.1 was then defined as comprising version 2.6 plus the two small ICUuP patches to fix AR.6210 & AR.6674.

It was then found that the co-adding function did not work correctly for channels 1 & 2, so a small patch was developed on top of software 2.6 to correct this. In addition, the patch to correct the spurious SU Off anomaly (AR.6963) was developed, yielding software version 2.6.2.

There is currently no proposed plan for the software on GOME-2 FM3/Metop-A to evolve. With over 3 years of operational experience, it can be safely assumed that any bugs have been ironed out. However, the EUMETSAT control system requires that each software delivery comes with an LDM file comprising the full EEPROM image, without any exceptions. Software version 2.6.2 did not include the default timelines. Another impact of this EUMETSAT control system requirement is that each LDM file is flight model specific, since the Flight Model identifier is hard coded in EEPROM. It is therefore proposed to have an additional delivery - 2.6.3a, (the letter “a” is the Metop Identifier). Since the EQSOL (AR.6210) patch is not required for FM1 & 2 due to a hardware fix, version 2.6.4b/c is proposed and defined as version 2.6.3a without the AR.6210 patch.

Table 6-2 is a summary of actual software versions, bright green being current.

Software Version	*Content*	*Configured as*	*Full image Available*	*Note*	*METOP*
2.5	Reference	New Release	Yes	At Launch	A
2.5.1	v2.5 + AR.6210, AR.6674 patches	Patches	No	Patches to ICUuP Only	A
2.6	v2.5 + SCIuP reload for AR.7050	New Release	Yes	Evolution of v2.5. Reloading of SCIuP only to fix AR.7050. ICUuP patches to fix AR.6210 and AR.6674 not included	A
2.6.1	v2.6 + AR.6210, AR.6674 patches	New Release	Yes	Evolution of 2.5.1	A
2.6.2	v2.6 + AR.6210, AR.6674, AR.6963 & 2.6 bug patches	New Release	Yes	Evolution of v2.6.1	A
2.6.3a	v2.6.2 plus EEPROM default timelines and Metop A identifier	New Release	Yes	Evolution of v2.6.2	A

Software Version	*Content*	*Configured as*	*Full image Available*	*Note*	*METOP*
2.6.4b	v2.6.2 less the AR.6210 patch, plus EEPROM default timelines and Metop B identifier	New Release	Yes	Evolution of v2.6.2	B
2.6.4c	v2.6.2 less the AR.6210 patch, plus EEPROM default timelines and Metop C identifier	New Release	Yes	Evolution of v2.6.2	C

Table 6-2 GOME-2 Software Versioning

6.3.1 Timelines and Onboard Tables

Table 6-3 shows the current status of Software and on-board tables. ***Note:*** In future releases, one or more pseudo tables will be defined to cover all DSMs that are not highly dynamic. This will include all DSMs requiring Standby-Idle transition for an update, plus DSMs that are not regularly updated by timelines.

Component	*Status*	*Comments*
CDHU ICU SW	Version 2.6.2	AR.6210 Ghost EQSOL Patch Uploaded AR.6674 Coffee Break Patch Uploaded AR.6963 Patch Uploaded
CDHU SCI SW	Version 2.6.2	AR.7050 Co-adding Patch Uploaded
SU SW	Version x.x	None.
GTL	Nominal	GOME_LTL_00_M02_CALNS0xx01 GOME_LTL_01_M02_CALNS4xx01 GOME_LTL_02_M02_CALNS5xx01 GOME_LTL_03_M02_PMDRAWNS01 GOME_LTL_04_M02_CALNS6xx01 GOME_LTL_05_M02_NOT960xx02 GOME_LTL_10_M02_NADIRxxx10 GOME_LTL_11_M02_NOT320xx00 GOME_LTL_12_M02_MOON1NSx01 GOME_LTL_13_M02_MOON2NSx01 GOME_LTL_14_M02_MOON3NSx01
GTL SEQ	Nominal	v.4.0
GTT	Empty	Not Used
Monitoring Parameters	Nominal	MDA_IGO1STM_DEFAULT.dts v1.1 MDA_IGO1RFD_DEFAULT.dts v1.1 MDA_IGO1XAS_DEFAULT.dts v1.1 MDA_IGO1XMN_DEFAULT.dts v1.1
PMD Bands	Nominal	MDA_IGO8PMD_DEFAULT.dts v1.1

Table 6-3: Onboard Tables Configuration

6.4 Operational Documentation Status

The latest GOME-2 IOM is v7 (Sep 2009).

7 CONCLUSION

Currently, all indicators of GOME health and performance are excellent, with the exception of problems relating to throughput, which stabilised in September 2012, with limited performance degradations in the UV.

The degradations observed for both the HCL and QTH lamps are just normal signs of aging and do not cause concern within the timeframe until 2018.

The trend in Scan Unit torque appears to have stabilised, and there is no reason to believe that this will be a limiting factor before 2018. In the meantime, ESA tribology experts will study the bearing design, use of the scan mirror and torque telemetry to determine possible mechanisms for the trend, its projected evolution and recommend any mitigating action which could be taken.

APPENDIX A MAPPING OF PHYSICAL SIGNATURES, INSTRUMENT COMPONENTS AND TM PARAMETERS

		GOM01	*GOM02*	*GOM03*	*GOM04*	*GOM05*	*GOM06*
	Test Title	**HKTLM Stability**	**SU Bearings Monitoring**	**HCL, QTH Lamp Monitoring**	**Spectral Stability**	**Detector response stability**	**Throughput**
	Description	Monitor Stability of HKTLM and Type 14 entries to determine health of Instrument	For each 171 Hz 1920 km and 960km swath torque profile, plot the average difference between all points on reference profile, separating for "turn arounds" and the main part of the cycle. Repeat for Mirror position.	Plot current and voltage profiles during operation and ensure they fit within envelope. For HCL Lamp monitor for Low Voltage Mode and Ignition Time in particular. SMR v WLS monitoring may indicate differential loss of throughput which could indicate lamp blackening.	SLS measurements are primarily used for pixel to wavelength mapping and also to monitor the spectral stability of the instrument which is important for the maintenance of product quality. The strength of the measured SLS lines is also an important result that must be used in the throughput monitoring. When the intensity of individual lines falls below specified thresholds they are no longer deemed reliable for use in spectral calibration. SLS measurements are made daily and the positions of spectral lines on the detectors are monitored.	LEDs can be used to monitor Pixel to Pixel gain which is used to correct for the pixel to pixel variation of quantum efficiency of the detectors, as well as for identification of hot or dead pixels. Pixel to Pixel gain is measured by using the LEDs mounted directly in front of each detector. LEDs illuminate the detectors uniformly with green light (ca 550 nm). By comparing the LED measurements with an LED spectrum smoothed over ~5 pixels, an estimate of the pixel-to-pixel gain can be made. By monitoring changes in pixel-to-pixel gain changes in the relative behaviour of the quantum efficiency of the detectors can be observed. This is a result must be fed back into other throughput monitoring so that relative changes in pixel performance do not appear as pixel dependent signatures.	By assessing various Instrument throughputs and comparing in various combinations, it is possible to identify individual components as a source of throughput loss.
Component	**Subcomponent**						
SU	**Bearings**	0x11 0x12 0x13 0x14 0x15 0x16 0x64 0xB1, sub 0x7	SU Mode SU Torque (all samples) SU Torque Shift (all samples) SU Position (all samples) **Torque Profile** **Position Profile**				
SU	**Scan Mirror**						Scan Mirror Contamination
CU	**HCL**	0x70, sub 0xC		HCL Status HCL Voltage HCL Current **HCL Ignition Time** **HCL Low Voltage Mode**			**HCL Lamp Degradation**
CU	**QTH**	0x70, sub 0xD		**Lamp Blackening**			**QTH Lamp Degradation**
CU	**SHUTTER**	0x70, sub 0xB 0x71					
CU	**DIFFUSER**						**Diffuser Contamination**
PMD	**COOLERS**	0x70, sub 0x0, 0x1 PMD temperatures					
PMD	**DETECTORS**	0xB1, sub 0x4, 0x5 0xB2, sub 0x4, 0x5 0xB3, sub 0x4, 0x5 PMD temperatures				**hot or dead pixels**	**Detctor Contamination**
FPA	**COOLERS**	0x70, sub 0x7, 0x8, 0x9, 0xA, 0x6 0xB1, sub 0x8, 0x9, 0xA, 0xB FPA temperatures Peltier Output V OB temp					

		GOM01	*GOM02*	*GOM03*	*GOM04*	*GOM05*	*GOM06*
	Test Title	**HKTLM Stability**	**SU Bearings Monitoring**	**HCL, QTH Lamp Monitoring**	**Spectral Stability**	**Detector response stability**	**Throughput**
	Description	Monitor Stability of HKTLM and Type 14 entries to determine health of Instrument	For each 171 Hz 1920 km and 960km swath torque profile, plot the average difference between all points on reference profile, separating for "turn arounds" and the main part of the cycle. Repeat for Mirror position.	Plot current and voltage profiles during operation and ensure they fit within envelope. For HCL Lamp monitor for Low Voltage Mode and Ignition Time in particular. SMR v WLS monitoring may indicate differential loss of throughput which could indicate lamp blackening.	SLS measurements are primarily used for pixel to wavelength mapping and also to monitor the spectral stability of the instrument which is important for the maintenance of product quality. The strength of the measured SLS lines is also an important result that must be used in the throughput monitoring. When the intensity of individual lines falls below specified thresholds they are no longer deemed reliable for use in spectral calibration. SLS measurements are made daily and the positions of spectral lines on the detectors are monitored.	LEDs can be used to monitor Pixel to Pixel gain which is used to correct for the pixel to pixel variation of quantum efficiency of the detectors, as well as for identification of hot or dead pixels. Pixel to Pixel gain is measured by using the LEDs mounted directly in front of each detector. LEDs illuminate the detectors uniformly with green light (ca 550 nm). By comparing the LED measurements with an LED spectrum smoothed over ~5 pixels, an estimate of the pixel-to-pixel gain can be made. By monitoring changes in pixel-to-pixel gain changes in the relative behaviour of the quantum efficiency of the detectors can be observed. This is a result must be fed back into other throughput monitoring so that relative changes in pixel performance do not appear as pixel dependent signatures.	By assessing various Instrument throughputs and comparing in various combinations, it is possible to identify individual components as a source of throughput loss.
FPA	**DETECTORS**	0x70, sub 0x2, 0x3, 0x4, 0x5 0xB1, sub 0x0, 0x1, 0x2, 0x3 0xB2, sub 0x0, 0x1, 0x2, 0x3 0xB3, sub 0x0, 0x1, 0x2, 0x3 FPA Temps				**hot or dead pixels**	**Detector Contamination**
SPEC	**TELESCOPE**						**Telescope contamination**
SPEC	**PRISMS**						
SPEC	**MIRRORS**						
SPEC	**GRATINGS**						
SPEC	**FOCUSSING OBJECTIVES**						
CDHS	**CDHU**	0x20, 0x21, 0x31, 0x44, 0x45, 0x4F, 0x51, 0x52, 0x55, 0x56, 0x65, 0x66, 0x77, 0x78, 0xB1 sub 0x6, 0xB9, 0xBB, 0xBE CDHU Power V EQ status					
CDHS	**GPDU**	0x70, sub 0x14 GPDU Power V EQ status					
OB							